Aus dem Zentrum für Medizinische Forschung
der Medizinischen Fakultät Mannheim
Direktor: Prof. Dr. med. Norbert Gretz

Influence of photobiomodulation with blue light on the metabolism, proliferation and gene expression of human keratinocytes

Inauguraldissertation
zur Erlangung des akademischen Grades
Doctor scientiarum humanarum (Dr. sc. hum.)
der
Medizinischen Fakultät Mannheim
der Ruprecht-Karls-Universität
zu
Heidelberg

vorgelegt von
Anja Becker

aus
Bad Bergzabern, Deutschland
2017

Dekan: Prof. Dr. med. Sergij Goerdt
Referent: Prof. Dr. med. Norbert Gretz

TABLE OF CONTENTS

Page

ABBREVIATIONS

AHR	Aryl hydrocarbon receptor
AHRE (XRE, DRE)	Aromatic hydrocarbon response element
AHRR	Aryl hydrocarbon receptor repressor
ALDH3A1	Aldehyde dehydrogenase 3 family member a1
ANOVA	Analysis of variance
ARNT	Aryl hydrocarbon receptor nuclear translocator
BL	Bright Light
bHLH	Basic helix-loop-helix
BrdU	Bromdeoxyuridine
Cdc37	Cell division cycle 37 control protein
CDKN1B (Kip1)	Cyclin-dependent kinase inhibitor 1B
CICZ	Indolo[3,2-b]carbazole-6-carboxylic acid
CLS	Cell Line Service
CYP	Cytochrome P450
FACS	Fluorescence activated cell sorting
dFICZ	6,12-diformylindolo[3,2- b]carbazole
DMEM	Dulbecco's Modified Eagle Medium
DMSO	Dimethylsulfoxid
E	Efficiency
EDTA	Ethylenediaminetetraacetic acid
EGFR (ERBB)	Epidermal growth factor receptor
ELISA	Enzyme-linked Immunosorbent Assay
EPRE (ARE)	Electrophile response element
ER	Endoplasmatic Reticulum
FACS	Fluorescent-Activated Cell Sorting
FAD	Flavin Adenine Dinucleotide
FBS	Fetal Bovine Serum
FDR	False Discovery Rate
FICZ	6-formylindolo[3,2-b]carbazole
GOBP	Gene Ontology Biological Processes
GSEA	Gene Set Enrichment Analysis

GSTA1	Glutathione S-transferase 1
HAAs	Heterocyclic aromatic amines/amides
HaCaT	Immortalized Human Keratinocytes
IKKβ	Inhibitor of kappa light polypeptide gene enhancer in B-cells kinase beta
IR	Infrared
Keap1	Kelch-like ECH-associated protein 1
KEGG	Kyoto Encyclopedia of Genes and Genomes
LLLT	Low Level Laser (Light) Therapy
NER	Named entity recognition
NES	Normalized Enrichment Score
NF-κB	Nuclear factor of kappa light polypeptide gene enhancer in B-cells 1
NQO1	NAD(P)H quinone oxidoreductase 1
Nrf2 (NFE2L2)	Nuclear factor erythroid 2 like 2
PAHs	Polycyclic aromatic hydrocarbons
PBM	Photobiomodulation
PBS	Phosphate Buffered Saline
PCR	Polymerase Chain Reaction
q	Real time
R²	Goodness-of-fit of linear regression
RB1	Retinoblastoma 1
ROM	Reactive oxygenated metabolite
ROS	Reactive Oxygen Species
RT	Reverse Transcriptase
TCDD	2,3,7,8-Tetrachlordibenzodioxin
TM	Textmining
TNF-α	Tumor necrosis factor alpha
TRADD	(TNF-α receptor-associated protein
UGT1A	UDP glucuronosyltransferase 1 family, polypeptide A
UV	Ultraviolet
VL	Visible Light
XMEs	Xenobiotic-metabolizing enzymes

XTT	Sodium 3´-[1-(phenylaminocarbonyl)-3,4-tetrazolium] bis(4-methoxy-6-nitro)benzene sulfonic acid hydrate
7-AAD	7-aminoactinomycinD

1   INTRODUCTION

1.1   Text mining

Scientific publications are the main media through which researchers gain knowledge and report their new findings. One of the most important systems that provides access to the biomedical literature is PubMed, which gives access to more than 26 million scientific literature citations from MEDLINE, life science journals and online books [1, 2]. Nowadays, the large and growing number of published studies in biomedicine, and their increasing rate of publication, provides an immense volume of information. However, it makes the task of identifying relevant studies in an unbiased way both time consuming and complex [1, 3, 4]. Consequently, researchers turn more and more to the use of text mining (TM), which comes with solutions for this problem offering automated methods to screen and extract compressed information concealed within vast numbers of publications and thereby increasing speed, quality and reproducibility of text processing [3, 5]. Marti Hearst provided a widely accepted definition of TM, which is "the discovery by computer of new, previously unknown information, by automatically extracting and relating information from different written resources, to reveal otherwise 'hidden' meanings" [6]. TM analysis typically involves a number of distinct steps combining techniques from information retrieval, artificial intelligence, natural language processing (NLP) and data mining to apprehend the complex analytical processing system of written language [7, 8].

Fleuren and Alkema provided a comprehensive summary of the different steps for TM analysis (Figure 1) [8].

The first step is called information retrieval (IR) where relevant textual resources like literature or text segments are retrieved in response to query terms [4, 8, 9]. This first step serves to preprocess the narrative text in order to classify the publications and consequently reduce the search time [4].
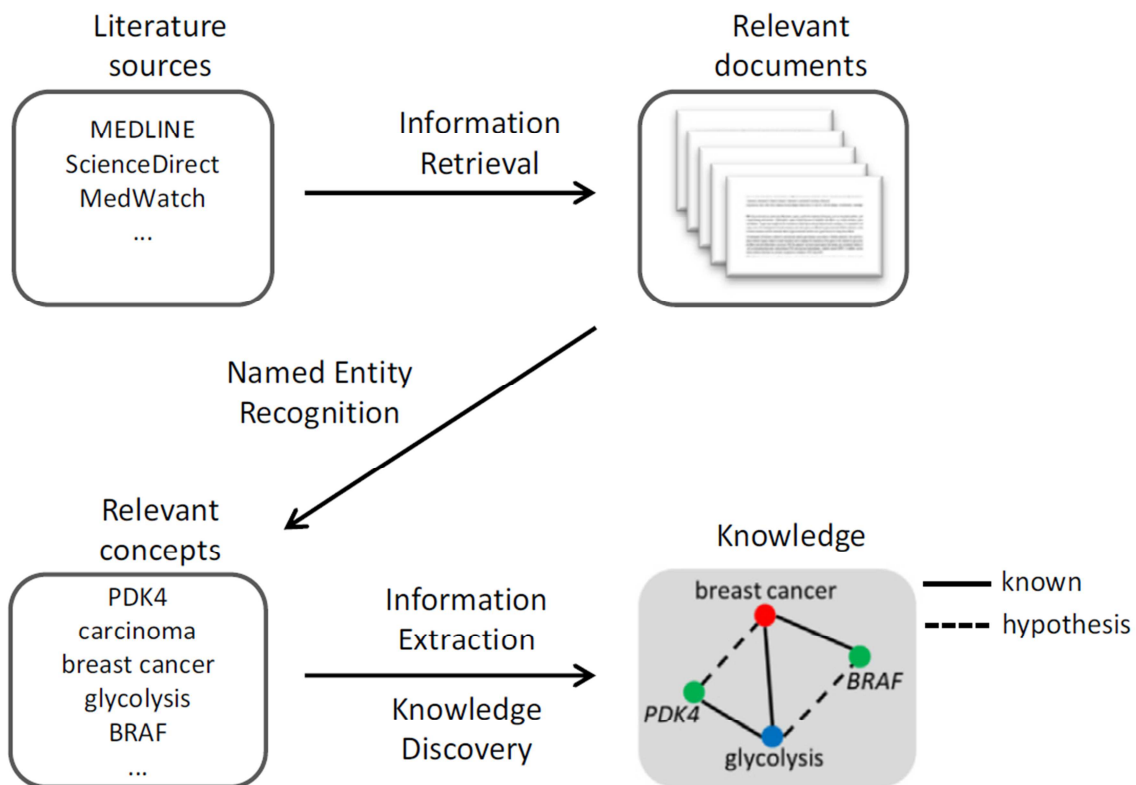
Figure 1: Overview of a typical TM workflow from Fleuren and Alkema: "A typical TM workflow starts with information retrieval (IR) to get relevant documents for a given subject of interest. Using named entity recognition (NER) these documents will be analyzed for the occurrence of specific keywords. Information extraction (IE) is about detecting links between the found keywords and can be done in a number of ways. During knowledge discovery (KD) links between keywords can be used to infer new relations, so called hidden relations that can be seen as 'true' new knowledge."[8]

As a second step, the selected publications can be examined using search algorithms where the results of the query are analyzed to enhance the process of IR and the recovered publications are classified according to their content and/or key-word matching [4]. Key-word matching is the analysis of occurrence of specific key-words in the publications and identification of relations between those keywords. To ease the identification of important parts of a publication sentence extraction can be performed, which depicts only those parts of the publication in which specific keywords occur [8]. Named entity recognition (NER) plays an essential part herein, with the keyword or a set of keywords being the named entity. These entities have to be linked to the specific concept of the publication, which can be defined as biological entity and can be referred to by multiple keywords [8].

As a next step, after performing IR and NER, the links between concepts in the text can be detected by using specialized algorithms. Additional context is given to the concepts by linking concepts together resulting in valuable knowledge which can be

used for further analysis. As scholarly publications are primarily written in text, natural language processing (NLP) is one of the most used approaches to extract this knowledge and can facilitate research productivity. It is able to extract key information from free text and converts it into structured knowledge [7-9].

The important last step in TM is the representation and visualization of results to simplify and clarify the complex network interaction of the selected publications and comprises many different possibilities like for example galaxy plots, landscapes and heat-maps. Graphs should demonstrate the correlations between different articles as well as cluster them to similar keywords.

In summary TM is a profitable method to select scientific articles according to related keywords thereby enabling a kind of pre-reading and simplifying the formulation of new hypothesis and initiating follow-up experiments [8, 10].

1.2 The human skin

The human skin is the largest organ of the body and serves as a protective barrier between the internal milieu and the environment thereby functioning as the body's first line of defense against infection and regulating temperature and fluid balance [11]. Furthermore, its complex cellular network constitutes an immunological barrier [12, 13]. The skin is organized in three primary layers, the epidermis, the dermis and the hypodermis (Figure 2).

The dermis comprises the fibroblasts and nerve endings, hair follicles, sweat glands, and blood vessels among other structures [11]. A basement membrane separates and connects epidermis and dermis with anchoring mature, epidermal melanocytes [11]. The epidermis, which is the outermost skin layer, is made up of a network of keratinocytes with interconnected melanocytes and scattered inflammatory cells [11]. It functions as the physiological barrier and can be divided into five layers: stratum corneum, stratum lucidum, stratum granulosum, stratum spinosum and stratum germinativum, which is also called stratum basale. The self-renewing property of the epidermis is maintained by the accurate regulation of keratinocyte proliferation, migration, differentiation, and apoptosis [14, 15]. The most essential structural constituents of keratinocytes are the intermediate filaments called cytokeratins; they play a crucial role in development and barrier function of the skin [16]. Proliferation of

keratinocytes takes place in the basal layer and is stimulated by various growth factors [14, 16].
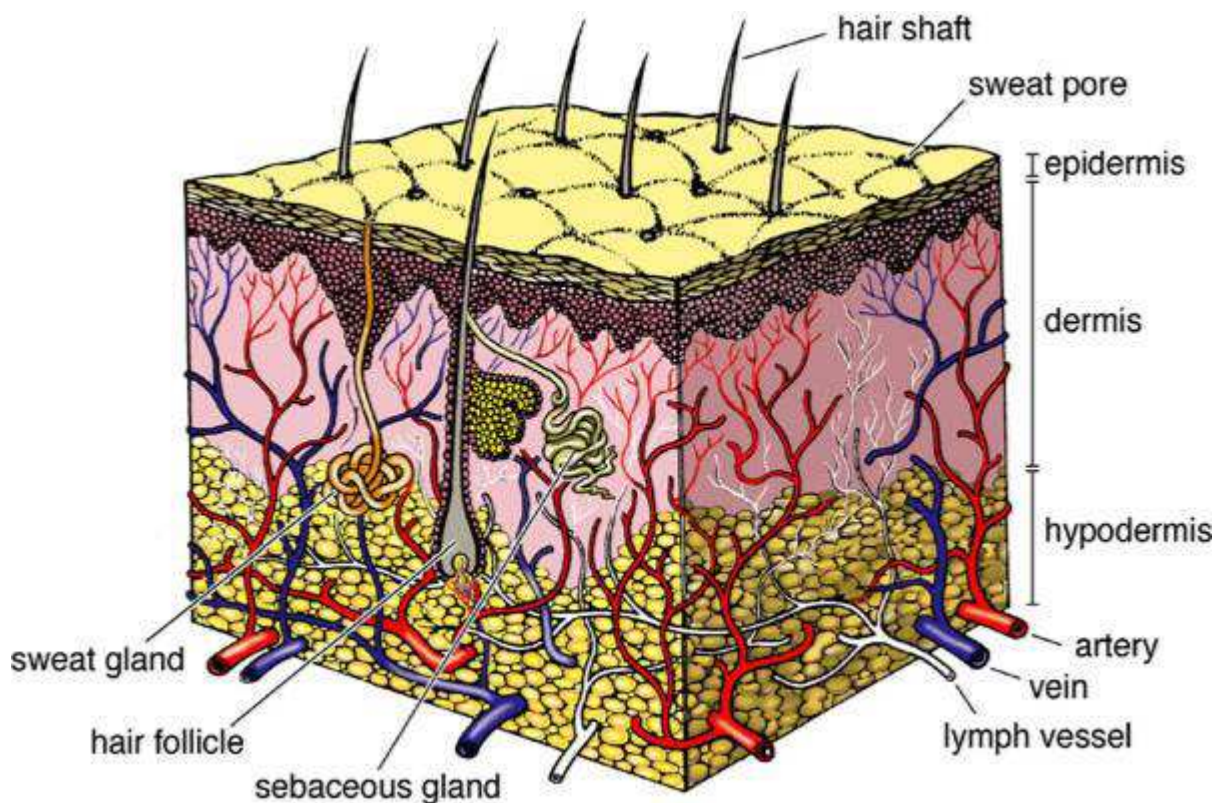

Figure 2: Physiology of the human skin [17].

Members of the epidermal growth factor (EGF), fibroblast growth factor (FGF), nerve growth factor (NGF), and insulin-like growth factor (IGF) families, as well as hepatocyte growth factor (HGF), granulocyte-macrophage colony stimulating factor (GM-CSF), and endothelin-1 stimulate keratinocyte growth while transforming growth factor-b, vitamin D3, and interferon-ɣ suppress their growth. Next to being regulated by growth factors, keratinocytes themselves are a source of various growth factors, chemokines and cytokines and play an important role in the skin's cytokine network [14].

Differentiation of keratinocytes occurs during migration from the basal layer towards the skin surface. In the following phase called cornification or keratinization, the cells progress from rounded cells to a flat form thereby building up the cornified outer layer of the skin [16]. It comprises cross-linked proteins (cornified cell envelope) and lipids (cornified lipid envelope) and is most affected by external stimuli [18].

Besides structural scaffolding, keratinocytes actively produce substances like cytokines, neurotransmitters and hormones [16] when exposed to external stimuli like temperature, pressure, pain, and light [19]. These are mediators of inflammation and

immune responses and are essentially connected to the pathophysiology of skin diseases such as psoriasis and atopic dermatitis, and play a crucial role in skin wound healing.[14, 20]

In summary, keratinocytes are not only present in all layers of the epidermis but are also the first cells to be in contact when exposed with external stimuli and are consequently more amenable to non-invasive treatments such as topical agents and photobiomodulation using blue light [21].

1.2.1 The human skin and light penetration

The behavior of light irradiation in the human skin respectively its penetration depth is an important issue that should be considered when using light as a therapeutic tool. Two factors influence the penetration depth of light through or into the skin which are optical light scattering and absorption of irradiation. Both vary according to wavelength respectively to frequency or energy of light (Figure 3) [22, 23].
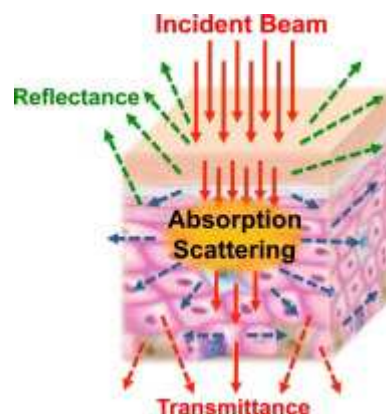

Figure 3: Light distribution in the human skin [22].

Furthermore, the penetration depth is reliant on the thickness of the skin, which is based on the number of the different cell layers and can vary depending on the location [23].

Blue light, which will be used in this study, is closest to UV in the visible spectrum. It penetrates about 0.7mm into the human skin, therefore does not directly affect deeper skin layers but mainly effects keratinocytes in the upper skin [23].

1.3 Photobiomodulation (PBM)

Light is connected to various functions of the human body like vitamin-D metabolism, circadian rhythm and the psychosocial state and consequently it is important for human health. Phototherapy (UV), photodynamic therapy (PDT) and skin rejuvenation as well as high power surgical lasers in ophthalmology, dermatology and oncology are treatment paradigms which are already used in medicine [24, 25]. Low level light/laser therapy (LLLT) with non-thermal, low power visible and near-infrared light is a less prominent therapeutic application which is used to stimulate wound healing, tissue regeneration and hair growth [26-28] or to reduce inflammation and alleviate pain [27, 29-32]. Blue light in particular is used for different medical treatments like psoriasis [33], neonatal jaundice [34] and back pain [35] and it is known to have anti-microbial [36], anti-inflammatory [37] and anti-proliferative effects [38, 39]. Thus, light therapy is a convenient, painless and inexpensive therapeutic intervention for different treatment paradigms gaining more and more attention [40]. However, the protocols for light therapy enclose a variety of different parameters which are not comparable easily. To introduce a more defined application a new term was introduced called photobiomodulation (PBM), which is a form of light therapy using the visible and infrared spectrum. It utilizes non-ionizing forms of light, comprising LEDs, lasers and broadband light and is non-thermal. The process involves endogenous chromophores, which elicit photophysical and photochemical events at various biological scales. Beneficial therapeutic outcomes are inter alia alleviation of pain or inflammation, immunomodulation, and promotion of wound healing as well as tissue regeneration [24]. What differs here from the previously used terms is that the biomodulation is only induced by the photons, heat stress induced by the light source as well as adding substances extracellular, like for PDT, has to be excluded.

1.3.1 Mechanisms of PBM

PBM has only an effect in living systems if the photons are absorbed by electronic absorption bands belonging to some molecular photoacceptors, or chromophores, which is stated by the first law of photobiology [41]. These chromophores almost always occur in one of two forms: metal complexes and conjugated π-electron systems [42] and are comprised in the human skin in a wide variety. They absorb light in at least one spectral range of the optical spectrum, like endogenous nucleic acids, aromatic amino acids, urocainic acid, tryptophan, tyrosine, NADPH, NADH cofactors,

cytochromes, flavins, flavoproteins, porphyrins, melanin and melanin precursors, protoporphyrin IX, bilirubin, haemoglobin, myoglobin, β-carotene or water molecules [23, 42].

Four possible mechanisms of light action on chromophores were described by Karu [43]. First, photoexcitation which can influence redox properties of carriers in the respiratory chain and thereby enhance electron transfer. Second, the partial conversion of the energy of excitation into heat, which can thereby lead to a localized temporary heating of absorbing chromophores. As a consequence, conformational changes may occur and thus biochemical activities may be triggered. Third, H_2O_2 or reactive oxygen species (ROS), which are metabolites of oxygen in the respiratory chain, might function as secondary messengers, leading to variation of redox activity of mitochondria and/or redox state of the cell, and furthermore to accelerated electron transfer. And fourth, photoabsorbing chromophores can directly be converted into photosensitizers which can transmit energy to adjacent molecules. Through that molecules can be activated and can induce chemical reactions. Moreover, this process is oxygen dependent and creates ROS, more precisely singlet oxygen. Photoabsorbing chromophores of the respiratory chain include porphyrins and flavoproteins, hemes, Fe-S centers, as well as terminal respiratory chain oxidase cytochrome C oxidase. Secondary reactions after light absorption are cellular signaling pathways, which also include the mitochondrial retrograde signaling [43, 44].

1.3.2 PBM dosages

One of the most important parameters to describe PBM is the energy (J) or energy density (J/cm^2). However, energy is based on the power and on the irradiation time (Energy (J) = Power (W) × Time (s)) and these two components have to be considered when talking about the dose in PBM as there is not necessarily reciprocity between them. Consequently, if the energy is constant but the two parameters are changed the biological outcome may be different. Important parameters and their correlations are listed in Table 1 and Table 2 from Huang et al. 2009 [42].

Defining an effective dose for a clinical use of PBM is still a critical point as the parameters of wavelength, irradiance, fluence and delivery protocol have to be clearly defined to achieve a specific biological scenario [45]. An important point to consider when creating a PBM protocol is its possible biphasic dose response

(**Arndt-Schulz curve**) [32], which is also called "hormesis" [46], first used by Stebbing in 1982 [47] and comprehensively reviewed by Calabrese [46, 48].

Many different studies in low-level light therapy (LLLT) presented this biphasic dose response [49, 50] and those dose dependent effects are frequently connected to the model of the "Arndt-Schulz Law" [51-54]. It states, that a weak stimulus can accelerate the vital activity, which can be even increased with higher stimuli. However, at some point a peak will be reached after which an increase of stimulus will first lead to suppressing the effect and finally inducing a negative response in vital activity [44, 55]. That means that beneficial therapeutic effects can be induced with low doses of light, whereas higher doses are harmful and therefore phototoxic leading to a need of defining a threshold for clinical use of PBM [32].

Table 1: Parameters involved in determining the LLLT "medicine" [42].

IRRADIATION PARAMETERS (*The Medicine*)		
Irradiation parameter	**Unit of measurement**	**Comment**
Wavelength	nm	Light is electromagnetic energy which travels in discrete packets that also have a wave-like property. Wavelength is measure in nanometers (nm) and is visible in the 400-700 nm range.
Irradiance/ Power density	W/cm^2	Often called Intensity, or Power Density and is calculated as Irradiance = Power (W)/Area (cm^2)
Pulse structure	Peak power (W) Pulse frequency (Hz) Pulse width (s) Duty cycle (%)	If the beam is pulsed then the Power should be the Average Power and calculated as follows: Average Power (W) = Peak Power (W) × pulse width (s) × pulse frequency (Hz)
Coherence	Coherence length depends on spectral bandwidth	Coherent light produces laser speckle, which has been postulated to play a role in the photobiomodulation interaction with cells and subcellular organelles.
Polarization	Linear polarized or circular polarized	Polarized light may have different effects than otherwise identical non-polarized light (or even 90-degree rotated polarized light). However, it is known that polarized light is rapidly scrambled in highly scattering media such as tissue (probably in the first few hundred μm).

Table 2: Parameters involved in determining the LLLT "dose" [42].

IRRADIATION TIME OR ENERGY DELIVERED (*The Dose*)		
Irradiation parameter	**Unit of measurement**	**Comment**
Energy (Joules)	J	Calculated as J = W x s This mixes medicine and dose into a single expression and ignores irradiance. Using Joules as an expression of dose is potentially unreliable as it assumes reciprocity (the inverse relationship between power and time).
Energy density	J/cm^2	Common expression of LLLT "dose" is energy density. This expression of dose again mixes medicine and dose into a single expression and is potentially unreliable as it assumes reciprocity relationship between power and time.
Irradiation time	s	In our view the safest way to record and prescribe LLLT is to define the four parameters of the medicine (See Table 1) and then define the irradiation time as "dose".
Treatment interval	Hours, days or weeks	The effects of different treatment intervals are underexplored at this time though there is sufficient evidence to suggest that this is an important parameter.

1.4 Aim of the project

During the last years PBM represented one of the main upcoming treatment approaches.

PBM has many advantages, it is noninvasive, cost-effective and easy to handle. Many promising effects of blue light are known comprising its anti-microbial [36], anti-inflammatory [37] and anti-proliferative effects [38, 39]. It is already used in different medical treatments for inter alia psoriasis [33], neonatal jaundice [34] and back pain [35] and could possibly be applied for a variety of other treatment paradigms if the effects would be more defined and estimable.

Although many reports describe the effectiveness of blue light, little is known about the mechanisms transducing the light induced signals from target molecules over downstream processes and/or gene expression to the biological effects [56] with additional difficulty of being hardly able to differentiate between primary and secondary effects.

Therefore, the aim of this project was to test the dosage dependent blue light effects on the immortalized human keratinocyte cell line HaCaT with following set up:

- Cell viability tests analyzing metabolism and proliferation, thereby selecting certain dosages for further experiments

- H_2O_2 concentration measurement to confirm a light induced ROS production

- FACS analysis for cell apoptosis as safety measurement to demonstrate that ROS production does not induce apoptosis, hence, does not harm the cells

- Comprehensive gene expression analysis using Affymetrix GeneChips to assess the safety and identify possible target genes for PBM using blue light

2 MATERIAL AND METHODS

2.1 Material

2.1.1 Equipment

BD FACSCalibur	BD Biosciences
Corning® 96 well plates, clear bottom	Sigma Aldrich
DMM230 Industrial Multimeter	Multimetrix
GeneChip Scanner 3000	Affymetrix
Human Gene 2.0 st arrays (Hugene-2_0-st)	Affymetrix
Incubator Heraeus	Thermo Scientific
Fluidics station 450	Affymetrix
Laminar Flow	Kendro Laboratory Products
LightCycler® 480 Multiwell Plate 96	Roche
Luna cell counter	Biozym
Lumileds LUXEON Rebel LXML-PR01-0275	Philips
Microplate Reader Infinite® 200 PRO	Tecan
Microscope	Leica
Dyad, Peltier Thermo Cycler	Bio-Rad
Pipettes	Gilson/Eppendorf
RNA Clean-Up and Concentration Micro Kit	Norgen
Vortexer Reax top	Heidolph
Water bath	Memmert

2.1.2 Software for statistical analysis

JMP Genomics 10	SAS

2.1.3 Chemicals and Kits

Amplex® UltraRed Reagent	Invitrogen
Cell Proliferation ELISA, BrdU (colorimetric)	Roche
cDNA Synthese Kit	Thermo Scientific
Chlorophorm	J.T. Baker
Colorimetric Cell Viability Kit III (XTT)	PromoKine (PromoCell GmbH)

Dulbecco's Modified Eagle Medium (DMEM)	Gibco
Dimethylsulfoxid (DMSO)	Sigma Aldrich
Ethanol	Emsure Merck
Fetal Bovine Serum (FBS)	Gibco
FITC Annexin V	BioLegend
FITC BrdU Flow Kit	BD Pharmingen™
Isopropanol	Sigma Aldrich
Light Cycler 96 DNA Green	Roche
Penicillin/Streptomycin	Gibco
Phosphate buffered saline (PBS)	Gibco
Propidiumiodid	Invitrogen
RevertAid H Minus First Strand-SuperScript Choice System	Invitrogen
Sodium Pyruvat	Gibco
Staurosporine	Sigma Aldrich
TRIzol Reagent	Ambion
Trypsin 0.25% EDTA	Gibco
Colorimetric Cell Viability Kit III (XTT)	PromoKine

2.1.4 Primer sequences

Primer sequences for CYP1A1, CYP1B1, ALDH3A, NQO1 and UGT1A were adopted from Brauze et al. 2014 [57]. Primers for FOS, IL8, Krt5 and the reference gene MOK were designed (2.2.11) and are depicted in Table 3.

Table 3: Primer specifications.

Gene name and Accession number	Sequence	Annealing Temperature Tm(°C)/t(s)	Efficiency	R^2
FOS	F: CACTCCAAGCGGAGACAGAC	63	1.92	0.96
NM_005252.3	R: AGGTCATCAGGGATCTTGCAG	61		
IL8	F: AGGAACCATCTCACTGTGTGT	59	2.14	0.97
NM_ 000584	R: CACCCAGTTTTCCTTGGGGTC	63		
Krt5	F: AACCTGGACCTGGATAGCATCA	62	1.80	0.78
NM_ 000424.3	R: ACATTGTCAATCTCGGCTCTCAG	63		
MOK	F: AGAGATCCAAGCACTGAGGC	60	2.12	0.98
NM_ 001272011.1	R: TACCAGCGGGTGGAGATGTA	60		

2.2 Methods

Methods were previously described [39, 58, 59] in short.

2.2.1 Literature search and Tex Mining

The systematic literature search to identify relevant references describing the effects of blue and red LED light on keratinocytes was performed (March 2015) in the electronic database MEDLINE using PubMed platform. The keywords included in the search were (blue light AND keratinocytes NOT photodynamic) or (red light AND keratinocytes NOT photodynamic). Therefore, publications dealing with therapies using not only photobiomodulation but heat, chemicals or other factors in addition were excluded. Additionally, papers were selected according to the following criteria: irradiation with visible blue and red light, stimulation of keratinocytes, performance of in vitro studies and the use of statistical methods. Papers were reviewed and summarized in tabular form. Due to heterogeneity between studies a meta-analysis was not performed. For further analysis and classification parameters were chosen connected to light irradiation, which are wavelength, energy density, power density, irradiation time and distance from the light source. Furthermore, the biological outcome was used to cluster the articles into three groups: cell proliferation, apoptosis and migration of keratinocytes. A three-dimensional scatterplot and a principal component analysis (PCA) were performed to summarize those results.

Finally, Text Mining was applied using statistical and learning methods. In this case abstracts, titles and Medical Subject Headings (MeSH) terms from different research publications were taken into account by copying them into the software R, version 3.2.0. For further analysis, the R-package tm was used and all text was saved in "corpus", which is a collection format for documents in R [60].

2.2.2 Cell culture

HaCaT cells (immortal human keratinocytes) from Cell Line Service (CLS) GmbH (Heidelberg/Germany) were cultured under standard conditions at 37°C with 5% CO_2. They were cultured in Dulbecco´s modified Eagle´s medium (DMEM) high glucose containing 10% fetal bovine serum (FBS), 1mM sodium pyruvate and 100U/mL penicillin/streptomycin (Gibco® by life technologies TM AG (Carlsbad/USA)) whereas

0.1% Trypsin-EDTA (1x) phenol red from Gibco® was used to detach the cells with a 10min incubation time. Sub-culturing ratios have been 2/10 to 3/10.

2.2.3 Irradiation with blue light

HaCaT cells were plated in black 96 well plates, with sterile clear flat bottom wells (Sigma Aldrich Co. LLC (St. Louis/USA)). These plates allow a direct microscopic cell viewing as well as a reduction of the background signal. Cell numbers were depending on the duration of experiment and are described in Table 4. No cells were seeded in the last column H, which served as chemical blank and only contained the cell culture medium. After seeding, cells were incubated 24h at 37°C with 5% CO_2. Medium was renewed and cells were illuminated with blue light for different irradiation times/energy densities (Table 5). The right half of the plate was taped with black foil for the no light negative control; consequently non-irradiated cells were kept under the same environmental conditions apart from light exposure. After a defined time experiments were conducted or cells were harvested with TRIzol Reagent (Ambion® by life technologies TM AG (Carlsbad/USA)) and stored at -80°C for further use in RNA isolation and following gene expression analysis with microarrays.
Lumileds LUXEON Rebel LXML-PR01-0275 were used (Koninklijke Philips N.V. (Eindhoven/Netherlands)) with an intensity of 23mW/cm^2 at an irradiation distance of 55mm, beam divergence of ±15° and a peak wavelength at 453 nm (blue light).

As trypsinization of 96 well plates turned out to inefficient using this cell line, cells were seeded in 6 well plates for cell counting with Luna Cell Counter and BrdU FACS. The no light control was not on the same plate. However, to eradicate the plate effect, cells were seeded well per well (well1 plate1, well1 plate2, well2 plate1, well2 plate2,…).

Table 4: Cell numbers for seeding into microwell plates depending on experiment duration.

Harvesting time [h]	Cell number per 96 well	Cell number per 6 well
0-24	10,000	160,000
48	5,000	80,000
72	2,500	40,000

Table 5: Irradiation parameters.

Irradiation time [min]	Power density [mW/cm²]	Energy density [J/cm²]
0	23	0
2.5	23	3.45
5.0	23	6.90
7.5	23	10.35
10.0	23	13.80
12.5	23	17.25
15.0	23	20.70
17.5	23	24.15
20.0	23	27.60
22.5	23	31.05
30.0	23	41.40
45.0	23	62.10
60.0	23	82.80
90.0	23	124.20
120.0	23	165.60

2.2.4 Cell proliferation tests

For analyzing proliferation of irradiated cells different approaches were tested including XTT test, a simple cell count using the LUNA Cell Counter from Biozym and colorimetric BrdU Cell Proliferation ELISA. Additionally, BrdU in combination with a nucleic dye was tested with FACS to classify a change in cell cycle phase proportion.

2.2.4.1 Cell metabolism (XTT) test

The Colorimetric Cell Viability Kit III (XTT) from PromoKine (PromoCell GmbH (Heidelberg/Germany)) was used as a first test to examine the effect of blue light irradiation. The assay is based on the formation of an orange formazan dye only by metabolic active and therefore viable cells. Consequently, an increasing absorbance directly correlates with the metabolism of living cells. The experiment was performed according to protocol with a 1h incubation time. For quantification spectrophotometric absorption measurements at 450nm and 640nm reference wavelength were used with Infinite® 200 PRO microplate reader (Tecan Group AG (Männedorf/Switzerland)). Experiments were done in three replicates and three repetitions. The raw absorbance values were normalized with the no light control. Based on OneWay-ANOVA, differential absorbance intensities were analyzed using

a commercial software package: JMP Genomics 10 from SAS. A false positive rate of a=0.05 was taken as the level of significance.

2.2.4.2 Cell counting with LUNA Cell Counter

In addition to XTT tests, a simple cell count using the LUNA Cell Counter from Biozym was used to confirm the impact of blue light induced metabolic changes on proliferation. After certain irradiation and harvesting times, cells were trypsinized with 1mL Trypsin per well (6 well plate), stopped with the same amount of cell culture medium and counted according to the recommendations of the manufacturer with the Luna Cell Counter (Biozym (Hessisch Oldendorf/Germany) using 1:2 Trypan blue. Experiments were done in three replicates and two repetitions. The cell count values were normalized with the starting cell number and no light control (Table 4). Based on OneWay-ANOVA, differential cell numbers were analyzed using a commercial software package: JMP Genomics 10 from SAS. A false positive rate of a=0.05 was taken as the level of significance.

2.2.4.3 Measuring newly synthesized cells with bromodeoxyuridine (BrdU) using Enzyme-linked immunosorbent assay (ELISA)

Furthermore, Colorimetric BrdU Cell Proliferation ELISA from Roche Diagnostics GmbH (Mannheim/Germany) was used for quantification of newly synthesized cells, respectively cell proliferation. BrdU labeling was done 1h after each irradiation with subsequent ELISA read out 24h after last labeling according to protocol. For quantification spectrophotometric absorption measurement was done at 450nm (with 640nm reference wavelength) with Infinite® 200 PRO microplate reader (Tecan Group AG (Männedorf/Switzerland)). Experiments were done in three replicates and two repetitions. The raw absorbance values were normalized with the no light control. Based on OneWay-ANOVA, differential absorption intensities were analyzed using a commercial software package: JMP Genomics 10 from SAS. A false positive rate of a=0.05 was taken as the level of significance.

2.2.4.4 Evaluating cell cycle phase with BrdU using Fluorescence-activated cell sorting (FACS)

For evaluating cell cycle phase proportion the FITC BrdU Flow Kit from BD Pharmingen™ (BD Biosciences (Heidelberg/Germany)) was used. After different irradiation and harvesting times, cells were trypsinized with 1mL Trypsin per well (6 well plate), stopped with the same amount of cell culture medium and prepared

according to the manufacturer´s protocol. 7-aminoactinomycin D (7-AAD) labeling was used to stain total DNA and consequently be able to categorize the different cell cycle phases with two-color flow cytometric analysis. Experiments were done in three replicates and two repetitions. The subsequent measurement was performed on a BD FACSCalibur (BD Biosciences (Heidelberg/Germany) while Flowing Software version 2.5.1 was used to perform a distribution analysis for statistical evaluation. Based on OneWay-ANOVA, differential distribution of cells in cell cycle phases were analyzed using a commercial software package: JMP Genomics 10 from SAS. A false positive rate of a=0.05 was taken as the level of significance.

2.2.5 Reactive oxygen species (ROS) measurement

Amplex UltraRed (Moelcular Probes, Invitrogen (Carlsbad/CA)) was used for measuring H_2O_2 concentrations in HaCaT cells modified from Chen et al. 2011 [56]. At defined time points after blue light irradiation 50µl 0,1M Potassium phosphate buffer pH 6,0 containing 100mM Amplex Ultrared and 0.2U/ml Horse radish peroxidase (Molecular Probes, Invtirogen (Carlsbad/CA)) was added to each well of the black 96 well plates and incubated for 30min at 37°C with 5% CO_2. Fluorescence was measured with the Infinite® 200 PRO microplate reader from underneath at λ_{ex}490nm/λ_{em}581nm (Tecan Group AG (Männedorf/Switzerland)). Experiments were done in three replicates and two repetitions. The raw fluorescence values were normalized with the no light control. Based on OneWay-ANOVA, differential fluorescence intensities were analyzed using a commercial software package: JMP Genomics 10 from SAS. A false positive rate of a=0.05 was taken as the level of significance.

2.2.6 Examining apoptosis using FACS

For marking of apoptotic cells with FITC labeled Annexin V (BioLegend (San Diego/USA)) and Propidiumiodide (PI) (InvitrogenTM by life technologies TM AG (Carlsbad/USA)) supernatant was harvested to collect possible apoptotic cells. After that, cells were washed with PBS, trypsinized and dissolved with the collected supernatant; $2x10^5$ cells were used. The cells were transferred to a 15ml Falcon tube and centrifuged 3min at RT and 2000x g. The supernatant was removed and the pellet was washed twice, first with PBS, secondly with Annexin-Binding Buffer (BioLegend (San Diego/USA)). Subsequently, the pellet was resuspended in 100µl

Annexin-Binding Buffer and cells were incubated with 5µl of Annexin V, and 2µl of PI 1mg/ml for 15min at RT in the dark. Finally, 100µl Annexin-Binding Buffer was added. For positive control 1µM Staurosporine (Sigma Aldrich Co. LLC (St. Louis/USA)) was added for 4h to HaCaT cells to induce apoptosis prior trypsinization. The subsequent measurement was performed on a BD FACSCalibur (BD Biosciences (Heidelberg/Germany) while Flowing Software version 2.5.1 was used to perform a distribution analysis for statistical evaluation. Based on OneWay-ANOVA, differential distribution of cells was analyzed using a commercial software package: JMP Genomics 10 from SAS. A false positive rate of a=0.05 was taken as the level of significance. Experiments were done in three replicates and two repetitions.

2.2.7 RNA Isolation for microarray analysis and quantitative real time PCR

For RNA isolation, modified from the TRIzol Reagent protocol, 200µl of chloroform was added for 1ml TRIzol. They were incubated for 2-3min at RT. Then the mixture was vortexed and centrifuged at 12000x g for 15min at 4° C to separate the organic from the aqueous phase. The aqueous upper phase was transferred into a new tube and precipitated with 500µl isopropanol. After incubation for 10min at RT, the mixture was centrifuged at 12000x g for 10min at 4° C. The supernatant was discarded. The pellet was washed twice with 1ml of ethanol and centrifuged at 12000x g for 5min at 4° C. After discarding the supernatant, the pellet was dried. Subsequently, the pellet was re-suspended in 20µl RNase-free water.

2.2.8 Gene expression analysis with Affymetrix GeneChips

After RNA isolation RNA was purified using the RNA Clean-Up and Concentration Micro Kit. cDNA synthesis was performed using the SuperScript Choice System according to the recommendations of the manufacturer. Using ENZO BioArray HighYield RNA Transcript Labeling Kit biotin-labeled cRNA was produced. A standard protocol from Affymetrix was used for the in vitro transcription (IVT). Quantification of cRNA was performed by spectrophotometric analysis with an A260/A280 ratio of 1.9 to 2.1. Fragmentation of the cRNA was achieved using Affymetrix defined protocol. For gene expression profiling, labeled and fragmented cRNA was hybridized to Affymetrix Hugene-2_0-st microarrays with an incubation of 16h at 45° C. The Affymetrix fluidics station 450 was used to wash the microarrays, scanning was performed with Affymetrix Genechip scanner 3000.

2.2.9 Bioinformatical evaluation of gene expression analysis

The Custom CDF Version 18 with Entrez based gene definitions was used for annotation [61]. Applying quantile normalization, the raw fluorescence intensity values were normalized. Based on OneWay-ANOVA, differential gene expression was analyzed using a commercial software package: JMP Genomics 10 from SAS. A false positive rate of a=0.05 with FDR correction was taken as the level of significance.

Gene Set Enrichment Analysis (GSEA) was used to determine whether defined lists (or sets) of genes exhibit a statistically significant bias in their distribution within a ranked gene list (see http://www.broadinstitute.org/gsea/ for details) [62]. Pathways belonging to various cell functions such as cell cycle or apoptosis were obtained from the public external database KEGG.

2.2.10 Reverse Transcription (RT) PCR

1µg of previously isolated RNA was used for the preparation of cDNA. RNA was filled up with distilled water to a total volume of 11µl. A master mix was prepared according to RevertAid H Minus First Strand cDNA Synthese Kit from Thermo Fisher Scientific Inc. (Waltham/USA). The 20µl reaction mixture was then used with the following program for the production of cDNA: 5min at 25°C, 60min at 42°C and 5min at 70°C. The cDNA was 1:10 diluted for further use in Real Time-PCR.

2.2.11 Primer design

Primer sequences for CYP1A1, CYP1B1, ALDH3A, NQO1 and UGT1A were adopted from Brauze et al. 2014 [57]. Primers for FOS, IL8, Krt5 and MOK (used as reference gene) were designed according to published genes sequences (NCBI-Gene) with PrimerBlast (http://www.ncbi.nlm.nih.gov/tools/primer-blast/) and span exon/exon boundaries. BLAST alignment search (http://blast.ncbi.nlm.nih.gov/Blast.cgi) was used to verify specificity. All Primers were purchased as DNA Oligo-Primer from Metabion International AG (Planegg, Steinkirchen/Germany).

2.2.12 Real Time-PCR (qPCR)

To verify expression of various genes in the microarray analysis, a Real Time-PCR (qPCR) was carried out with SYBR Green. The reaction mixture consisted of 5µl 1:10

diluted cDNA, 4.8µl water, 10µl SYBR Green master mix and 0.1µl each primer (LightCycler 96 DNA Green, Roche Diagnostics GmbH (Mannheim/Germany)). DNA Oligo-Primer from Metabion International AG (Planegg, Steinkirchen/Germany) were used with a concentration of 100µM, therefore end concentration in the reaction mix was 0.5µM. The qPCR was programmed as follows: 10 min 95°C, 45x(10 sec 95°C, 10 sec at Primer specific Tm, 10 sec 72°C), 10 sec 95°C, 1 min 65°C, 1 sec 97°C. Experiments were done in three replicates and two repetitions. For evaluation Roche LightCycler® 96 Application Software and JMP Genomics 10 from SAS were used.

3 RESULTS

3.1 Literature overview

To get an overview on literature for the effects of blue and red visible light on human keratinocytes PubMed was used to perform a search with the key words (blue light AND keratinocytes NOT photodynamic) and (red light AND keratinocytes NOT photodynamic), which resulted in 148 hits. To exclude non relevant studies a selection was taken by reading all the abstracts and dismissing papers not directly linked to blue and red light stimulation of cells. Finally, 8 articles were selected for blue light along with 4 publications for red light stimulation of keratinocytes. An evaluation was performed by extracting the different irradiation parameters for all articles, assigning them to resulting light effects and clustering the analysis into the three groups of proliferative effect (red), anti-proliferative effect (blue) and apoptotic effect (green). Articles, which were selected due to their connection to light effects but did not contain any information on proliferation or apoptosis of irradiated cells were represented with the color code black. To analyze the multivariate data, a principal component analysis (PCA) was executed. The 2 dimensional plots depict which components have the highest influence on the outcome (proliferation, anti-proliferation or apoptosis) and show the variances in the data set. The PCA demonstrates a clustering of the single effects and reveal the components wavelength, irradiation time, energy density and the proliferation as the most important ones (Figure 4).

Furthermore, a three-dimensional scatterplot was created to plot the three main characterized parameters containing wavelength, power density and the resulting energy density (Figure 5).

The 8 selected articles for blue light comprised the spectral region from 412 to 470nm with a wide range of tested power and energy densities. The described effects on cells include all three groups of proliferation, anti-proliferation and apoptosis. The effects cannot be assigned to a certain wavelength, power density or energy density. The search for the effect of red light on human keratinocytes was inconclusive.
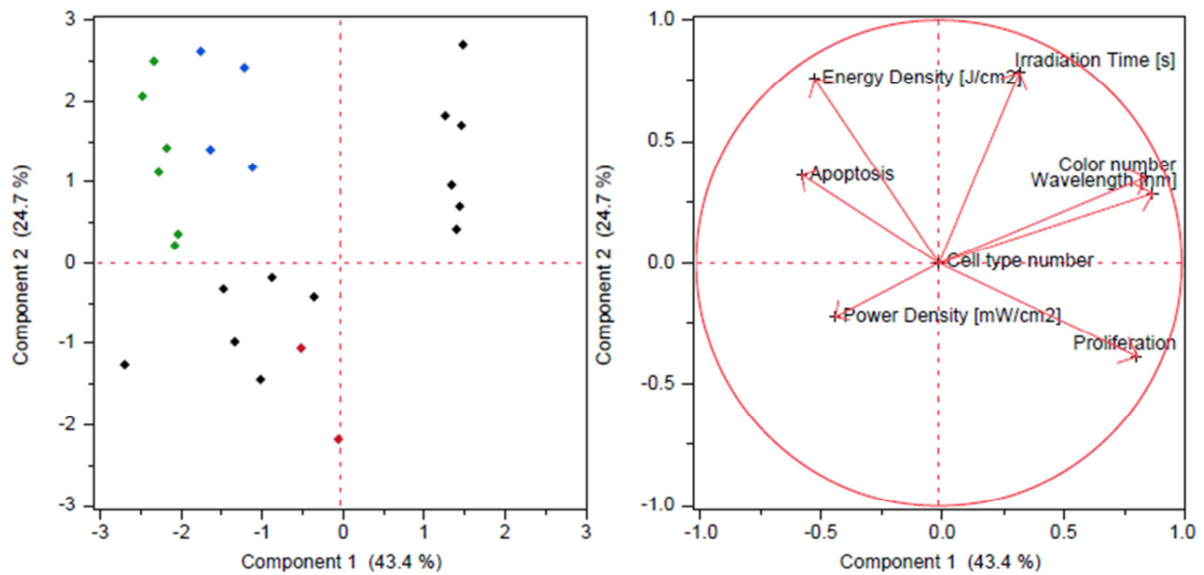
Figure 4: Principal component analysis: analysis of the literature search for visible light effects of blue and red light on keratinocytes with (A) showing the clustering of the predefined effects and (B) identifying the parameters with the highest impact on the clustering process depicted in (A). Red: pro-proliferative effect, blue: anti-proliferative effect, green: apoptotic effect, black: did not contain any information on proliferation or apoptosis.
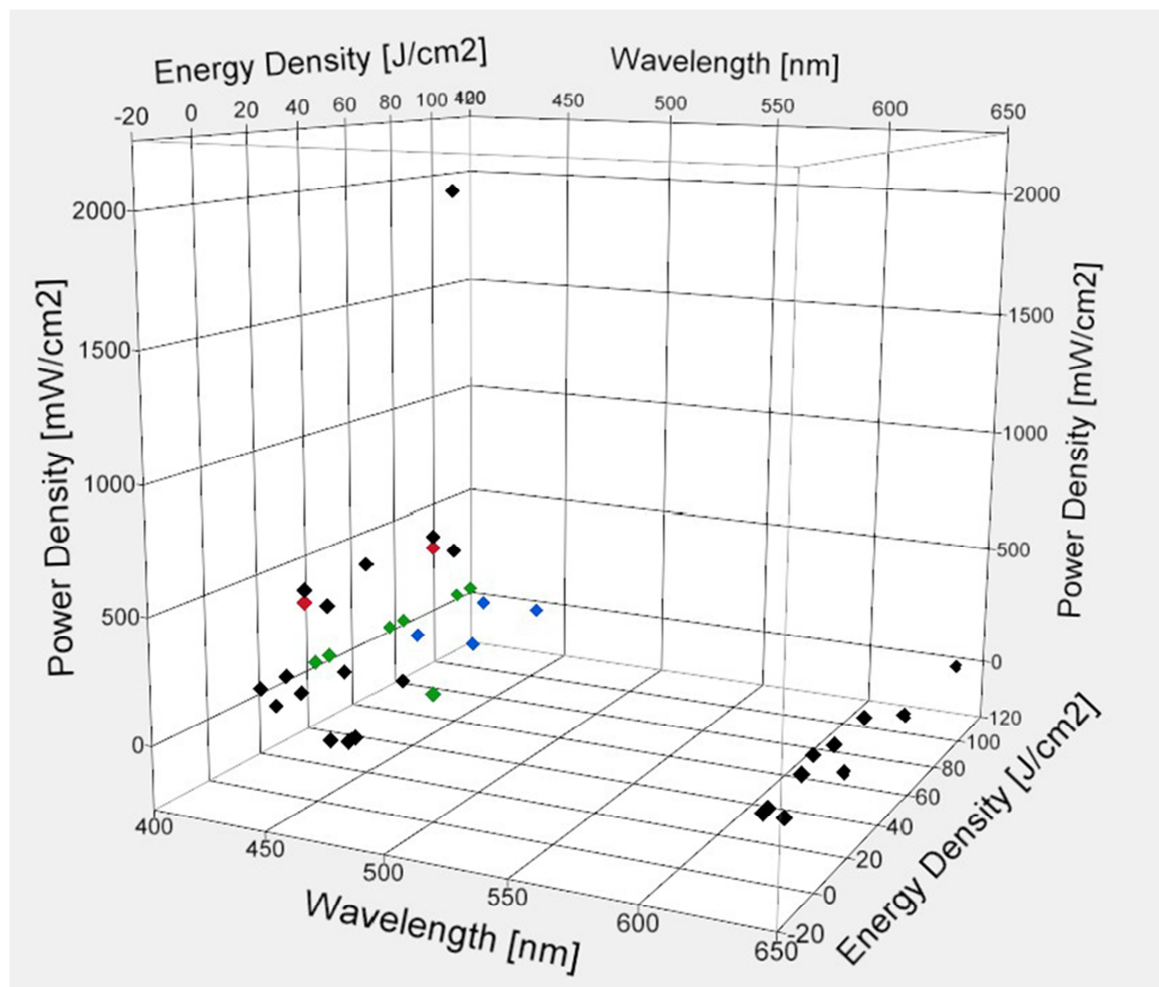

Figure 5: Scatterplot to analyze the literature search for visible light effects of blue and red light on keratinocytes depicting the correlation of wavelength, power density and energy density. Red: proliferative effect, blue: anti-proliferative effect, green: apoptosis, black: did not contain any information on proliferation or apoptosis.

3.1.1 Text Mining

To get a better overview of the relation between scientific articles and blue and red light effect on keratinocytes text mining was applied in a next step. In this process, the same or similar keywords served to cluster the corresponding publications into groups to simplify the selection procedure. Different kinds of data illustrations are available when using this method like density plot (Figure 6), galaxy plot (Figure 7) or 2D landscape (Figure 8).

Text Mining clustered the relevant articles into 5 groups depicted in different colors in all three figures (Figure 6, Figure 7 Figure 8). For instance, cluster 1 includes all articles containing keywords like microscope, stain and skin, whereas papers assigned to cluster 4 show keywords like light, blue and cell. Due to the given keywords the latter one is considered to be the most appropriate cluster for this study (Figure 6, Figure 7 Figure 8).

The density plot in Figure 6 depicts the occurrence of relevant papers per year over a time period from 1977 to 2015 (Figure 6). Furthermore, it demonstrates the development of increasing interest and attention to light therapy and its treatment possibilities over the last decade.

The galaxy plot (Figure 7) is based on a PCA with every data point corresponding to one article. The proximity of the data points resembles the relationship between the related articles and, similar to the density plot, the publications are clustered into the 5 groups according to keywords and color-coded respectively.

An additional indication about the emerging and high impact topics of the literature search for the effect of blue and red light on human keratinocytes is depicted with the 2D landscape in Figure 8, which visualizes the clustering process of the documents in the form of maps.
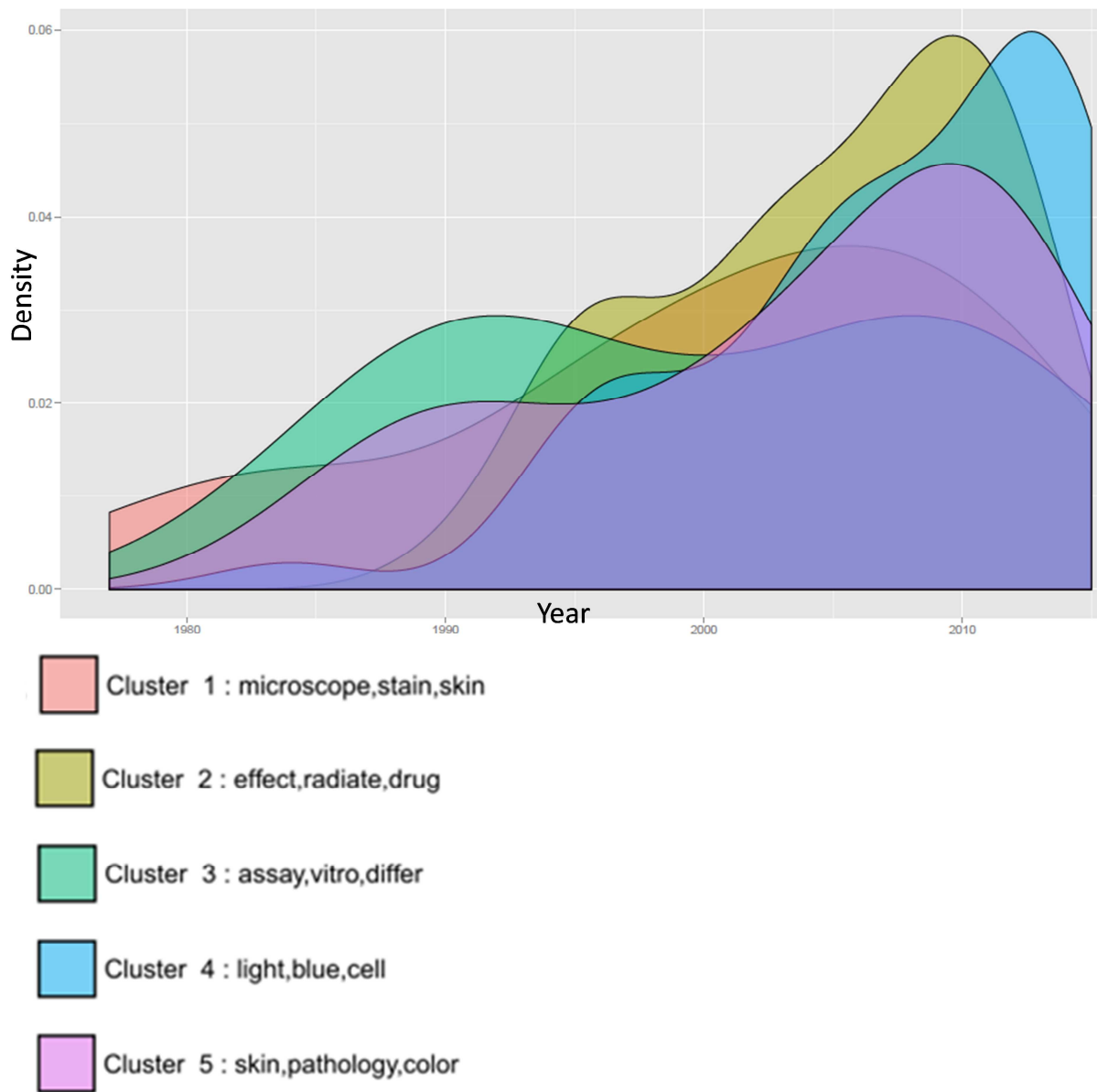
Figure 6: Density plot describing the literature search regarding red and blue light as well as keratinocytes per year by cluster from 1977 to 2015.
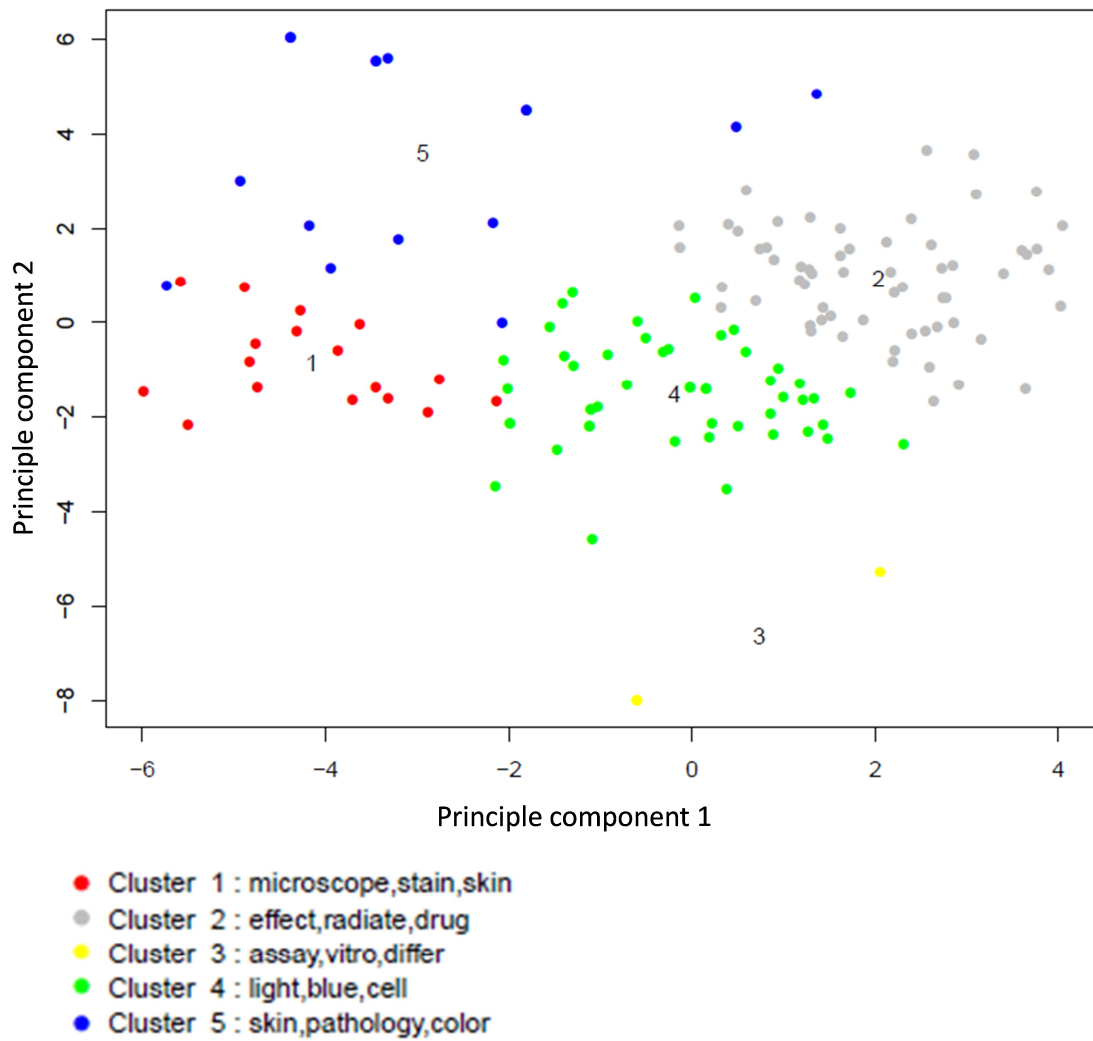
Figure 7: Galaxy plot for text mining defining the thematic distance of several publications describing the literature search regarding red and blue light as well as keratinocytes.
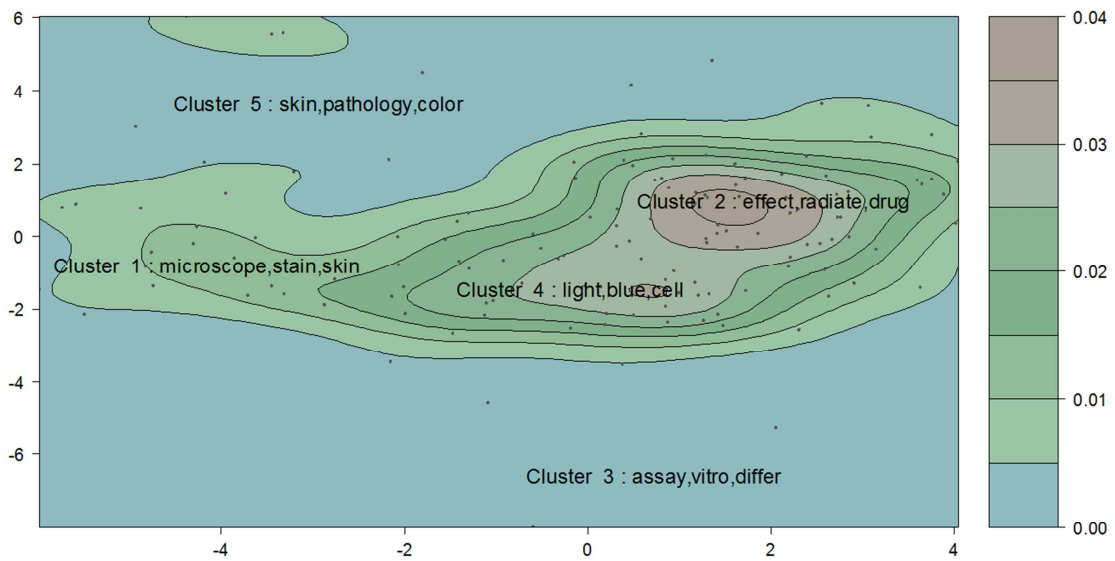

Figure 8: 2D landscape of text mining plotting the literature clusters with differences in height describing the literature search regarding red and blue light as well as keratinocytes.

3.2 Blue light irradiation leads to a PBM characteristic biphasic dose response curve in human keratinocytes

As changes in cell metabolism are faster and more pronounced compared to changes in cell proliferation the Colorimetric Cell Viability Kit III (XTT) from PromoKine (PromoCell GmbH (Heidelberg/Germany)) was used as a first test to examine the effect of blue light irradiation.

XTT tests of HaCaT cells were performed with different irradiation times and measured at the harvesting time point (harvesting time) 24h after irradiation to study the dose effect of PBM with blue light on cell metabolism (Figure 9).
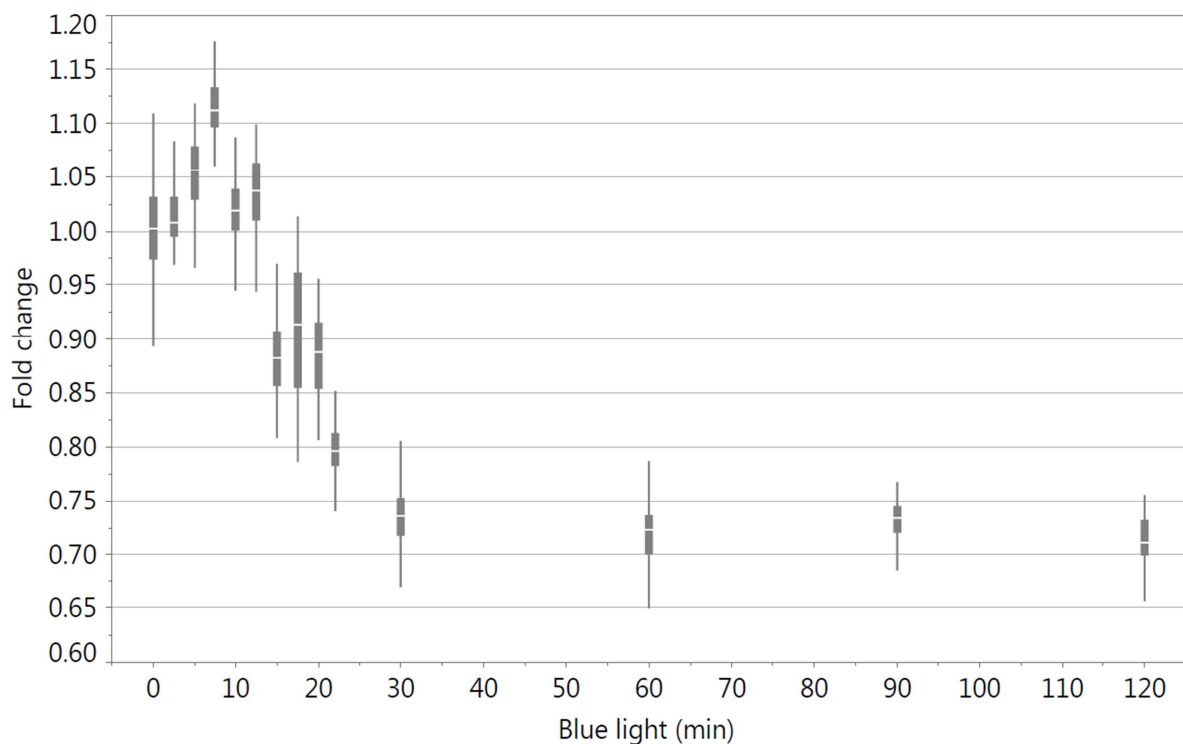

Figure 9: XTT test results of different irradiation times: 2.5, 5, 7.5, 10, 12.5, 15, 17.5, 20, 22.5, 30, 45, 60, 90 and 120min with cell harvesting 24h after irradiation. The box-and-whisker plots represent the distribution of XTT data values. These are ranked into quartiles, which divide the data set into a box of four equal groups; the band inside the box reflects the median. The whiskers extend from the ends of the box to the outermost data point that falls within the distances calculated as follows: 3rd quartile+1.5*(interquartile range) and 1st quartile-1.5*(interquartile range).

With short exposure times of 5min (6.9J/cm²), 7.5min (10.35J/cm²), 10min (13.5J/cm²) and 12.5min (17.25J/cm²) cell metabolism was significantly increased with a maximal effect of 12% (p<0.0001*) with 7.5min (10.35J/cm²) blue light.

After 15min cell metabolism was significantly decreased (p<0.0001) by 12%, with even more pronounced effect of 29% for 30min (41.4J/cm²) of blue light irradiation (p<0.0001). The effect seems to be constant after 30min; there was no further decrease in cell metabolism with longer irradiation times up to 120min irradiation.

7.5min (10.35J/cm²) respectively 30min (41.4J/cm²) were chosen in subsequent experiments to test the blue light effect after different harvesting times in the proliferative phase respectively the anti-proliferative phase of PBM.

3.3 Anti-proliferative phase of blue light irradiation - 30min (41.4J/cm²) blue light irradiation

3.3.1 The decrease in cell metabolism after 30min (41.4J/cm²) blue light irradiation in HaCaT cells, which lasts until at least 24h, is gone 48h after irradiation

XTT tests of HaCaT cells were conducted at different harvesting times after 30min (41.4J/cm²) of blue light irradiation to examine the time course of the anti-proliferative effect of this dose. Already 1h after irradiation the metabolism of the cells was decreased by 6% (p<0.0001) with even more pronounced effect of 9% (p<0.0001) after 3h, 16% (p<0.0001) after 6h to 18% (p<0.0001) after 12h, and finally reaching its maximum with 29% decrease (p<0.0001) 24h after irradiation. 48h after irradiation metabolism of irradiated cells was again on the same level as the no-light control cells (Figure 10).
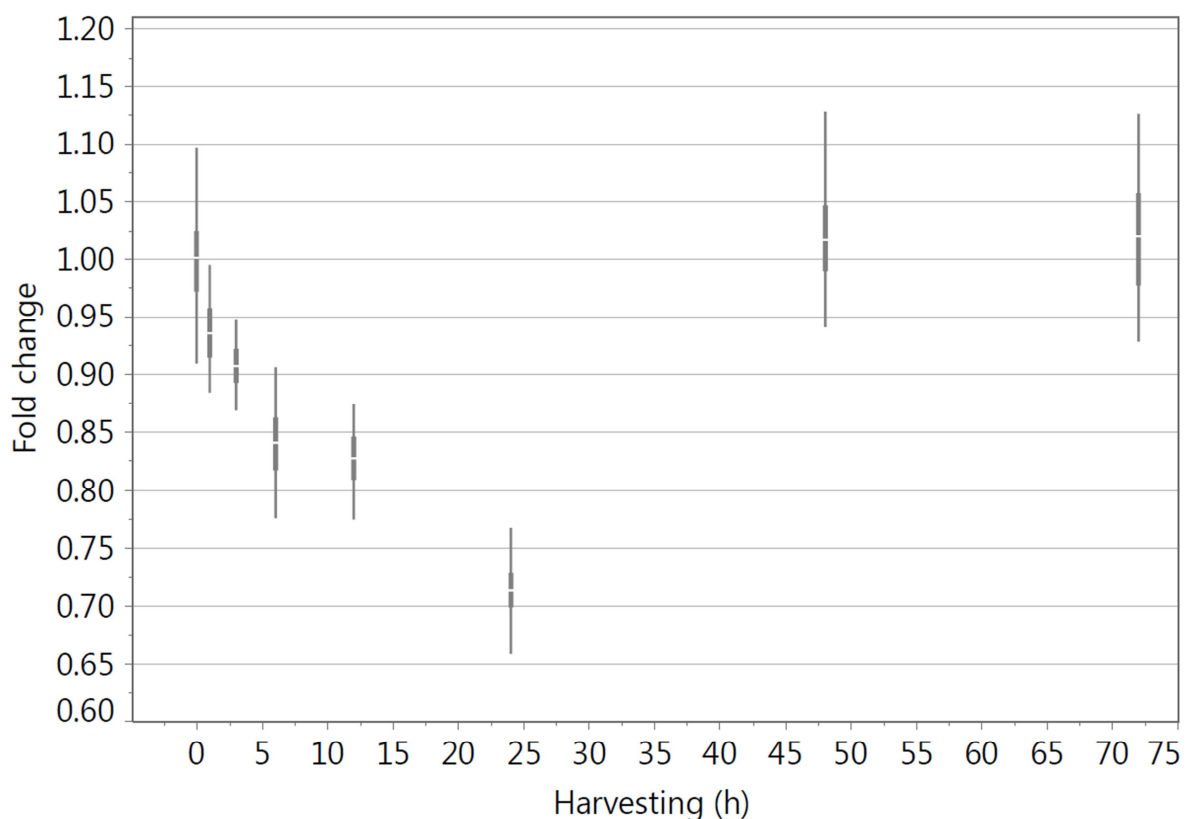

Figure 10: XTT test results at the different time points of cell harvesting: 1h, 3h, 6h, 12, 24h, 48h and 72h after 30min (41.4J/cm²) of blue light irradiation. (For legend see Figure 9).

3.3.2 Consecutive irradiations with 30min (41.4J/cm²) of blue light each 24h can prolong the inhibition of cell metabolism in HaCaT cells

As the effect of decreased metabolism disappeared 48h after blue light irradiation, consecutive irradiations with 30min (41.4J/cm²) of blue light were performed each 24h. When irradiated more than once the effect could be prolonged, metabolism of HaCaT cells was even more decreased compared to a single irradiation from 32% decrease to 34% decrease (p<0.0001), however, the effect between two and three irradiations did not change significantly (p=0.518) and depicts a decrease in metabolism of 35% (p<0.0001) for irradiated cells compared to the no-light control cells (Figure 11).
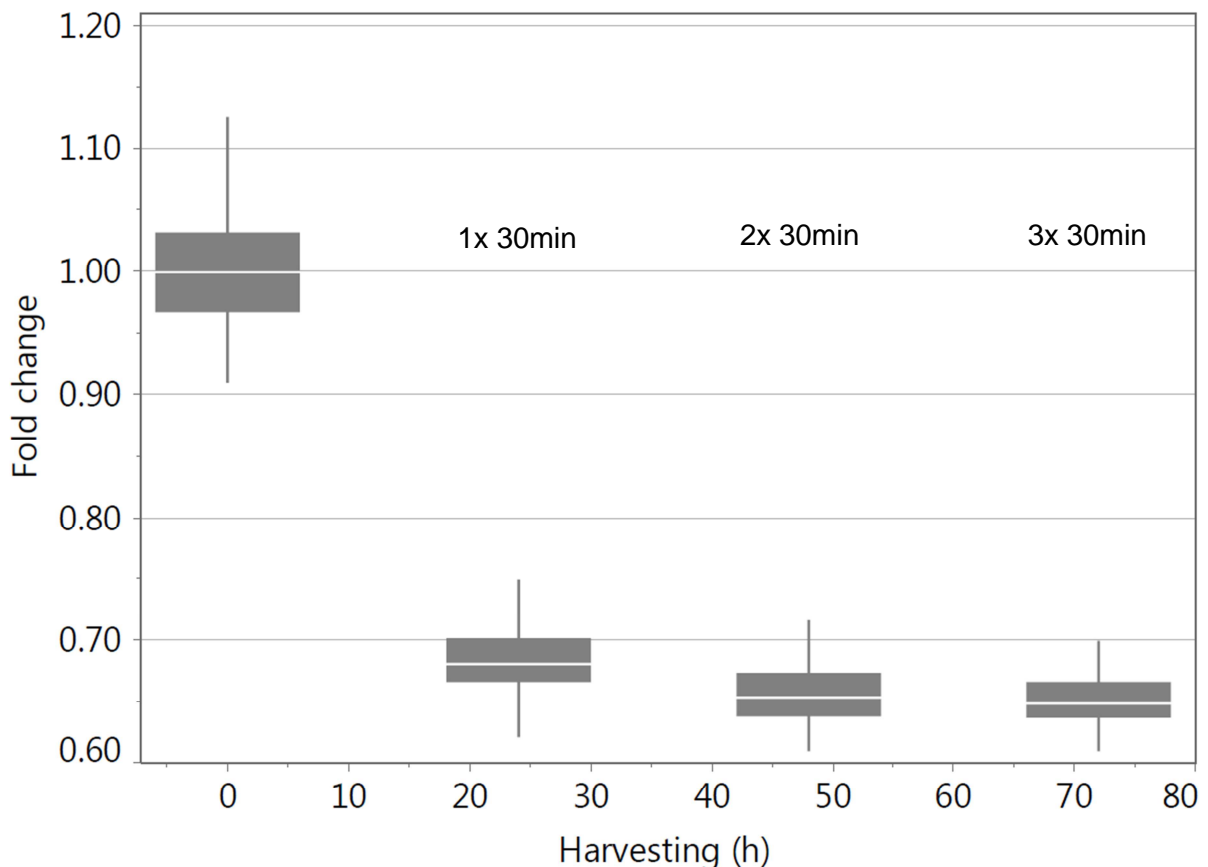

Figure 11: XTT test results of the different numbers of 30min (41.4J/cm²) blue light irradiations harvested 24h after the respective last irradiation. (For legend see Figure 9).

3.3.3 30min (41.4J/cm²) blue light irradiation of HaCaT cells leads to a decrease in cell proliferation 24h after irradiation and can be increased by consecutive irradiations each 24h

Cell counting and BrdU ELISA of HaCaT cells were conducted at different harvesting times after 30min (41.4J/cm²) of blue light irradiation to examine the time course of

the anti-proliferative effect of this dose. As the doubling time of HaCaT cells is 24h, an effect on cell proliferation was not expected before 24h after irradiation and therefore fits to cell counting results. A lower cell count of 20% (p=0.0159) was noted 24h after irradiation, which could be intensified with consecutive irradiations each 24h with 37% (p=0.0130) 48h after irradiation and 37% (p=0.0034) 72h after irradiation. BrdU, which is a pyrimidine analogue being incorporated instead of thymidine into the DNA of proliferating cells, was tested for 24h, 48h and 72h harvesting. The extend of BrdU ELISA was less than for cell counting results, however depicted a corresponding anti-proliferative result with no effect on cell proliferation 24h after irradiation, but decreasing effect with consecutive irradiations each 24h with 6% (p=0.0315) 48h after irradiation and 14% (p<0.0001) 72h after irradiation (Figure 12).
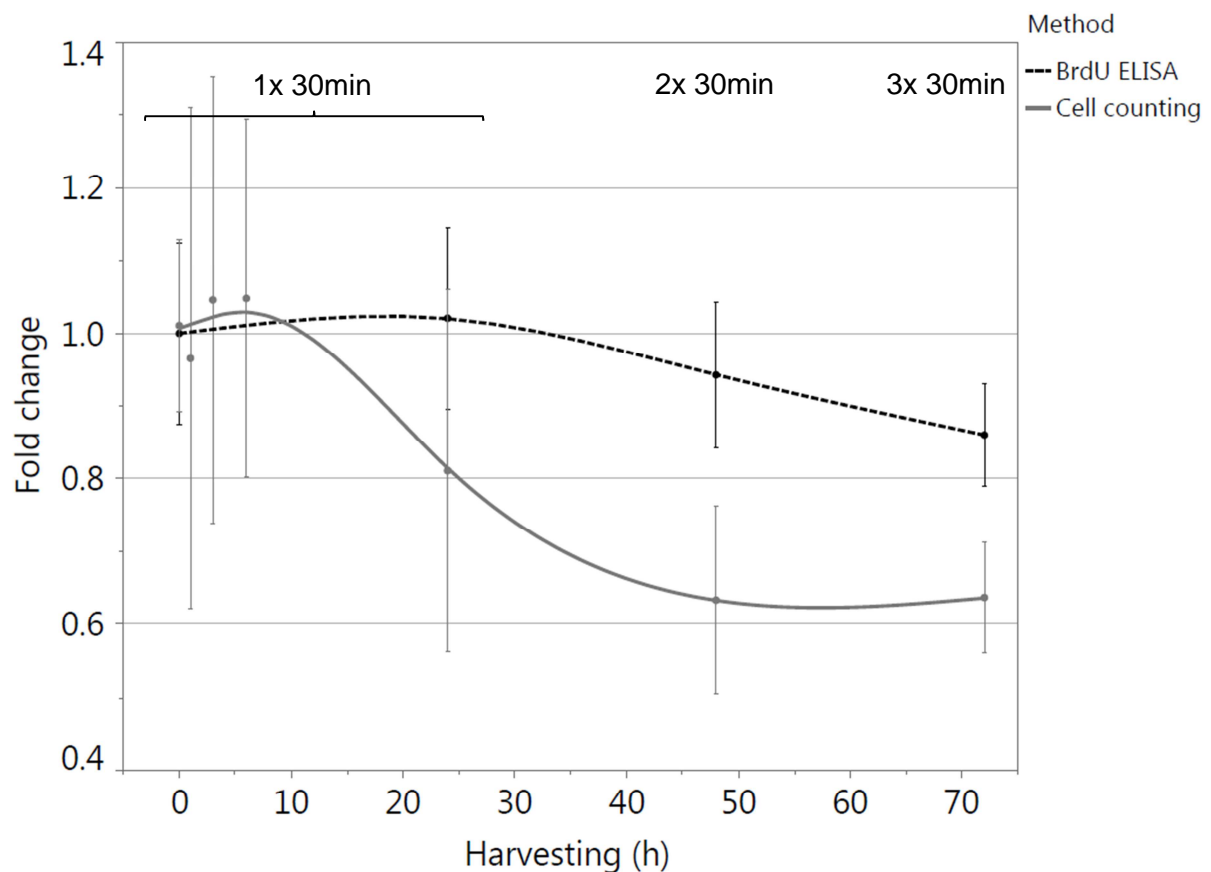

Figure 12: Cell count and BrdU ELISA at the different time points of cell harvesting: 1h, 3h, 6h, 12, 24h, 48h and 72h after different numbers of 30min (41.4J/cm²) of blue light irradiation. Dots display mean values with SD.

3.3.4 Consecutive irradiations with 30min (41.4J/cm²) of blue light each 24h induce a change in cell cycle phase proportion of HaCaT cells leading to an increase in S-phase cells and decrease in G_0/G_1-phase cells

To test the cell cycle phase proportion of HaCaT cells after 30min (41.4J/cm²) of blue light irradiation immunofluorescent BrdU staining was used in combination with 7-AAD, which binds to total DNA. Already 24h after irradiation cell proportion was slightly shifted from G_0/G_1 to S-phase (1% (p=0.7102)). This shift was increased by consecutive irradiations each 24h to 1.3% (p=0.5201) 48h after irradiation and a significant increase of 5.8% (p=0.0368) 72h after irradiation (Figure 13).

Figure 13: BrdU FACS results of the different numbers of 30min (41.4J/cm²) blue light irradiations harvested 24h after the respective last irradiation. Bars display mean values with SD.

3.3.5 30min (41.4J/cm^2) of blue light irradiation increases H_2O_2 concentration in HaCaT cells immediately after irradiation

As light is known to induce production of ROS, respectively H_2O_2, we measured H_2O_2 concentrations in HaCaT cells at different harvesting times after 30min (41.4J/cm²) of

blue light irradiation, with a first time point at 30min according to incubation time. H_2O_2 concentration was increased 1.26 fold (to 126%) 30min after blue light irradiation (p<0.0001). Followed by a decrease to 93% 1h after irradiation (p<0.0001), H_2O_2 concentration alternated between 99% after 3h (p=0.7585) to 96% after 6h (p<0.0001) and finally 105% after 24h (p<0.0001) (Figure 14).
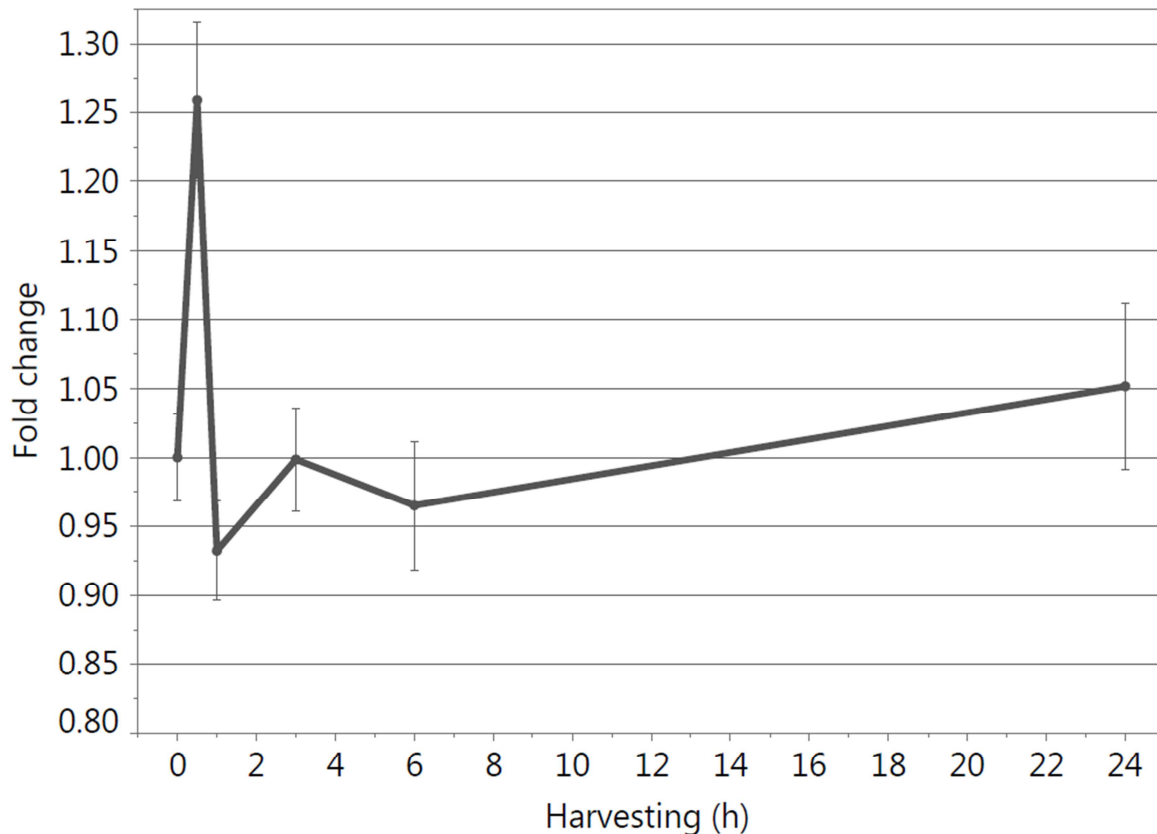

Figure 14: ROS measurement of 30min (41.4J/cm²) blue light irradiation for different harvesting times. Dots display mean values with SD.

3.3.6 30min (41.4J/cm^2) of blue light irradiation does not induce apoptosis in HaCaT cells

Fluorescence-activated cell sorting (FACS) was applied to test a possible apoptotic effect of blue light on HaCaT cells 24h after 30min (41.4J/cm²) irradiation. Cells were labeled with Annexin V, which binds to the phospholipid membrane component phosphatidylserine on the cell surface during early apoptosis and propidiumiodide which intercalates with DNA and therefore shows late apoptosis and cell necrosis. Staurosporine treated cells served as a positive control for induced apoptosis resulting in 40% living cells and 60% dead cells. Both untreated and light-treated cells exhibited a significant difference to the positive control (p<0.0001). Untreated as

well as blue light treated cells contained ~85% living cells and ~15% dead cells. Thus, that dose of blue light did not induce apoptosis in HaCaT cells (Figure 15, Figure 16).

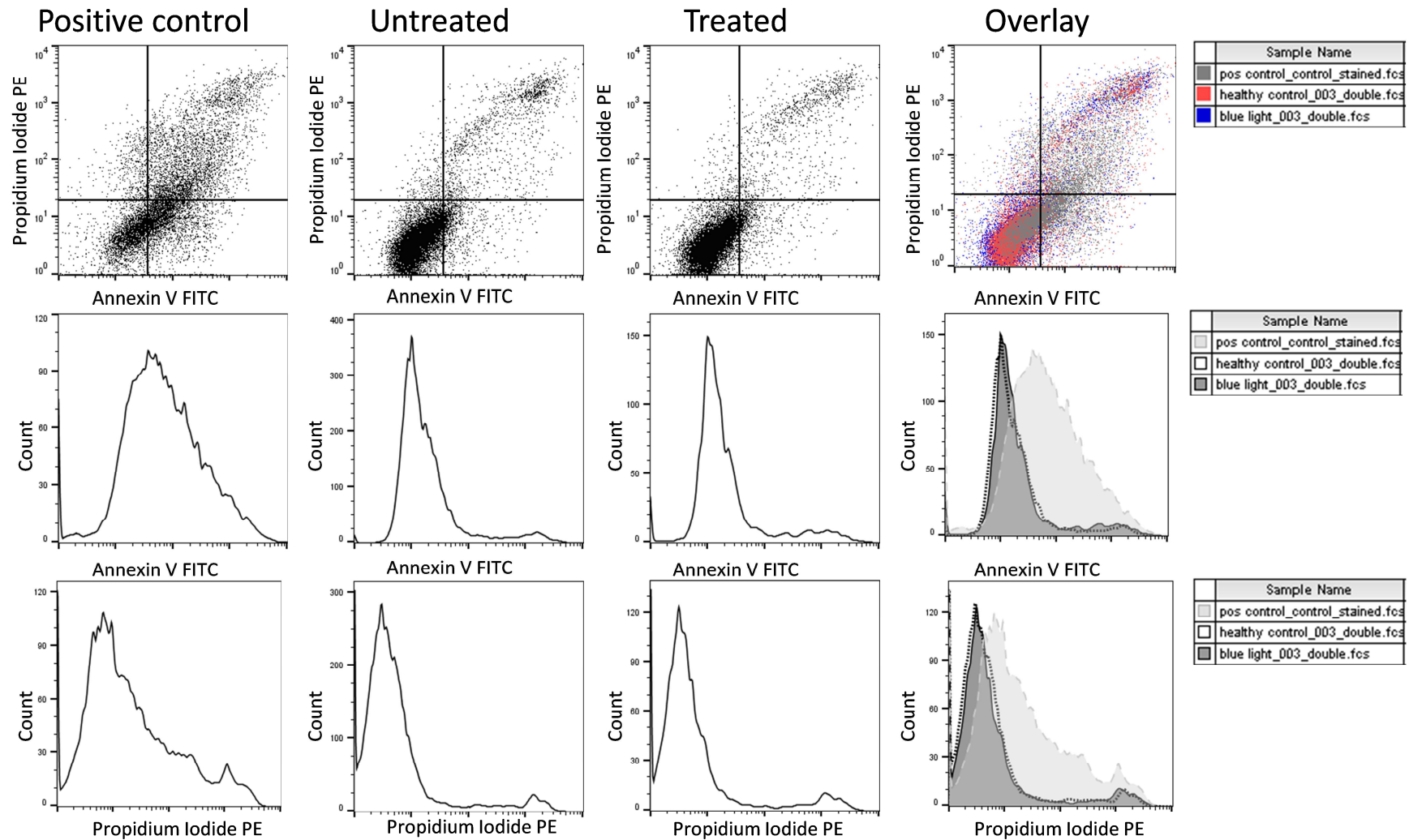Figure 15: FACS analysis 24h after 30min (41.4J/cm²) of blue light irradiation. The four quadrants can be distinguished as follows: lower left quadrant=intact cells, lower right quadrant=early apoptosis, upper right quadrant=late apoptotic or secondary necrotic apoptotic cells and upper left quadrant=primary necrotic cells. 30min (41.4J/cm²) of blue light did not induce apoptosis in HaCaT cells.

Figure 16: FACS analysis 24h after 30min (41.4J/cm²) of blue light irradiation. For comparison between live and dead cells from Figure 15 the lower left quadrant was used for the numbers of intact cells and the other three quadrants were taken together to show the amount of dead cells. There is no distinction between early or late apoptosis or necrosis. 30min (41.4J/cm²) of blue light did not induce apoptosis in HaCaT cells. Bars display mean values with SD.

3.3.7 Gene expression analysis of HaCaT cells at different time points after 30min (41.4J/cm^2) of blue light irradiation reveals a time course in photobiomodulatory blue light effects

After examining the distribution and performing batch normalization to exclude a plate effect a cluster analysis and PCA were performed. As a next step an ANOVA was

performed and already 1h after irradiation a change in gene expression could be observed. However, differentially regulated genes increased in number with increasing harvesting time after blue light irradiation from 1358 genes after 1h, to 1686 genes after 3h, to 2192 genes after 24h (Table 6 and link: uploaded data: Gene list microarrays).

Genes that stand out were cytochrome P450 family 1 subfamily A member 1 (CYP1A1) and CYP1B1, which were both highly upregulated for all three harvesting time points, with significant p-values for 3h and 24h (Figure 17).

Table 6: Significantly deregulated genes and GSEA of 30min (41.4J/cm²) blue light irradiation (Irradiation time in minutes, harvesting time in h).

Irradiation time	30min	30min	30min
Harvesting time	**1h**	**3h**	**24h**
Significant differentially expressed genes	1318	1624	2323
Significant upregulated genes	641	834	1158
Pathways containing upregulated genes	144	128	132
Significant pathways containing upregulated genes with FDR <25%	3	15	15
Significant pathways containing upregulated genes with nominal p-value <5%	7	20	18
Significant downregulated genes	677	790	1165
Pathways containing downregulated genes	136	152	148
Significant pathways containing downregulated genes with FDR <25%	0	2	0
Significant pathways containing downregulated genes with nominal p-value <5%	5	16	3

In Figure 17, the volcano plots depict the regulation of single genes after 30min (41.4J/cm²) of blue light irradiation, with values higher than 0 being up-regulated and lower values being down-regulated. The red line represents the threshold of significance showing that for example the gene encoding (CYP1A1) is regulated by blue light with significant values at 3h and 24h after irradiation.
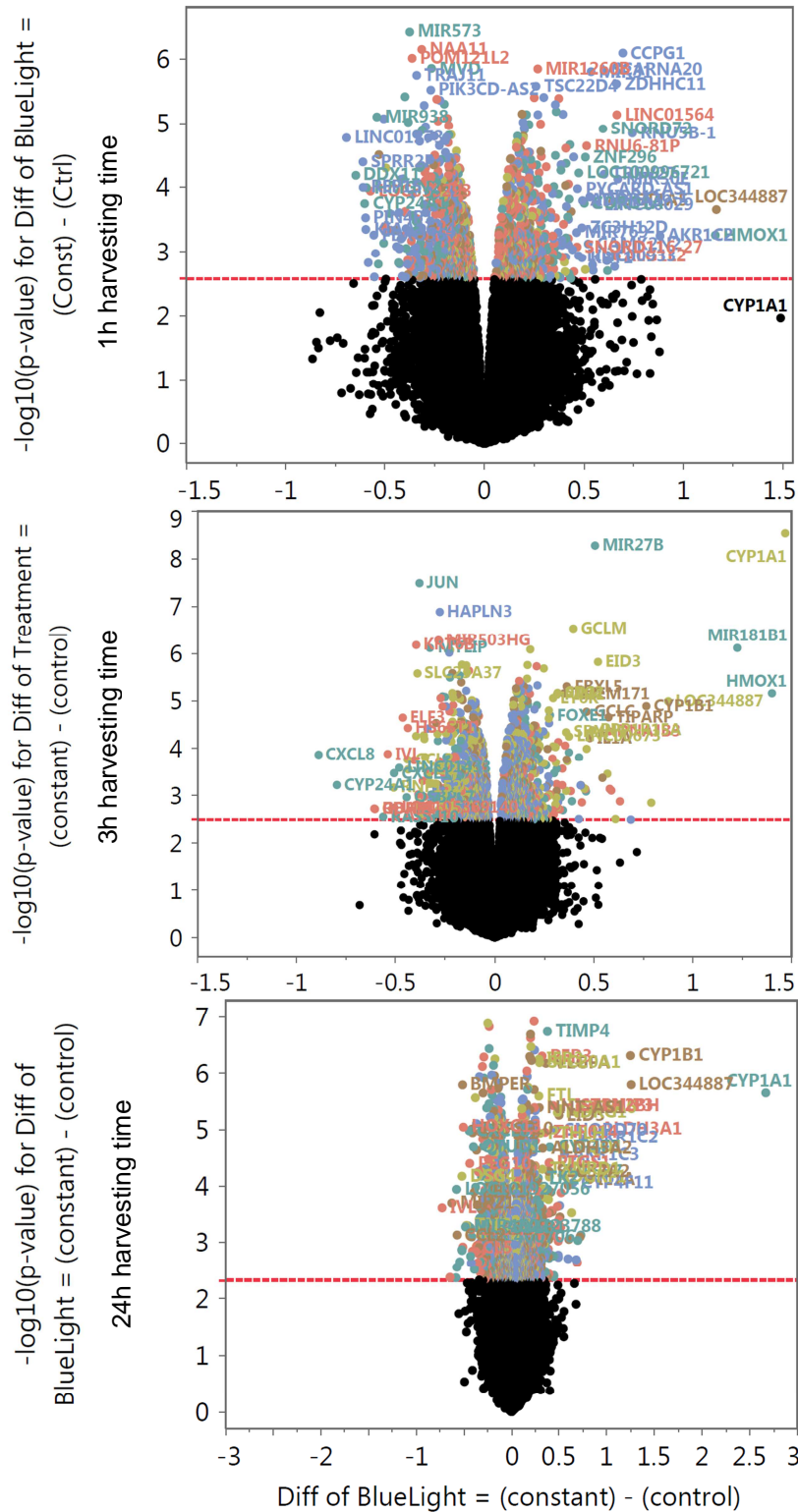

Figure 17: Gene expression analysis - volcano plot 1h, 3h and 24h after 30min (41.4J/cm²) blue light irradiation.

In a next step, gene set enrichment analysis (GSEA) was performed using Kyoto Encyclopedia of Genes and Genomes (KEGG) database (Table 7 and link: uploaded data: GSEA). Pathways containing the highest number of deregulated genes are depicted in Figure 18. Already 1h after blue light irradiation genes connected to steroid hormone biosynthesis, metabolism of xenobiotics by cytochrome P450, chemical carcinogenesis and tryptophan metabolism were upregulated. The number of genes and intensity of upregulation increased for all these pathways with time from 1h to 3h and 24h after irradiation. On the other hand, pathways containing downregulated genes that were reduced already 1h after irradiation are processes like NF-κB signaling pathway, TNF signaling pathway, T cell receptor signaling pathway and TGF-β signaling pathway. These pathways are mainly linked to inflammation and infection. For NF-κB signaling pathway and TNF signaling pathway, downregulation increased from 1h to 3h, whereas it slightly decreased for T cell receptor signaling pathway and TGF-β signaling pathway. Nevertheless, 24h after irradiation downregulation was higher for all these pathways when compared to 1h after irradiation. Although rheumatoid arthritis was slightly upregulated 1h after irradiation, the pathway was significantly downregulated 3h and 24h after irradiation. DNA replication was downregulated for 1h and 3h after blue light irradiation. Interestingly, 24h after irradiation DNA replication was slightly upregualted.

Table 7: Gene expression analysis of 30min (41.4J/cm²) blue light irradiation- time course of Normalized Enrichment Score (NES) for selected pathways for further evaluation of gene expression results.

No.	NAME	Main Category	Sub Category	30 1h NES	30 3h NES	30 24h NES
1	Arylhydrocarbon receptor (AhR) signaling pathway	1. Metabolism	1.11 Xenobiotics biodegradation and metabolism	1.09	1.95	2.24
2	Tryptophan metabolism	1. Metabolism	1.5 Amino acid metabolism	0.92	2.00	2.06
3	Steroid hormone biosynthesis	1. Metabolism	1.3 Lipid metabolism	1.31	1.85	1.97
4	Ovarian steroidogenesis	5. Organismal Systems	5.2 Endocrine system	1.25	1.70	1.92
5	Metabolism of xenobiotics by cytochrome P450	1. Metabolism	1.11 Xenobiotics biodegradation and metabolism	1.13	1.83	1.87
6	Chemical carcinogenesis	6. Human Diseases	6.1 Cancers: Overview	1.16	2.03	1.85
7	Drug metabolism - other enzymes	1. Metabolism	1.11 Xenobiotics biodegradation and metabolism	0.68	1.16	1.52
8	Glycolysis / Gluconeogenesis	1. Metabolism	1.1 Carbohydrate metabolism	0.90	0.84	1.33
9	Drug metabolism - cytochrome P450	1. Metabolism	1.11 Xenobiotics biodegradation and metabolism	1.03	1.25	1.26

10	**mTOR signaling pathway**	3. Environmental Information Processing	3.2 Signal transduction	0.71	-0.86	1.06
11	**Inflammatory mediator regulation of TRP channels**	5. Organismal Systems	5.7 Sensory system	-0.80	-1.01	1.01
12	**Circadian rhythm**	5. Organismal Systems	5.9 Environmental adaptation	-0.62	0.81	0.91
13	**Terpenoid backbone biosynthesis**	1. Metabolism	1.9 Metabolism of terpenoids and polyketides	0.78	-0.89	0.91
14	**ErbB signaling pathway**	3. Environmental Information Processing	3.2 Signal transduction	-0.82	-0.87	0.85
15	**Wnt signaling pathway**	3. Environmental Information Processing	3.2 Signal transduction	-0.99	1.17	0.85
16	**Notch signaling pathway**	3. Environmental Information Processing	3.2 Signal transduction	0.52	-0.84	0.84
17	**Mismatch repair**	2. Genetic Information Processing	2.4 Replication and repair	-0.50	-0.87	0.77
18	**VEGF signaling pathway**	3. Environmental Information Processing	3.2 Signal transduction	1.11	-0.74	0.74
19	**Citrate cycle (TCA cycle)**	1. Metabolism	1.1 Carbohydrate metabolism	0.72	-0.76	0.70
20	**DNA replication**	2. Genetic Information Processing	2.4 Replication and repair	0.39	-1.16	0.68
21	**Cell cycle**	4. Cellular Processes	4.3 Cell growth and death	-0.30	0.53	-0.52
22	**Oxidative phosphorylation**	1. Metabolism	1.2 Energy metabolism	0.93	-0.97	-0.55
23	**p53 signaling pathway**	4. Cellular Processes	4.3 Cell growth and death	0.65	0.83	-0.58
24	**RNA transport**	2. Genetic Information Processing	2.2 Translation	-0.79	-0.91	-0.59
25	**Steroid biosynthesis**	1. Metabolism	1.3 Lipid metabolism	-1.07	-1.19	-0.64
26	**AMPK signaling pathway**	3. Environmental Information Processing	3.2 Signal transduction	-0.86	-0.88	-0.68
27	**RNA degradation**	2. Genetic Information Processing	2.3 Folding, sorting and degradation	-0.76	-1.16	-0.73
28	**Estrogen signaling pathway**	5. Organismal Systems	5.2 Endocrine system	-0.92	-0.83	-0.79
29	**Longevity regulating pathway**	5. Organismal Systems	5.9 Aging	-0.72	-0.82	-0.79
30	**Protein processing in endoplasmic reticulum**	2. Genetic Information Processing	2.3 Folding, sorting and degradation	-0.47	0.52	-0.80
31	**cAMP signaling pathway**	3. Environmental Information Processing	3.2 Signal transduction	0.72	1.06	-0.82
32	**Longevity regulating pathway**	5. Organismal Systems	5.9 Aging	-0.90	-1.12	-0.84
33	**NOD-like receptor signaling pathway**	5. Organismal Systems	5.1 Immune system	0.94	-1.71	-0.90
34	**Regulation of lipolysis in adipocytes**	5. Organismal Systems	5.2 Endocrine system	-0.82	-0.74	-0.90
35	**Ras signaling pathway**	3. Environmental Information Processing	3.2 Signal transduction	-0.71	-0.85	-0.91
36	**Phototransduction**	5. Organismal Systems	5.7 Sensory system	-0.81	1.24	-0.92
37	**Apoptosis - multiple**	4. Cellular Processes	4.3 Cell growth and death	0.97	-1.35	-0.95

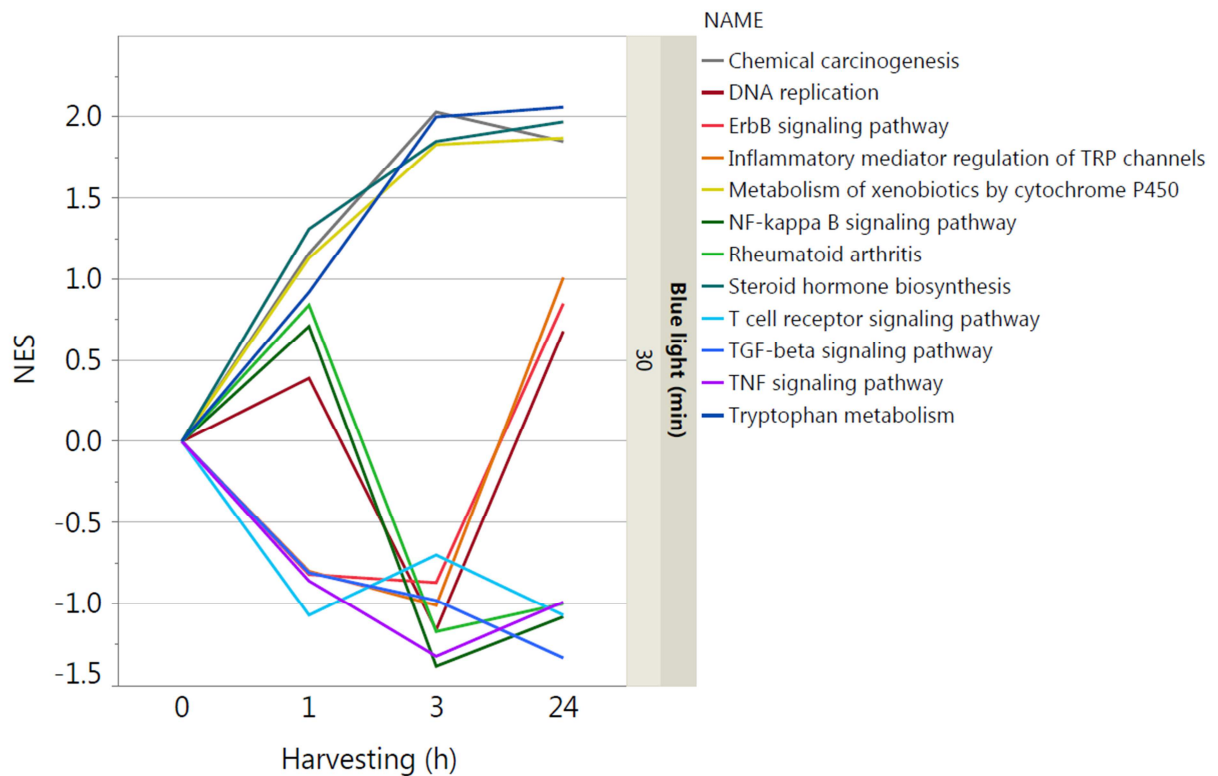|	**species**					
38	**Toll-like receptor signaling pathway**	5. Organismal Systems	5.1 Immune system	-0.81	-1.25	-0.96
39	**Cell adhesion molecules (CAMs)**	3. Environmental Information Processing	3.3 Signaling molecules and interaction	-0.93	0.84	-0.98
40	**PI3K-Akt signaling pathway**	3. Environmental Information Processing	3.2 Signal transduction	0.75	0.82	-0.99
41	**TNF signaling pathway**	3. Environmental Information Processing	3.2 Signal transduction	-0.86	-1.32	-0.99
42	**Rheumatoid arthritis**	6. Human Diseases	6.3 Immune diseases	0.84	-1.17	-1.00
43	**Pertussis**	6. Human Diseases	6.8 Infectious diseases: Bacterial	0.81	-1.15	-1.01
44	**Apoptosis**	4. Cellular Processes	4.3 Cell growth and death	-0.59	-1.03	-1.02
45	**Chemokine signaling pathway**	5. Organismal Systems	5.1 Immune system	-1.28	-1.07	-1.03
46	**Jak-STAT signaling pathway**	3. Environmental Information Processing	3.2 Signal transduction	0.82	1.13	-1.03
47	**Calcium signaling pathway**	3. Environmental Information Processing	3.2 Signal transduction	-0.85	1.32	-1.04
48	**T cell receptor signaling pathway**	5. Organismal Systems	5.1 Immune system	-1.07	-0.70	-1.07
49	**NF-kappa B signaling pathway**	3. Environmental Information Processing	3.2 Signal transduction	0.71	-1.38	-1.08
50	**Circadian entrainment**	5. Organismal Systems	5.9 Environmental adaptation	-0.91	-0.92	-1.11
51	**B cell receptor signaling pathway**	5. Organismal Systems	5.1 Immune system	-0.85	0.90	-1.12
52	**FoxO signaling pathway**	3. Environmental Information Processing	3.2 Signal transduction	-0.88	-0.91	-1.12
53	**MAPK signaling pathway**	3. Environmental Information Processing	3.2 Signal transduction	-0.87	0.87	-1.16
54	**Rap1 signaling pathway**	3. Environmental Information Processing	3.2 Signal transduction	0.91	-1.10	-1.20
55	**Primary immunodeficiency**	6. Human Diseases	6.3 Immune diseases	0.74	-0.64	-1.27
56	**TGF-beta signaling pathway**	3. Environmental Information Processing	3.2 Signal transduction	-0.81	-0.98	-1.33
57	**Melanoma**	6. Human Diseases	6.2 Cancers: Specific types	-0.76	-0.68	-1.38

Figure 18: Gene expression analysis of 30min (41.4J/cm²) blue light irradiation - time course of NES for selected pathways for further evaluation of gene expression results.

3.3.8 Gene expression analysis reveals upregulation of aryl hydrocarbon receptor target genes

CYP1A1 and CYP1B1 were both highly upregulated for all three harvesting time points leading to the identification of a possible functionality of their transcription factor aryl hydrocarbon receptor (AHR) after blue light irradiation. Tryptophan metabolism and chemical carcinogenesis are both pathways containing significantly upregulated genes and are connected to AHR. As KEGG does not provide such a pathway, an AHR pathway was designed (Figure 19) using a literature search containing inter alia the "AHR battery genes" CYP1A1, CYP1A2, CYP1B1, aldehyde dehydrogenase 3 family member a1 (ALDH3A1), NAD(P)H quinone oxidoreductase 1 (NQO1), UDP glucuronosyltransferase 1 family, polypeptide A (UGT1A), glutathione S-transferase 1 (GSTA1) and genes encoding AHR and its contributors aryl hydrocarbon receptor nuclear translocator (ARNT) and aryl hydrocarbon receptor repressor (AHRR). Additionally, genes deregulated downstream after AHR activation like cyclin-dependent kinase inhibitor 1B (CDKN1B, also KIP1), nuclear factor erythroid 2 like 2 (Nrf2, also NFE2L2) and tumor necrosis factor (TNF-a) receptor-associated protein (TRADD) are depicted. The AHR signaling pathway (Figure 20)

44

was upregulated for all three time points with p=0.242 after 1h, p=0.004 after 3h and p<0.0001 24h after blue light irradiation. The time course of the gene expression analysis for these mentioned genes is illustrated in Figure 21 and Table 8 to help describing that AHR is a possible target for blue light irradiation as explained in the discussion.

CYP1A1, CYP1B1, ALDH3A1, NQO1 and UGT1A5 were upregulated already 1h after blue light irradiation, which was stable up to 3h. CYP1A1, CYP1B1 ALDH3A1 and NQO1 showed an even higher upregulation in gene expression 24h after irradiation, whereas UGT1A kept the same level (Figure 21). AHRR was considerably upregulated 3h after blue light irradiation, while CDKN1B was upregulated after 1h and 3h, but downregulated 24h after irradiation. CYP1A2 was alternating from downregulation after 1h to upregulation after 3h and not regulated after 24h. GSTA1 was not considerably regulated, whereas NFE2L2 (Nrf2) was upregualted after 3h and 24h. TRADD was downregulated for all three time points with a maximum after 3h.
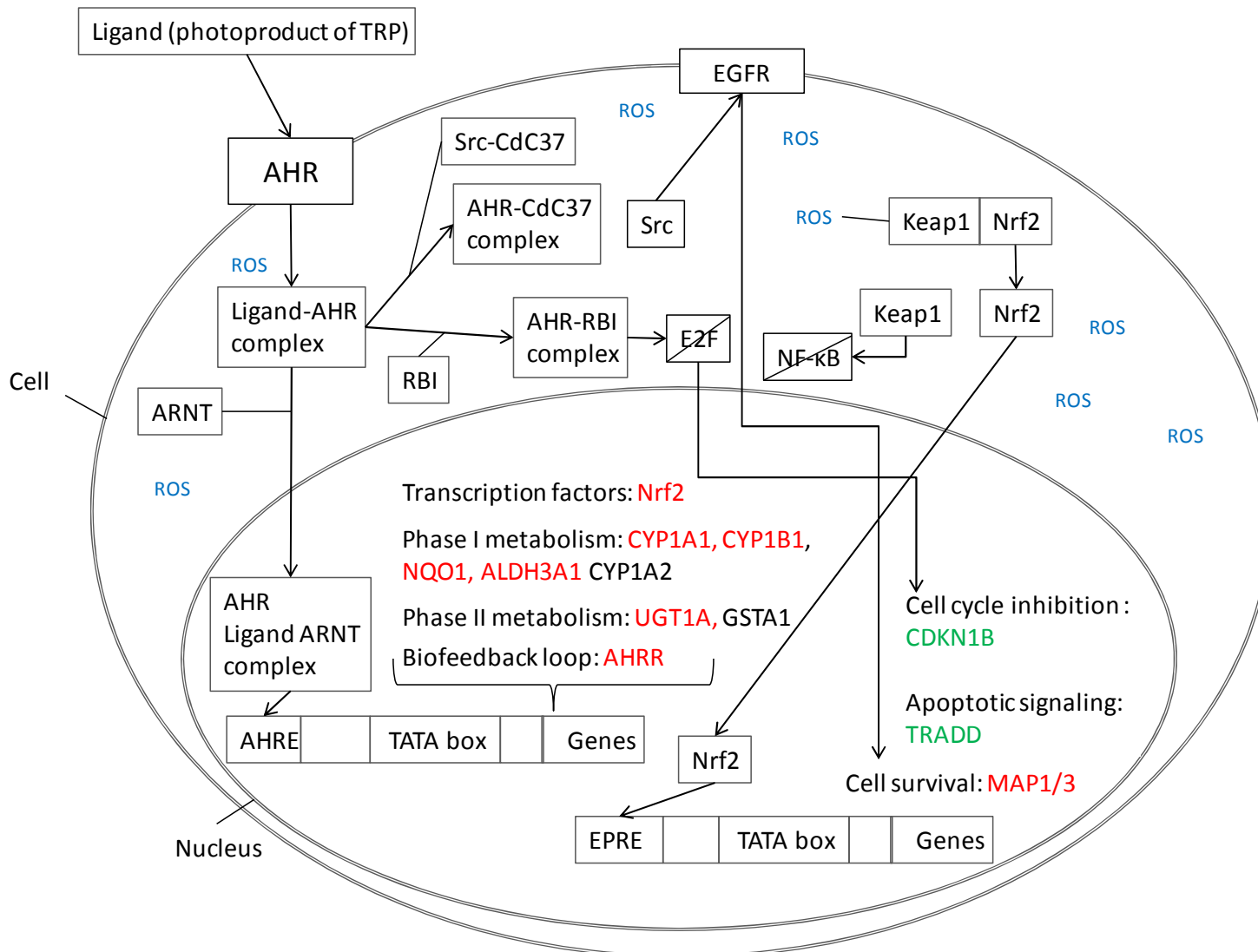
Figure 19: Aryl Hydrocarbon Receptor (AHR) signaling pathway for 30min (41.4J/cm²) blue light irradiation and 24h harvesting time. Red: upregulated gene expression after AHR activation, green: downregulated gene expression after AHR activation
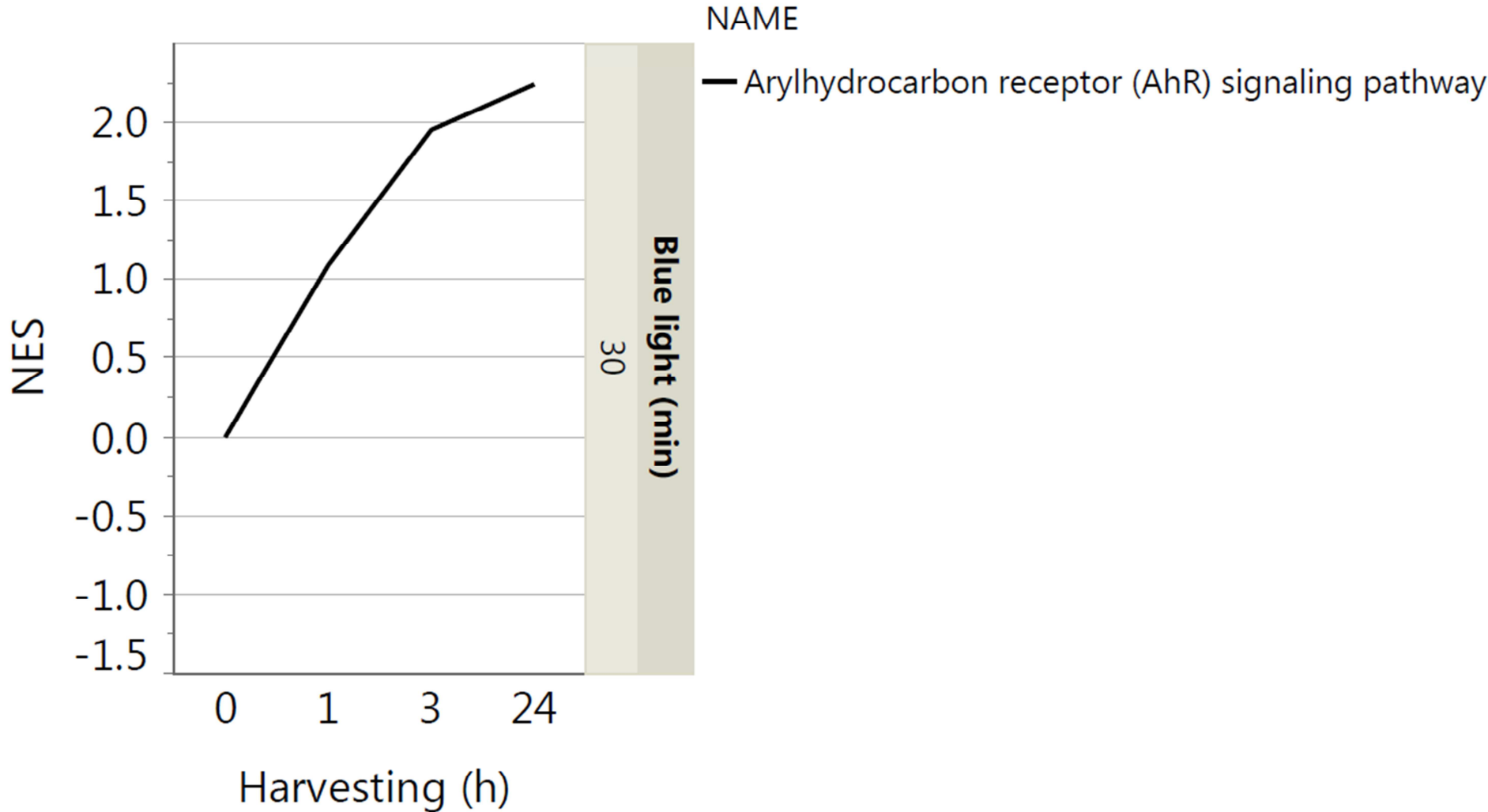
Figure 20: Gene expression analysis of 30min (41.4J/cm²) blue light irradiation - time course of the Aryl Hydrocarbon Receptor (AHR) signaling pathway.

Table 8: Gene expression analysis of 30min (41.4J/cm²) blue light irradiation - time course of selected AHR inducible genes for further evaluation of gene expression results.

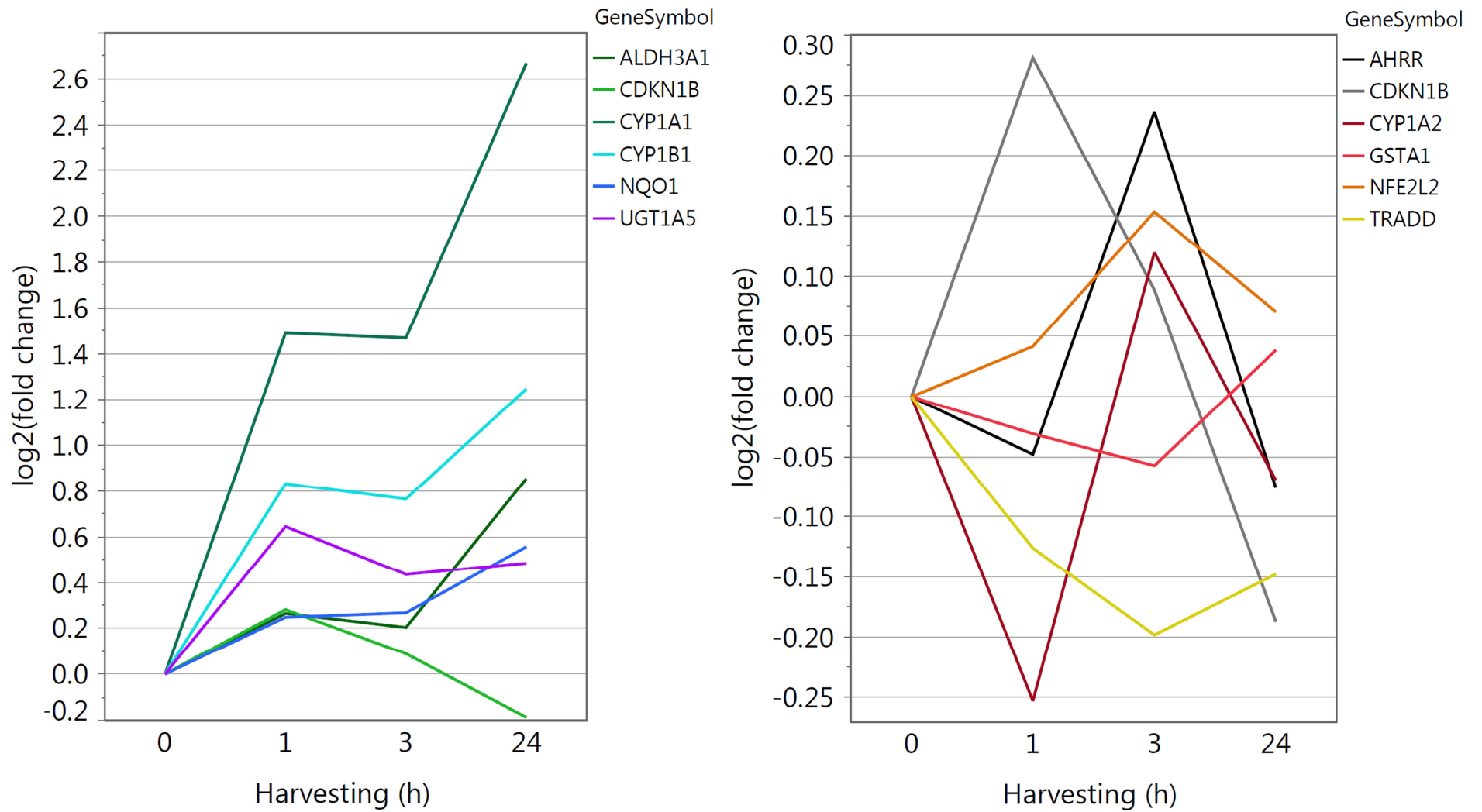| Gene name	30min 1h log$_2$(fold change)	30min 1h -log$_{10}$(p-value)	30min 1h Adjusted p-value	30min 3h log$_2$ (fold change)	30min 3h -log$_{10}$(p-value)	30min 3h Adjusted p-value	30min 24h log$_2$(fold change)	30min 24h -log$_{10}$(p-value)	30min 24h Adjusted p-value
AHR	-0.01	0.092	0.904	-0.01	0.129	0.875	0.06	1.918	0.086
AHRR	-0.05	0.206	0.796	0.24	1.788	0.118	-0.08	0.588	0.489
ALDH3A1	0.26	1.797	0.128	0.20	1.122	0.264	0.85	5.006	0.002
CDKN1B	0.28	1.724	0.139	0.09	0.687	0.453	-0.19	2.411	0.045
CYP1A1	1.49	1.962	0.105	1.47	8.539	0.000	2.67	5.654	0.001
CYP1A2	-0.25	1.812	0.126	0.12	0.984	0.315	-0.07	0.600	0.480
CYP1B1	0.83	2.403	0.062	0.77	4.890	0.004	1.25	6.312	0.001
GSTA1	-0.03	0.098	0.900	-0.06	2.270	0.065	0.04	0.576	0.495
NFE2L2	0.04	0.884	0.357	0.15	1.298	0.212	0.07	1.529	0.142
NQO1	0.25	1.208	0.247	0.27	3.982	0.010	0.56	4.687	0.003
TRADD	-0.13	2.873	0.036	-0.20	0.995	0.310	-0.15	0.955	0.299
UGT1A5	0.64	3.784	0.0153	0.44	3.207	0.021	0.49	1.541	0.140
ERK1	0.08	1.105	0.277	0.010	0.106	0.899	0.07	1.394	0.168

Figure 21: Gene expression analysis of 30min (41.4J/cm²) blue light irradiation - time course of selected AHR inducible genes for further evaluation of gene expression results.

3.3.9 Verification of genes from chips with qPCR

To confirm microarray results, genes were selected for real time PCR (qPCR). Criteria for selection were pathways with high normalized enrichment scores (NES) and/or fold changes of specific genes and connection to AHR signaling pathway. qPCRs were performed with RNA samples from harvesting time 24h after 30min of blue light irradiation, which were beforehand used for gene expression analysis. qPCR results match with the previously obtained gene expression results with CYP1A1, CYP1B1, ALDH3A1, NQO1 and UGT1A being significantly upregulated and FBJ murine osteosarcoma viral oncogene homolog (FOS), interleukin 8 (IL8) and keratin 5 (Krt5) being significantly downregulated (Figure 22).
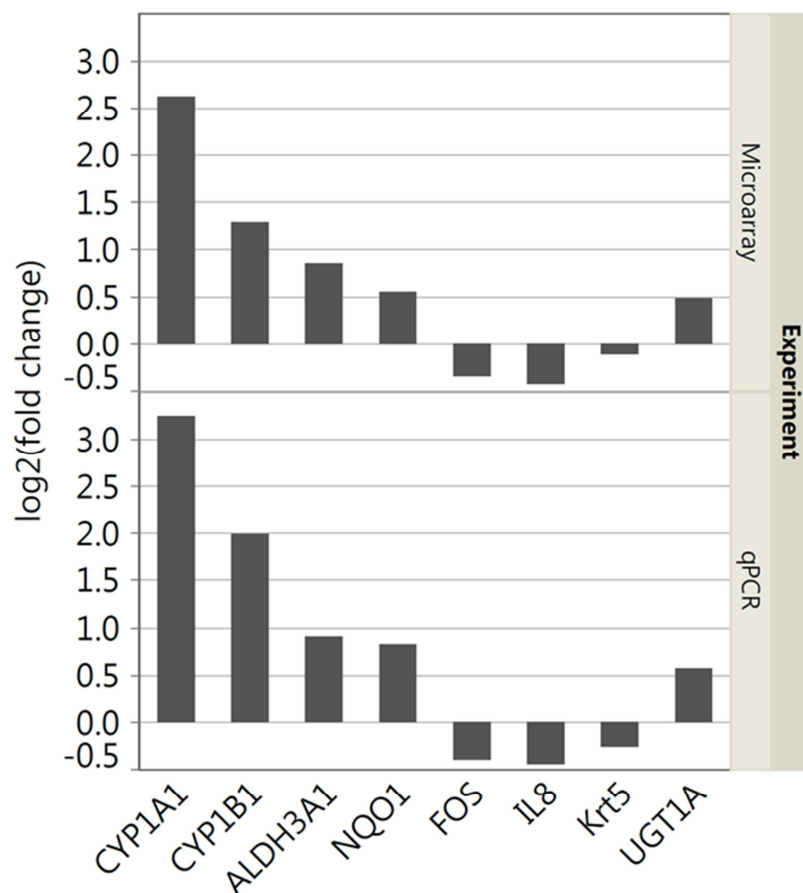

Figure 22: qPCR of selected genes verifies gene expression analysis results.

3.4 Proliferative phase of blue light irradiation - 7.5min (10.35J/cm²) blue light irradiation

3.4.1 Irradiation with 7.5min (10.35J/cm²) of blue light does significantly increase the metabolism of HaCaT cells

Cell metabolism of HaCaT cells was investigated at different harvesting times after blue light irradiation with 7.5min (10.35J/cm²). A fast increase of metabolism by 19% was achieved 1h after irradiation ($p<0.0001$). Compared to the no light control, 3h after irradiation cell metabolism was increased by 4% ($p<0.0001$), 2% ($p<0.0001$) after 6h and 1% ($p<0.0001$) after 12h. The irradiation resulted in an increase of metabolism by 12% ($p<0.0001$) 24h after blue light irradiation and attenuated to an increase of 2% ($p<0.0001$) after 48h and 4% ($p<0.0001$) after 72h (Figure 23).
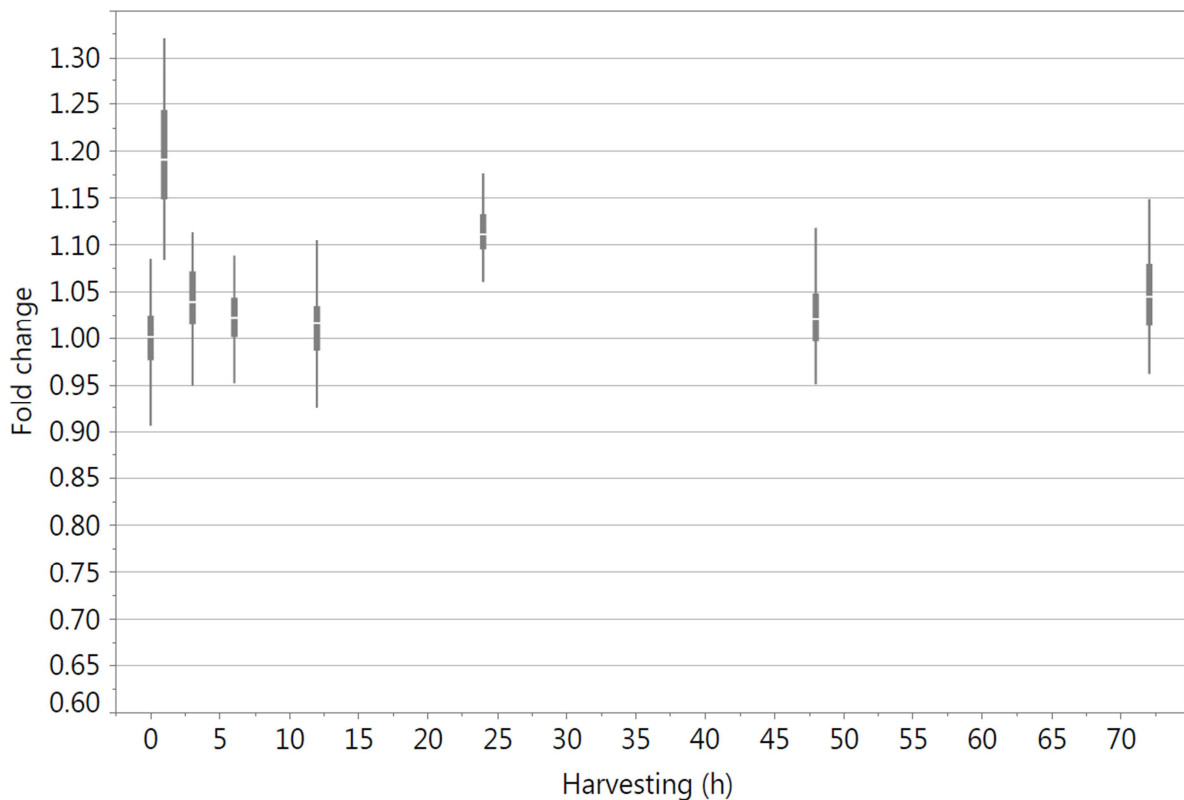

Figure 23: XTT results of different time points of harvesting after 7.5min (10.35J/cm²) blue light irradiation. (For legend see Figure 9).

3.4.2 Consecutive irradiations with 7.5min (10.35J/cm²) of blue light each 24h lead to an increase in metabolism for one and two consecutive irradiations, followed by a decrease for the third irradiation in HaCaT cells

As the proliferative effect decreased 48h after blue light irradiation (Figure 23) consecutive irradiations with 7.5min (10.35J/cm²) of blue light were performed each 24h. When irradiated twice, metabolism of HaCaT cells was not significantly different from the single irradiation of 12% (p=0.058) with a 10% increase of metabolism (significant when compared to the no light control (p<0.0001)); however, after three consecutive irradiations metabolism of irradiated cells was decreasing by 7% (p<0.0001) compared to the no-light control cells (Figure 24).
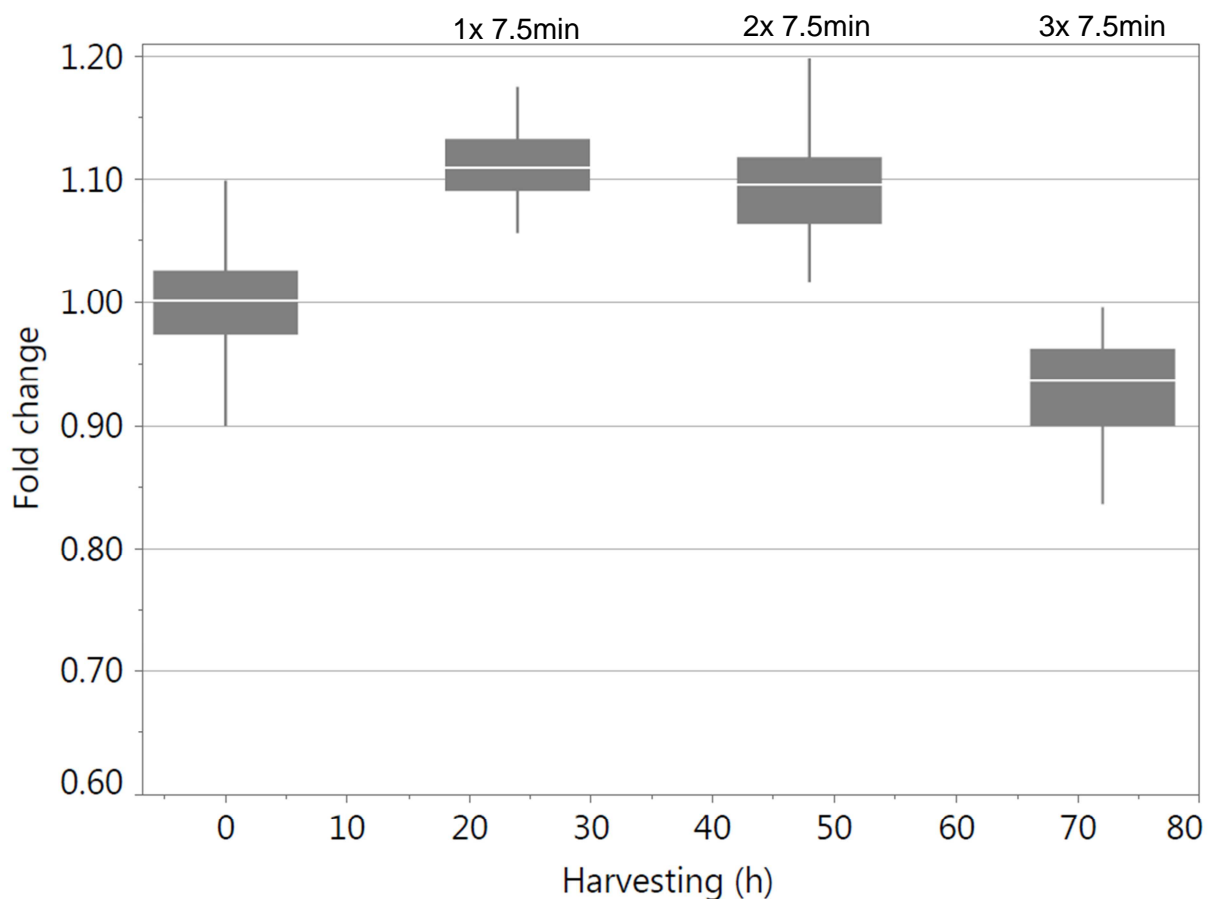

Figure 24: XTT test results of the different numbers of 7.5min (10.35J/cm²) blue light irradiations 24h after the last irradiation. (For legend see Figure 9).

3.4.3 Consecutive irradiations with 7.5min (10.35J/cm²) of blue light each 24h lead to an increase in proliferation for one and two consecutive irradiations, followed by a decrease for the third irradiation in HaCaT cells

Cell counting and BrdU ELISA of HaCaT cells were conducted at different harvesting times after 7.5min (10.35J/cm²) of blue light irradiation to examine the time course of the anti-proliferative effect of this dose. As the doubling time of HaCaT cells is 24h, an effect on cell proliferation was not expected before 24h after irradiation and therefore fits to cell counting results. An increase in cell number of 8% (p=0.2265) was induced 24h after irradiation. The effect was decreasing with two consecutive irradiations each 24h with 15% (p=0.1169) 48h after irradiation, to 25% (p=0.0562) 72h after irradiation.

BrdU was tested for 24h, 48h and 72h harvesting. The extend of BrdU ELISA was less than for cell counting results, however depicted a corresponding proliferative result with increase in cell proliferation of 7% (p<0.001) 24h after irradiation and no effect with two and three consecutive irradiations (Figure 25).
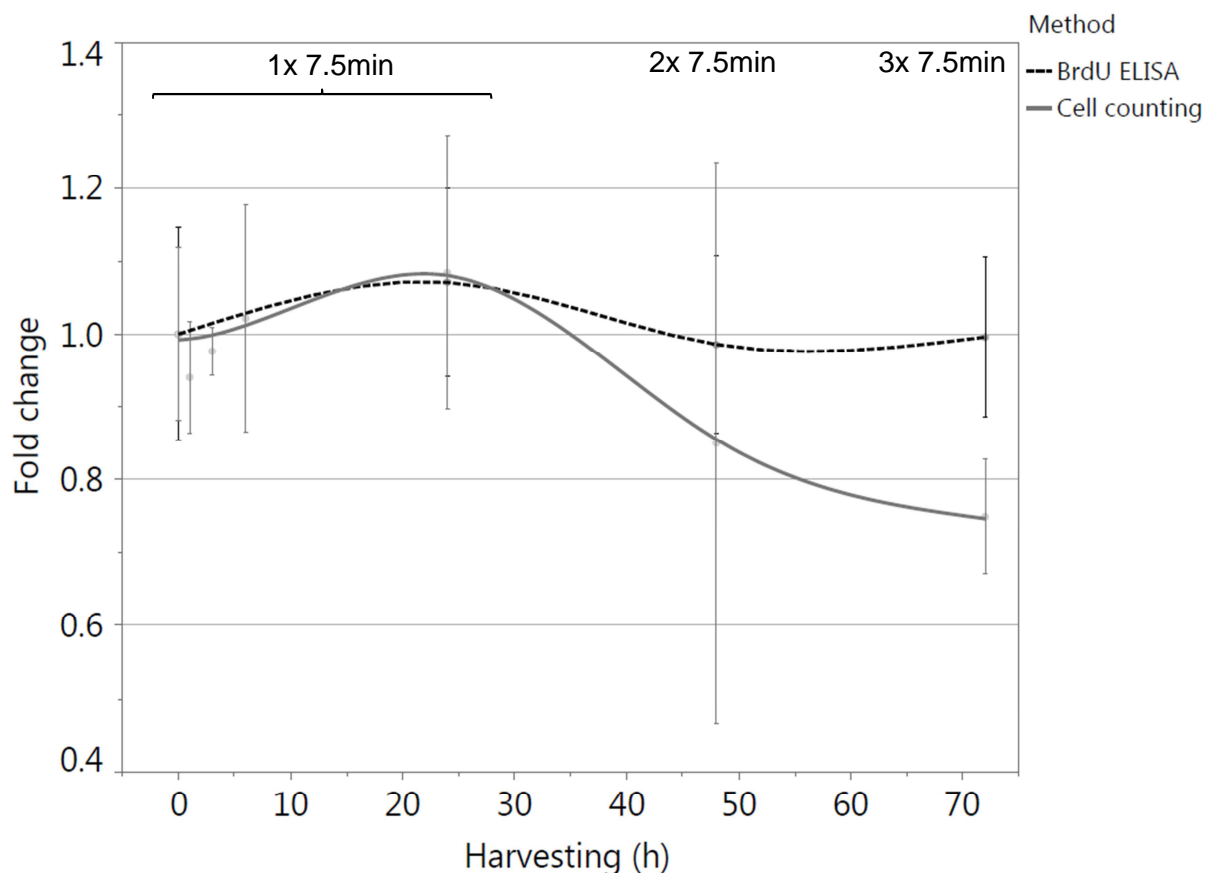

Figure 25: Cell count and BrdU ELISA at the different time points of cell harvesting: 1h, 3h, 6h, 12, 24h, 48h and 72h after different numbers of 7.5min (10.35J/cm²) of blue light irradiation. Dots display mean values with SD.

3.4.4 Consecutive irradiations with 7.5min (10.35J/cm²) of blue light each 24h induce a change in cell cycle phase proportion of HaCaT cells leading to an increase in S-phase cells for one and two consecutive irradiations, followed by a decrease for the third irradiation

To test the cell cycle phase proportion of HaCaT cells after 7.5min (10.35J/cm²) of blue light irradiation immunofluorescent BrdU staining was used in combination with 7-AAD, which binds to total DNA. The shift in cell cycles phases was not significant, however, already 24h after irradiation a slight shift of cell proportion from G_0/G_1 to S-phase (1% (p=0.8211)) was observed, which increased after two consecutive irradiations each 24h to 2% (p=0.4033) 48h after irradiation. However, it shifted back from S-phase to G_0/G_1 to -2% (p=0.5152) S-phase cells 72h after irradiation (Figure 26).
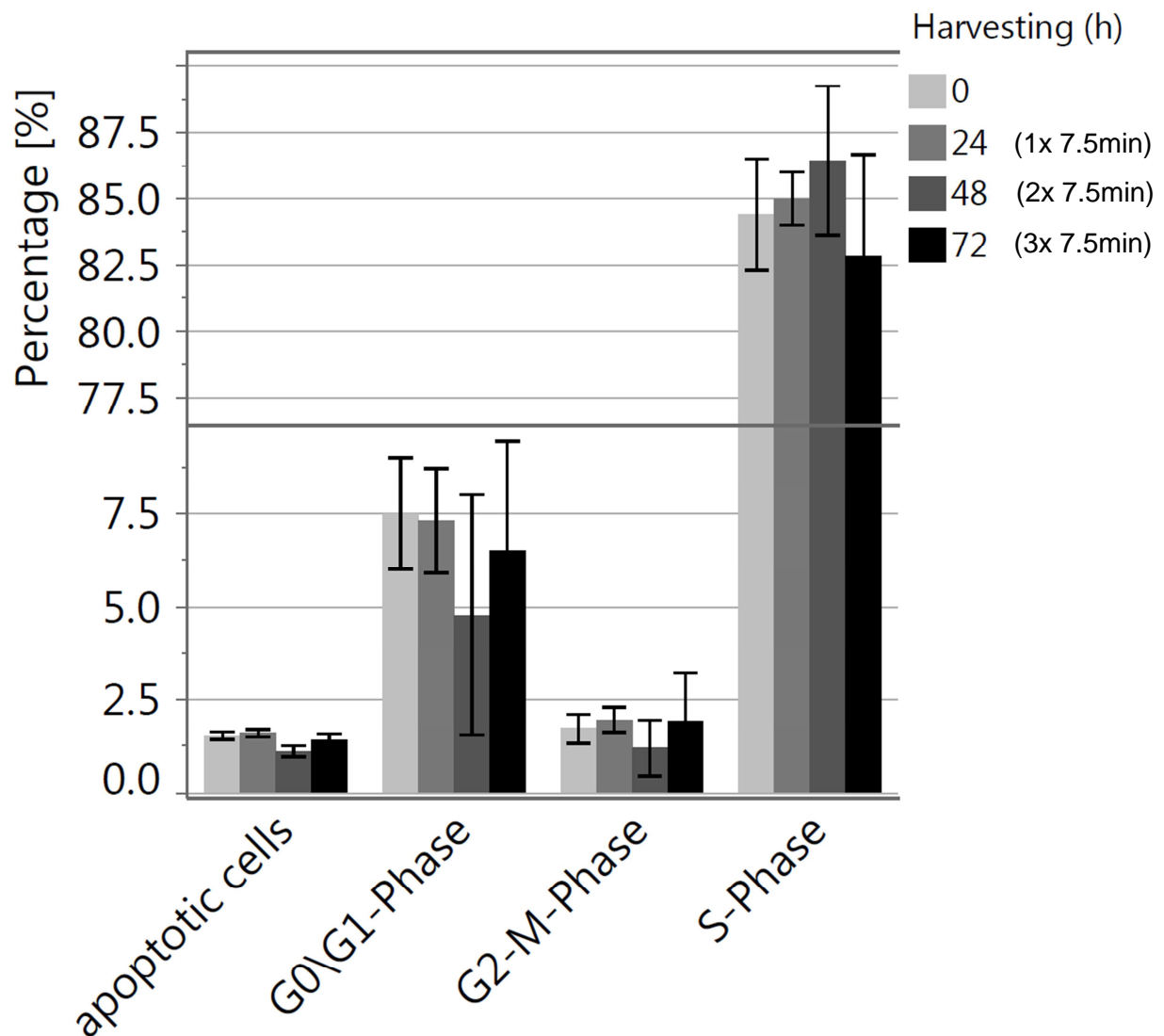

Figure 26: BrdU FACS results of the different numbers of 7.5min (10.35J/cm²) blue light irradiations harvested 24h after the respective last irradiation. Bars display mean values with SD.

3.4.5 7.5min ($10.35J/cm^2$) of blue light irradiation increases H_2O_2 concentration in HaCaT cells immediately after irradiation

H_2O_2 concentrations were measured in HaCaT cells at different time points after 7.5min ($10.35J/cm^2$) blue light irradiation, with a first time point at 30min according to incubation time of the reagent AmplexUltraRed. A high increase of H_2O_2 was noted 30min after blue light irradiation with 184% more H_2O_2 compared to the no light control cells ($p<0.0001$) followed by 59% ($p<0.0001$) 52.5min after irradiation. However, the effect could be balanced by the cells to a normal level already 1h after irradiation (0.9% after 1h ($p=0.7622$), -3% after 3h ($p=0.5511$), -11% after 6h ($p=0.0157$), 2% after 24h ($p=0.6351$)) (Figure 27).
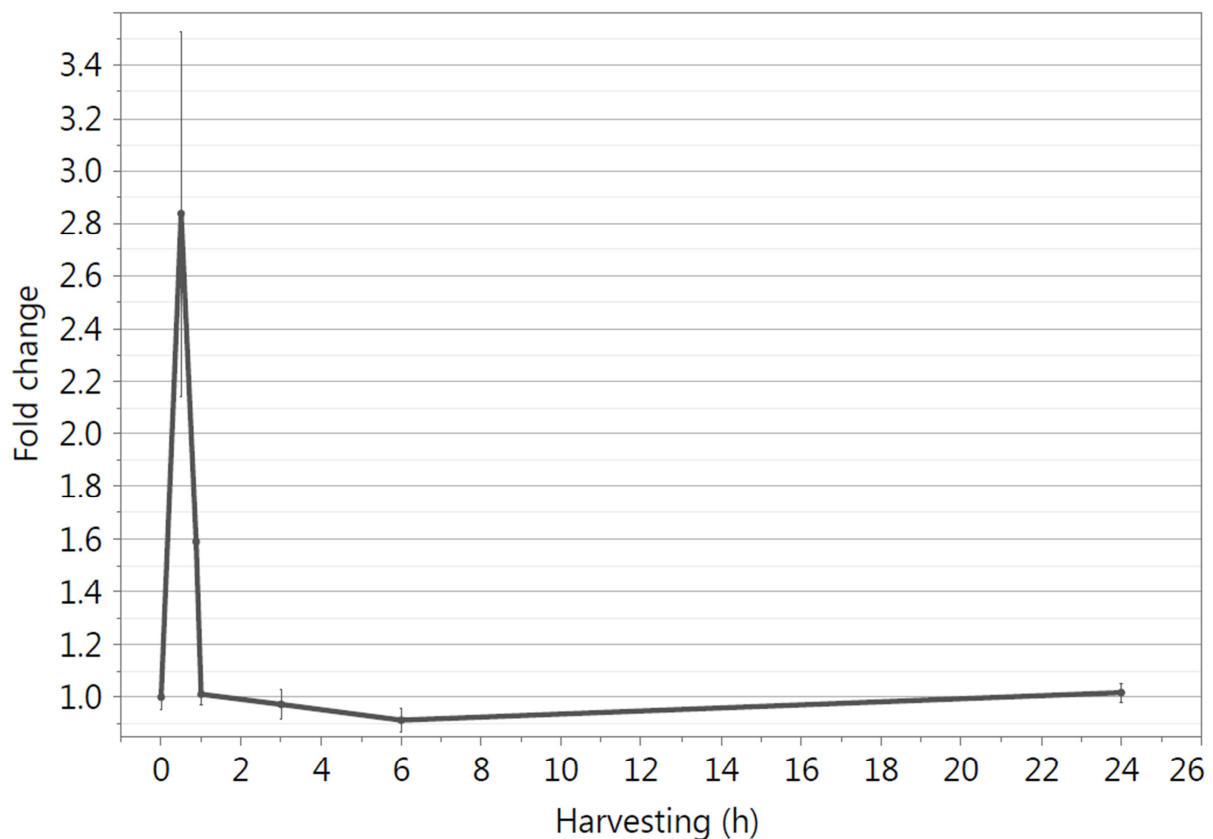

Figure 27: ROS measurement of 7.5min ($10.35J/cm²$) blue light irradiation for different harvesting times. Dots display mean values with SD.

3.4.6 7.5min (10.35J/cm^2) of blue light irradiation does not induce apoptosis in HaCaT cells

Fluorescence-activated cell sorting (FACS) was applied to test a possible apoptotic effect of blue light on HaCaT cells 24h after 7.5min (10.35J/cm²) irradiation. Staurosporine treated cells served as a positive control for induced apoptosis resulting in 40% living cells and 60% dead cells. Both untreated and light-treated cells exhibited a significant difference to the positive control (p=0.0165 for treated, p=0.0104 for untreated). Untreated as well as blue light treated cells contained ~75% living cells and ~25% dead cells. Thus, that dose of blue light did not induce apoptosis in HaCaT cells (Figure 28, Figure 29).

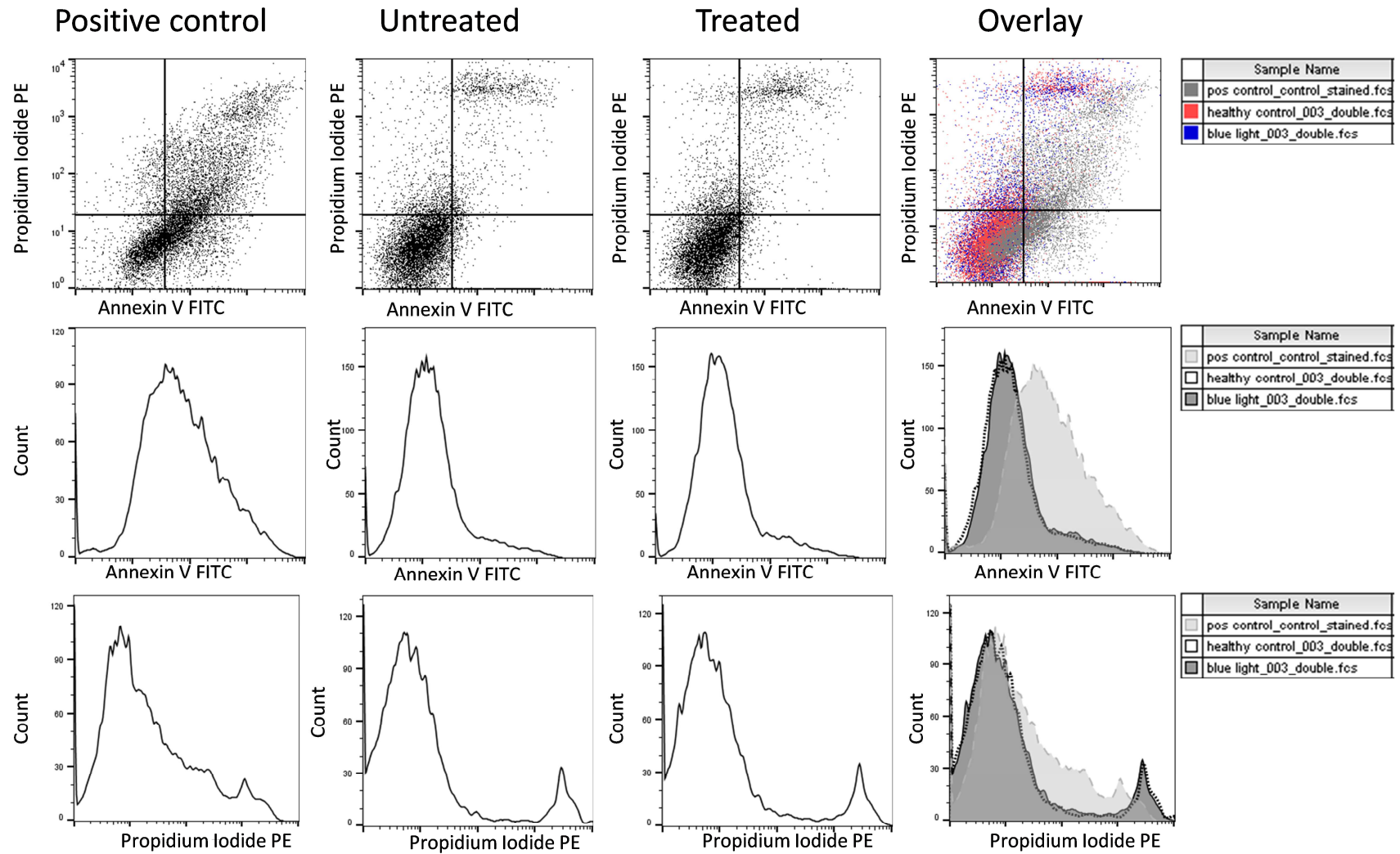Figure 28: FACS analysis 24h after 7.5min (10.35J/cm²) of blue light irradiation. The four quadrants can be distinguished as follows: lower left quadrant=intact cells, lower right quadrant=early apoptosis, upper right quadrant=late apoptotic or secondary necrotic apoptotic cells and upper left quadrant=primary necrotic cells. 7.5min (10.35J/cm²) of blue light did not induce apoptosis in HaCaT cells.

Figure 29: FACS analysis 24h after 7.5min (10.35J/cm²) of blue light irradiation. For comparison between live and dead cells from Figure 28 the lower left quadrant was used for the numbers of intact cells and the other three quadrants were taken together to show the amount of dead cells. There is no distinction between early or late apoptosis or necrosis. 7.5min (10.35J/cm²) of blue light did not induce apoptosis in HaCaT cells. Bars display mean values with SD.

3.4.7 Gene expression analysis of HaCaT cells at different time points after 7.5min (10.35J/cm^2) reveals the time course of photobiomodulatory blue light effect and upregulation of aryl hydrocarbon receptor target genes

After examining the distribution and performing batch normalization to exclude a plate effect a cluster analysis and PCA were performed. As a next step an ANOVA was

performed. Already 1h after irradiation a change in gene expression can be observed with 1137 genes significantly differentially expressed. 3h after irradiation the number of significantly differentially expressed genes decreased to 888. However, the number increased again and reached its maximum 24h after irradiation with 1292 significantly differentially expressed genes (Table 9).

Table 9: Significantly deregulated genes and GSEA of 7.5min (10.35J/cm²) blue light irradiation (Irradiation time in minutes, harvesting time in h).

Irradiation time	7.5min	7.5min	7.5min
Harvesting time	1h	3h	24h
Significant differentially expressed genes	1137	888	1292
Significant upregulated genes	477	430	668
Pathways containing upregulated genes	110	144	168
Significant pathways containing upregulated genes with FDR <25%	0	0	4
Significant pathways containing upregulated genes with nominal p-value <5%	3	10	16
Significant downregulated genes	660	485	624
Pathways containing downregulated genes	170	136	112
Significant pathways containing downregulated genes with FDR <25%	1	0	0
Significant pathways containing downregulated genes with nominal p-value <5%	19	3	5

In Figure 30 the volcano plots depict the regulation of single genes after 7.5min (10.35J/cm²) of blue light irradiation, with values higher than 0 being up-regulated and lower values being down-regulated. The red line represents the threshold of significance showing that for example the gene encoding (CYP1A1) is significantly upregulated by blue light 24h after irradiation.
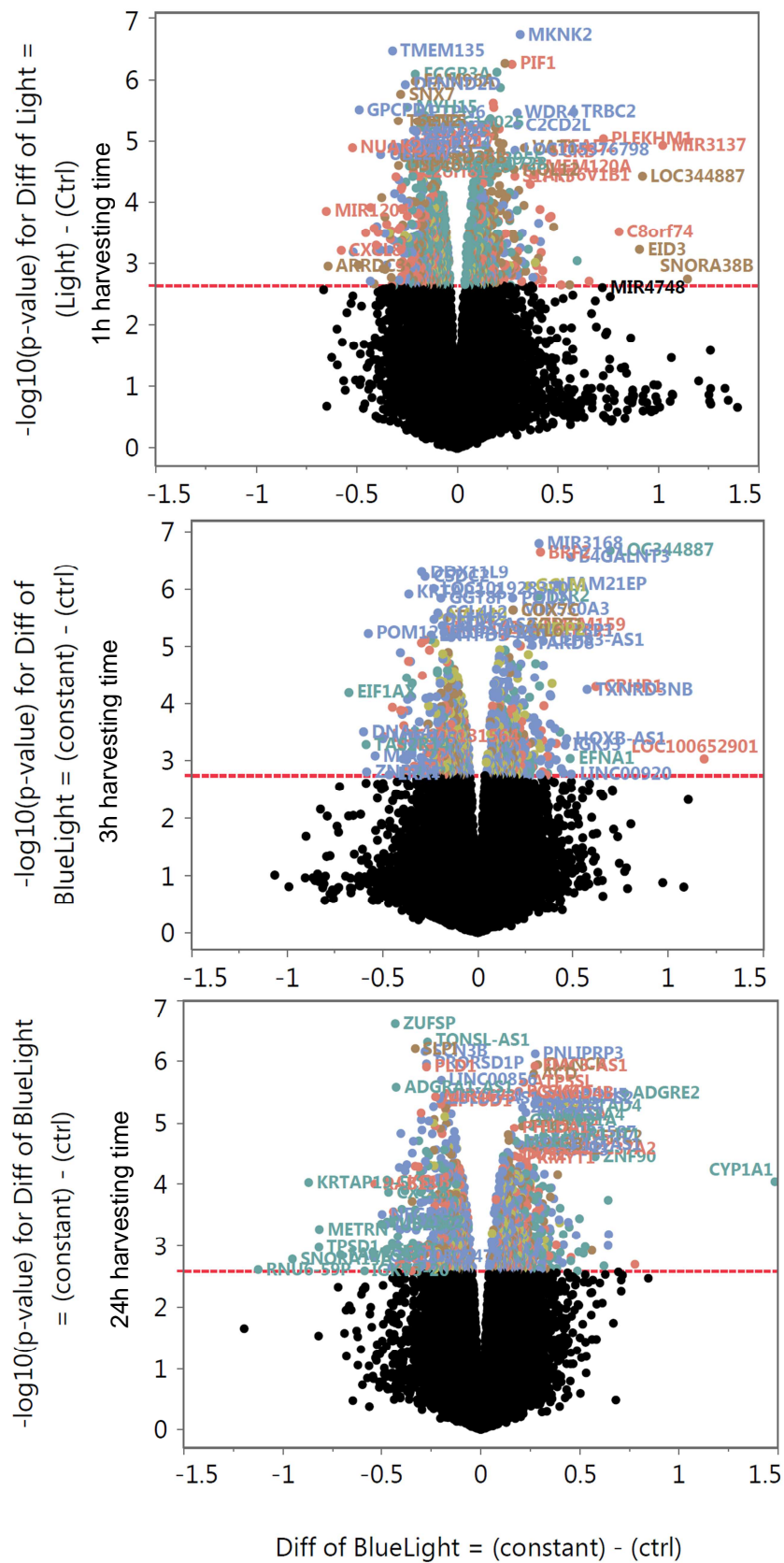
Figure 30: Gene expression analysis of 7.5min (10.35J/cm²) blue light irradiation - volcano plot 1h, 3h and 24h after blue light irradiation.

Using KEGG database a GSEA was performed (Table 9 and Table 10). To compare the proliferative phase of the dose response curve induced by PBM with blue light with the anti-proliferative phase, pathways, which were previously described in Becker et al. 2016 [59] and additionally are highly deregulated after 7.5min (10.35J/cm²) blue light irradiation and/or connected to the AHR signaling pathway, are depicted in Figure 31.

Table 10: Gene expression analysis of 7.5min (10.35J/cm²) blue light irradiation - time course of NES for selected pathways for further evaluation of gene expression results.

No.	NAME	Main Category	Sub Category	7.5 1h NES	7.5 3h NES	7.5 24h NES
1	Ovarian steroidogenesis	5. Organismal Systems	5.2 Endocrine system	1.04	0.95	1.92
2	Steroid hormone biosynthesis	1. Metabolism	1.3 Lipid metabolism	1.27	-1.13	1.79
3	Arylhydrocarbon receptor (AhR) signaling pathway	1. Metabolism	1.11 Xenobiotics biodegradation and metabolism	0.95	0.51	1.78
4	Metabolism of xenobiotics by cytochrome P450	1. Metabolism	1.11 Xenobiotics biodegradation and metabolism	1.44	-1.19	1.65
5	VEGF signaling pathway	3. Environmental Information Processing	3.2 Signal transduction	0.94	-0.81	1.59
6	Chemical carcinogenesis	6. Human Diseases	6.1 Cancers: Overview	1.26	0.95	1.53
7	NF-kappa B signaling pathway	3. Environmental Information Processing	3.2 Signal transduction	0.84	-0.77	1.43
8	Circadian rhythm	5. Organismal Systems	5.9 Environmental adaptation	-1.33	-0.87	1.38
9	ErbB signaling pathway	3. Environmental Information Processing	3.2 Signal transduction	0.80	0.74	1.36
10	Tryptophan metabolism	1. Metabolism	1.5 Amino acid metabolism	-0.58	1.23	1.24
11	Drug metabolism - cytochrome P450	1. Metabolism	1.11 Xenobiotics biodegradation and metabolism	1.12	-0.94	1.13
12	Regulation of lipolysis in adipocytes	5. Organismal Systems	5.2 Endocrine system	0.96	1.16	1.12
13	Calcium signaling pathway	3. Environmental Information Processing	3.2 Signal transduction	0.78	-0.94	1.11
14	Longevity regulating pathway	5. Organismal Systems	5.9 Aging	0.99	-0.50	1.11
15	mTOR signaling pathway	3. Environmental Information Processing	3.2 Signal transduction	-1.27	0.84	1.09
16	Inflammatory mediator regulation of TRP channels	5. Organismal Systems	5.7 Sensory system	0.91	-0.88	1.08
17	DNA replication	2. Genetic Information Processing	2.4 Replication and repair	0.50	1.09	0.99
18	Drug metabolism - other enzymes	1. Metabolism	1.11 Xenobiotics biodegradation and metabolism	0.98	0.91	0.97
19	MAPK signaling pathway	3. Environmental Information	3.2 Signal transduction	0.81	-0.77	0.96

			Processing	-0.92	-1.16	0.94

#	Pathway	Category	Subcategory			
			Processing			
20	B cell receptor signaling pathway	5. Organismal Systems	5.1 Immune system	-0.92	-1.16	0.94
21	Melanoma	6. Human Diseases	6.2 Cancers: Specific types	-0.88	1.11	0.93
22	Longevity regulating pathway	5. Organismal Systems	5.9 Aging	0.92	-0.68	0.92
23	Ras signaling pathway	3. Environmental Information Processing	3.2 Signal transduction	-0.95	0.72	0.92
24	Protein processing in endoplasmic reticulum	2. Genetic Information Processing	2.3 Folding, sorting and degradation	0.72	0.57	0.88
25	AMPK signaling pathway	3. Environmental Information Processing	3.2 Signal transduction	-0.92	-0.57	0.87
26	Terpenoid backbone biosynthesis	1. Metabolism	1.9 Metabolism of terpenoids and polyketides	-1.37	1.45	0.84
27	Circadian entrainment	5. Organismal Systems	5.9 Environmental adaptation	-1.00	-1.12	0.84
28	Chemokine signaling pathway	5. Organismal Systems	5.1 Immune system	-0.85	-1.20	0.81
29	Estrogen signaling pathway	5. Organismal Systems	5.2 Endocrine system	-0.75	-0.97	0.81
30	Pertussis	6. Human Diseases	6.8 Infectious diseases: Bacterial	-1.75	-0.69	0.80
31	Wnt signaling pathway	3. Environmental Information Processing	3.2 Signal transduction	-1.07	-1.07	0.79
32	Jak-STAT signaling pathway	3. Environmental Information Processing	3.2 Signal transduction	-1.07	-0.83	0.74
33	PI3K-Akt signaling pathway	3. Environmental Information Processing	3.2 Signal transduction	-1.12	0.83	0.73
34	RNA transport	2. Genetic Information Processing	2.2 Translation	-0.77	0.62	0.69
35	Mismatch repair	2. Genetic Information Processing	2.4 Replication and repair	0.68	1.04	0.62
36	Notch signaling pathway	3. Environmental Information Processing	3.2 Signal transduction	-0.95	0.64	0.62
37	p53 signaling pathway	4. Cellular Processes	4.3 Cell growth and death	-1.25	0.71	-0.58
38	Glycolysis / Gluconeogenesis	1. Metabolism	1.1 Carbohydrate metabolism	-1.21	-0.87	-0.65
39	Cell cycle	4. Cellular Processes	4.3 Cell growth and death	-0.78	0.65	-0.68
40	Apoptosis	4. Cellular Processes	4.3 Cell growth and death	-1.12	0.81	-0.74
41	Rap1 signaling pathway	3. Environmental Information Processing	3.2 Signal transduction	-0.83	0.94	-0.75
42	Steroid biosynthesis	1. Metabolism	1.3 Lipid metabolism	-1.09	-1.07	-0.79
43	T cell receptor signaling pathway	5. Organismal Systems	5.1 Immune system	1.01	-1.04	-0.79
44	Apoptosis - multiple species	4. Cellular Processes	4.3 Cell growth and death	-1.05	0.46	-0.82
45	Toll-like receptor signaling pathway	5. Organismal Systems	5.1 Immune system	-1.43	0.91	-0.87
46	Cell adhesion molecules (CAMs)	3. Environmental Information Processing	3.3 Signaling molecules and interaction	-0.85	0.90	-0.89
47	FoxO signaling pathway	3. Environmental Information	3.2 Signal transduction	-0.94	0.56	-0.89

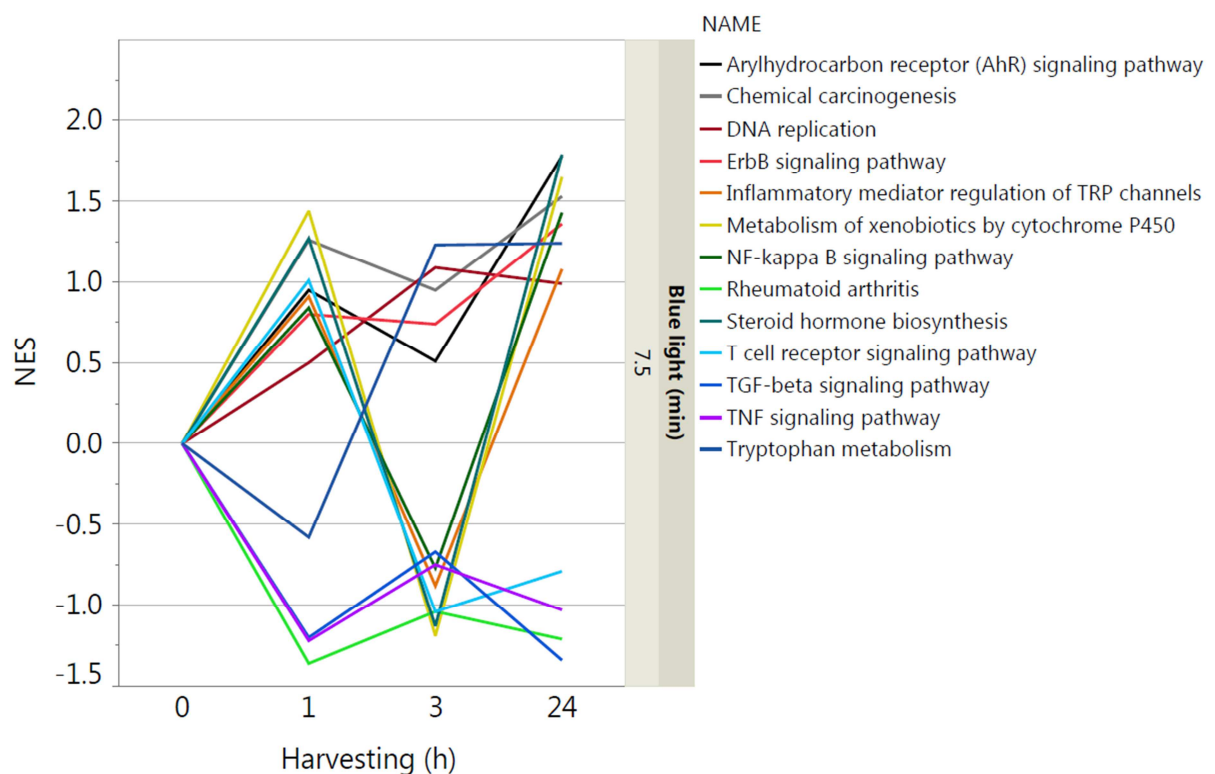|						
			Processing			
48	**Citrate cycle (TCA cycle)**	1. Metabolism	1.1 Carbohydrate metabolism	-0.78	1.09	-0.89
49	**cAMP signaling pathway**	3. Environmental Information Processing	3.2 Signal transduction	0.74	-0.98	-0.96
50	**NOD-like receptor signaling pathway**	5. Organismal Systems	5.1 Immune system	-1.36	-0.78	-1.03
51	**TNF signaling pathway**	3. Environmental Information Processing	3.2 Signal transduction	-1.22	-0.75	-1.03
52	**RNA degradation**	2. Genetic Information Processing	2.3 Folding, sorting and degradation	-1.03	1.03	-1.16
53	**Primary immunodeficiency**	6. Human Diseases	6.3 Immune diseases	-0.95	-1.07	-1.19
54	**Rheumatoid arthritis**	6. Human Diseases	6.3 Immune diseases	-1.36	-1.04	-1.21
55	**TGF-beta signaling pathway**	3. Environmental Information Processing	3.2 Signal transduction	-1.20	-0.67	-1.34
56	**Phototransduction**	5. Organismal Systems	5.7 Sensory system	0.69	0.66	-1.41
57	**Oxidative phosphorylation**	1. Metabolism	1.2 Energy metabolism	-0.98	1.25	-1.46

Figure 31: Gene expression analysis of 7.5min (10.35J/cm²) blue light irradiation - time course of NES for selected pathways for further evaluation of gene expression results.

Already 1h after 7.5min (10.35J/cm²) blue light irradiation genes connected to AHR signaling pathway, chemical carcinogenesis, DNA replication, ErbB signaling pathway, metabolism of xenobiotics by cytochrome P450, NF-κB signaling pathway,

steroid hormone biosynthesis and T cell receptor signaling pathway were upregulated. AHR signaling pathway, chemical carcinogenesis, DNA replication and ErbB signaling pathway were upregulated for all three harvesting times whereas metabolism of xenobiotics by cytochrome P450, NF-κB signaling pathway, steroid hormone biosynthesis and T cell receptor signaling pathway alternated between downregulation 3h after irradiation to upregulation 24h after irradiation. Consistently downregulated pathways were Rheumatoid arthritis, TGF-β signaling pathway and TNF signaling pathway. Additionally, Tryptophan metabolism was downregulated 1h after irradiation, however, upregulated 3h and 24h after irradiation. The time course of gene expression analysis at different time points after 7.5min (10.35J/cm²) blue light irradiation of highly deregulated genes and genes connected to the AHR signaling pathway are illustrated in Figure 32, Figure 33 and Table 11. CYP1A1, ALDH3A1 and NQO1 were slightly downregulated at 1h after irradiation, however, 3h and 24h after irradiation they were upregulated. GSTA1 was considerably upregulated only 3h after irradiation and CYP1B1 only 24h after irradiation. UGT1A was upregulation 1h after irradiation but downregulated after 3h and 24h after irradiation, while CDKN1B and TRADD were upregulated after 1h and 3h, but downregulated 24h after irradiation. AHRR, CYP1A2 and NFE2L2 (Nrf2) are not considerably regulated.

Table 11: Gene expression analysis of 7.5min (10.35J/cm²) blue light irradiation - time course of selected AHR inducible genes for further evaluation of gene expression results.

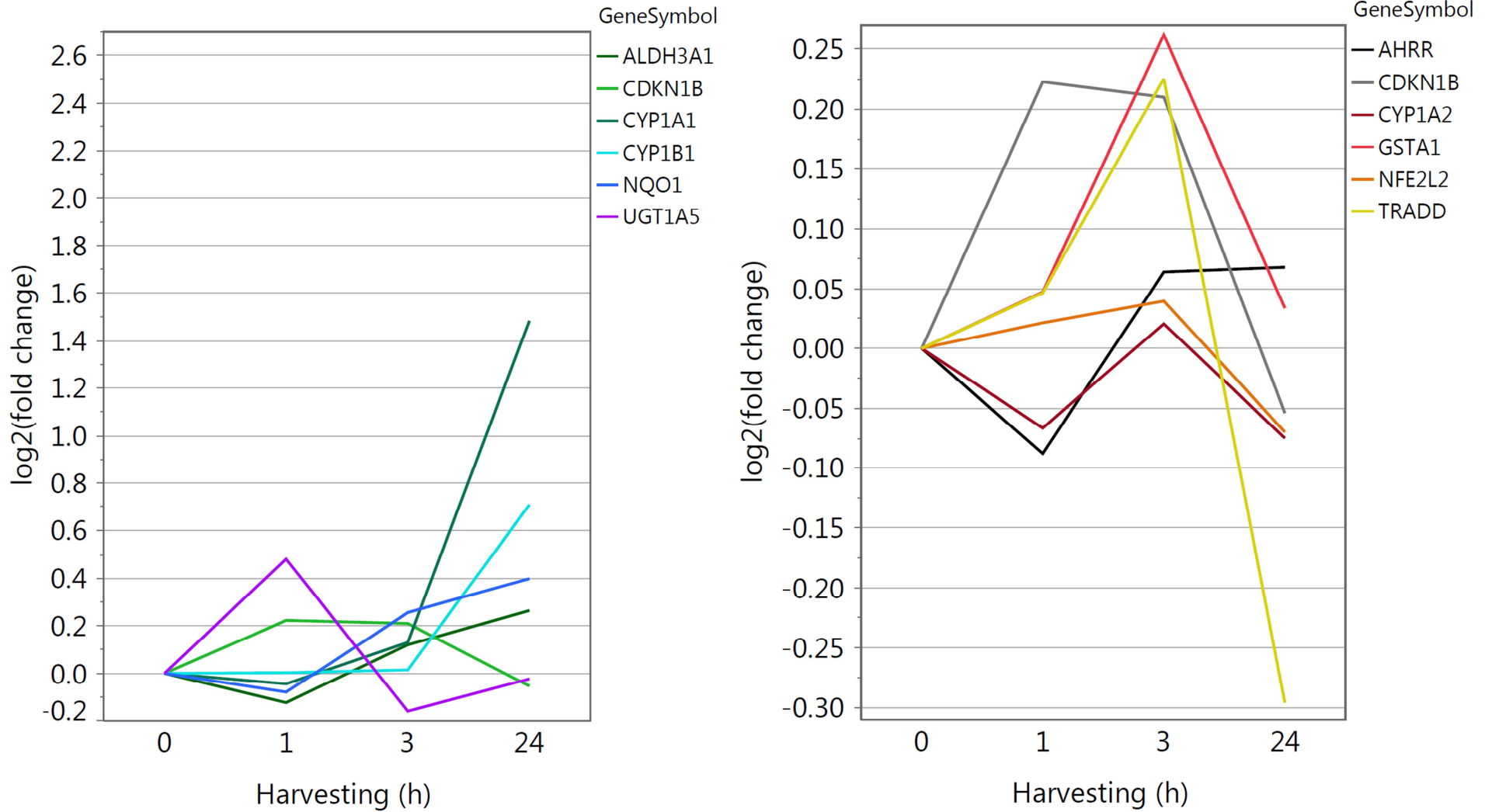| Gene name	7.5min 1h log$_2$(fold change)	7.5min 1h -log$_{10}$(p-value)	7.5min 1h Adjusted p-value	7.5min 3h log$_2$ (fold change)	7.5min 3h -log$_{10}$(p-value)	7.5min 3h Adjusted p-value	7.5min 24h log$_2$(fold change)	7.5min 24h -log$_{10}$(p-value)	7.5min 24h Adjusted p-value
AHR	-0.07	1.357	0.223	-0.07	1.553	0.186	-0.04	0.321	0.714
AHRR	-0.09	1.359	0.222	0.06	0.252	0.746	0.07	0.106	0.900
ALDH3A1	-0.12	0.919	0.363	0.12	1.231	0.262	0.26	0.778	0.423
CDKN1B	0.22	0.986	0.337	0.21	2.488	0.066	-0.05	0.231	0.788
CYP1A1	-0.04	0.286	0.737	0.13	1.737	0.152	1.48	4.043	0.011
CYP1A2	-0.07	0.442	0.619	0.02	0.103	0.890	-0.07	0.556	0.550
CYP1B1	0.00	0.040	0.962	0.01	0.447	0.594	0.71	2.259	0.072
GSTA1	0.05	0.284	0.739	0.26	0.804	0.412	0.03	0.065	0.938
NFE2L2	0.02	0.121	0.886	0.04	0.203	0.791	-0.07	0.546	0.556
NQO1	-0.08	0.396	0.653	0.26	2.084	0.104	0.40	3.376	0.021
TRADD	0.05	0.464	0.605	0.23	1.645	0.168	-0.30	1.354	0.210
UGT1A5	0.48	3.601	0.0176	-0.160	0.715	0.451	-0.02	0.048	0.955
ERK1	0.10	2.239	0.080	0.126	0.442	0.597	0.025	0.225	0.794

Figure 32: Gene expression analysis of 7.5min (10.35J/cm²) blue light irradiation - time course of selected AHR inducible genes for further evaluation of gene expression results.
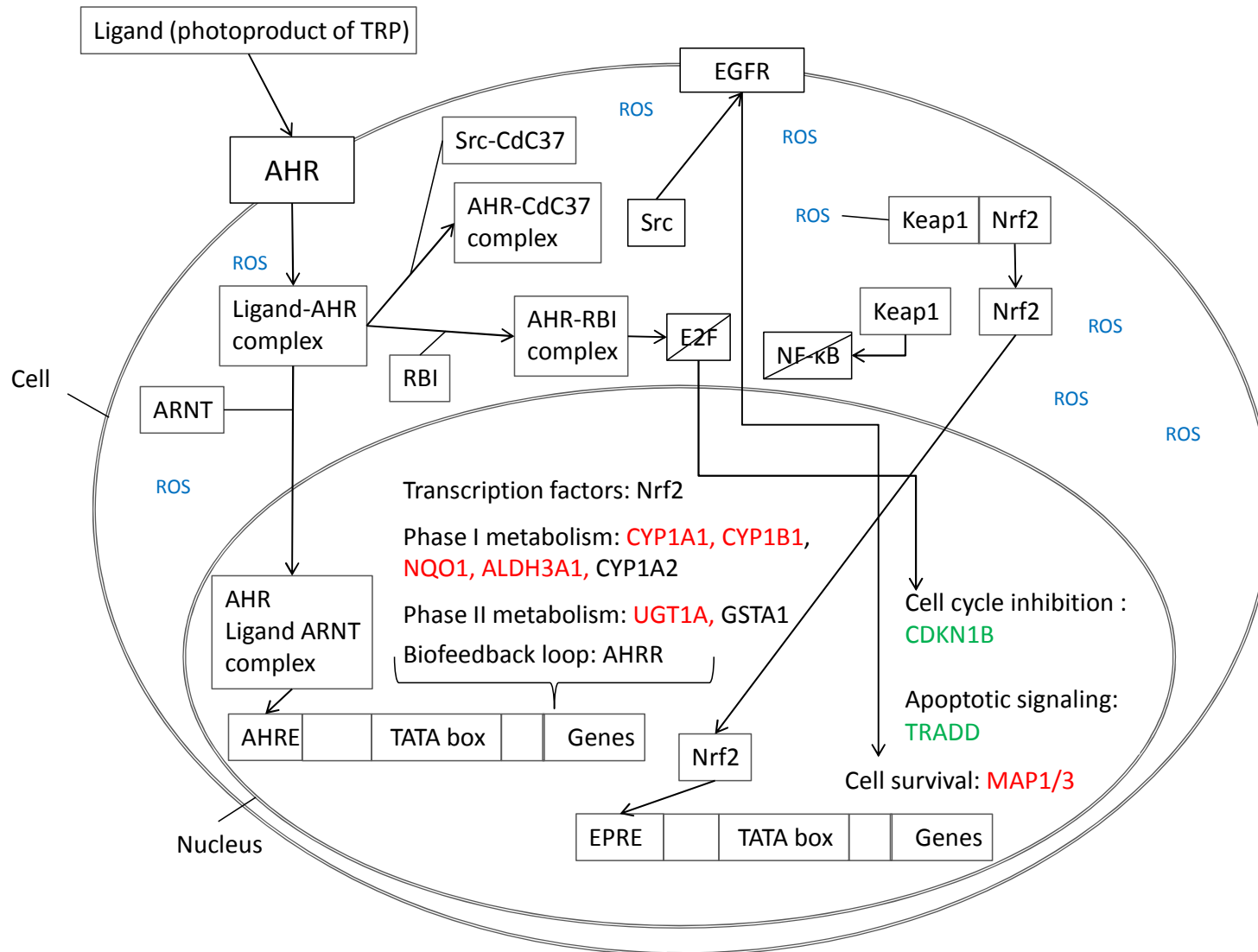
Figure 33: Aryl Hydrocarbon Receptor (AHR) signaling pathway for 7.5min (10.35J/cm²) blue light irradiation and 24h harvesting time. Red: upregulated gene expression after AHR activation, green: downregulated gene expression after AHR activation.

3.4.8 Verification of genes from chips with qPCR

Also for 7.5min (10.35J/cm²) blue light irradiation real time PCR (qPCR) was conducted to confirm selected genes of microarray results. qPCRs were performed with RNA samples from harvesting time 24h after 7.5min of blue light irradiation, which were beforehand used for gene expression analysis. qPCR results match with the previously obtained gene expression results with CYP1A1, CYP1B1, ALDH3A1 and NQO1 being significantly upregulated and FBJ murine osteosarcoma viral oncogene homolog (FOS), interleukin 8 (IL8) and keratin 5 (Krt5). UGT1A was not significantly regulated, however, showed a shift to downregulation in both experiments (Figure 34).
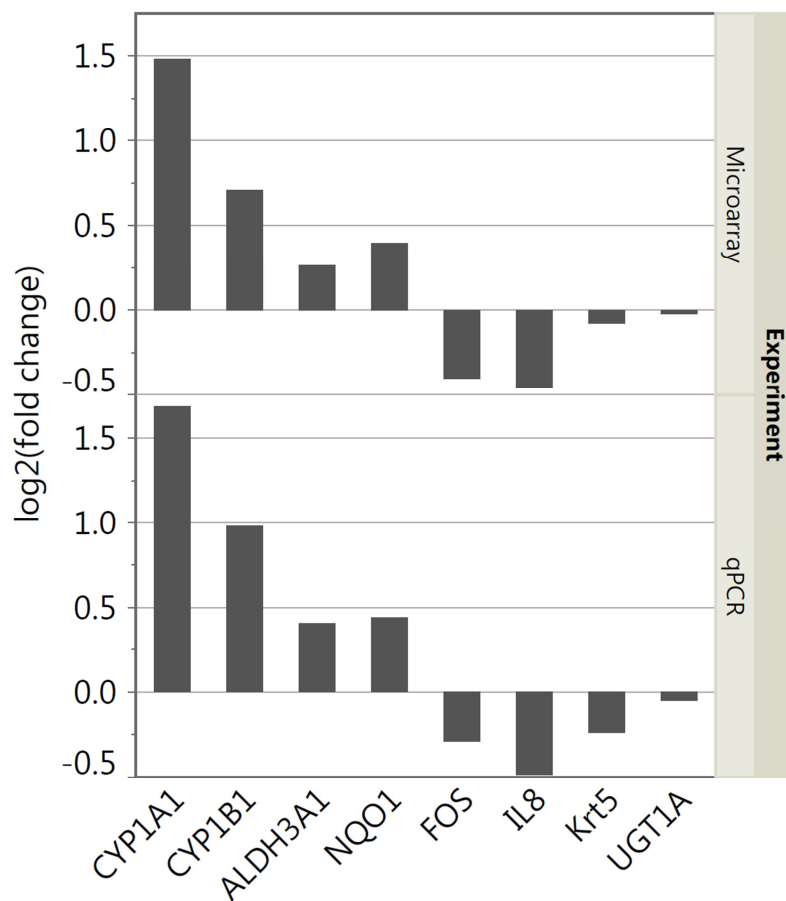

Figure 34: qPCR of selected genes verifies gene expression analysis results.

4 DISCUSSION

The literature search for the effect of blue visible light on keratinocytes showed as main light effects the induction of proliferation, reduction of proliferation and even induction of apoptosis (Figure 5). Results seemed to be cell type specific and not clearly assignable to a certain dose. Therefore, as a first experiment different irradiation times respectively energy densities were tested on HaCaT cells to obtain an overview for dose effects.

PBM using blue light irradiation induces a biphasic dose response curve in human immortalized keratinocytes with an increase in metabolism for low doses and a decrease in metabolism for higher doses *in vitro* (Figure 9) [58]. Two irradiation times were chosen to test the difference between proliferative and anti-proliferative phase of this biphasic curve. 7.5min (10.35J/cm²) blue light irradiation showed the highest increase in metabolism (Figure 9) and was consequently chosen for the proliferative phase. For the anti-proliferative phase 30min (41.4J/cm²) blue light irradiation was selected as this was the lowest dose where the highest decrease in metabolism was found (Figure 9). To explain the photobiomodulatory effect of blue light irradiation with the selected doses functional experiments were performed. Therefore, cell metabolism and proliferation were tested using XTT, cell counting, BrdU ELISA and BrdU FACS, ROS concentrations were measured and, for safety, apoptosis was analyzed using FACS. Furthermore, a comprehensive evaluation of gene expression analysis for the time points 1h, 3h and 24h after blue light irradiation was conducted.

4.1 Anti-proliferative phase

Viability tests demonstrated the inhibitory effect of 30min (41.4J/cm²) blue light on cell metabolism and proliferation, with BrdU FACS pointing out a shift of irradiated cells to the S-phase of cell cycle. Those effects could be prolonged with consecutive irradiations each 24h. ROS measurement confirmed a high increase of ROS directly after irradiation, which is expected after light treatment. However, ROS could be balanced to normal level quite fast and apoptosis test using FACS excluded any apoptotic induction of the used light dosage. Gene expression results were fitting to preceding experiments and revealed AHR as possible target for blue light irradiation.

XTT, cell counting and BrdU labeling were performed to investigate the metabolism and cell proliferation of HaCaT cells at different time points after a 30min (40.4J/cm²)

irradiation with blue light (Figure 10 - Figure 13). Already 1h after irradiation the metabolism of the cells was decreased and reached its maximum decrease 24h after irradiation. 48h after irradiation the effect was gone. However, it could be prolonged with consecutive irradiations every 24h. As changes in cell metabolism are faster and more pronounced compared to changes in cell proliferation, proliferation tests are expected to show smaller results which occur later then metabolic changes. Therefore, proliferation with cell counting and BrdU ELISA showed matching results compared with XTT test. Cell proliferation was decreased 24h after irradiation and the effect was more pronounced with consecutive irradiations every 24h. Hence it would be suggested to irradiate at least once per day if an anti-proliferative effect is desired.

H_2O_2 concentrations were tested in cells to confirm a light induced ROS production. ROS levels were increased 1.26 fold 30min after irradiation (Figure 14). Interestingly, the cells could balance that rise already after 1h and concentrations alternated between slightly increased and decreased until 24h after irradiation. These results fit to the phenomenon called mitohormesis, which is the adaptive response of mitochondria to varying ROS levels. In general, ROS, which are produced mainly in mitochondria, are signaling molecules induced by stress and an increased demand for readily available energy, which triggers the retrograde response; a process resulting in transcriptional changes in the nucleus [63, 64]. In more detail, ROS oxidize e.g. thiol groups on cysteine residues thereby activating downstream processes by changing functions of the enzymes in a signaling pathway [65] leading to a reversible signal transduction mechanism [66]. They are able to precondition the organism thereby inducing cellular defense mechanisms that finally serve as a long-term protective shield [67] and even prevent cellular damage [63, 64]. Furthermore, this process activates detoxification routes which finally result in a reduction of the initial signaling molecules and explain how the HaCaT cells could reduce H_2O_2 concentrations already 1h after blue light irradiation (Figure 14).

While low concentrations of ROS act in a protective way [68] high concentrations of ROS are well known to be able to irreversibly destroy cellular structures [68]. Although, gene expression analysis did not show any cell repair mechanisms, FACS analysis was used to test for apoptosis of the cells 24h after 30min (41.4J/cm²) of blue light irradiation. The cells did not show any signs of apoptosis (Figure 15 and Figure 16),

which fits to the hypothesis that light-induced ROS concentrations are not too high and do not damage the cells.

Gene expression analysis revealed a high number of deregulated genes already one 1h after irradiation, with even increasing numbers for 3h and highest numbers 24h after irradiation (Table 6). Subsequent GSEA depicted that blue light deregulates a variety of pathways in a time dependent manner (Table 7 and Figure 18), with some pathways already deregulated 1h after irradiation, which consequently induce the early response of blue light irradiation.

One of those early pathways is the pathway of metabolism of xenobiotics by CYPs (Table 7 and Figure 18) with CYP1A1, which is also known as aryl hydrocarbon hydroxylase [69], and CYP1B1 as highly upregulated genes (Figure 21). They are best known for their metabolic activation of polycyclic aromatic hydrocarbons (PAHs) and heterocyclic aromatic amines/amides (HAAs) to electrophilic reactive intermediates [69-71]. Their gene expression is regulated by a heterodimeric transcription factor consisting of the aryl hydrocarbon receptor nuclear translocator (ARNT) and the aryl hydrocarbon receptor (AHR) [70, 71]. The latter belongs to the group of basic helix-loop-helix (bHLH) PAS (homologous to Per/ARNT/Sim) proteins [72] and is a ligand activated transcription factor usually defined as transcriptional regulator connected to adaptive xenobiotic response [73]. The ligand binding pocket of the AHR is able to fit a large number of planar, hydrophobic compounds [74] with PAHs and HAAs as well-known exogenous ligands [75]. However, rising evidence led to the discovery of the existence of endogenous AHR ligands [75] indicating that physiological functions of AHR are important for normal cell development and immune responses [73, 76].

AHR serves not only as an internal oxygen and redox status sensor, but also recognizes low molecular-weight compounds and light [77, 78] with endogenous ligands derived from tryptophan due to UV or visible light exposure induced photolytic destruction/photo-oxidation [12, 72, 75]. As the epidermis, consisting mainly of keratinocytes, has a high tryptophan content, the irradiation of keratinocytes with 453nm blue light for 30min respectively 41.4J/cm² may be able to induce the production of high affinity AHR ligands like 2,3,7,8-Tetrachlordibenzodioxin (TCDD), 6-formylindolo[3,2-b]carbazole (FICZ), 6,12-diformylindolo[3,2- b]carbazole (dFICZ) and oxi FICZ carboxylic acid type originating from indolo[3,2-b]carbazole-6-carboxylic acid (CICZ) which are natural substrates for CYPs present in skin cells [72]. After ligand binding AHR, which is located in the cytoplasm in its inactive state, forms a

heterodimer with ARNT and translocates to the nucleus. Subsequently, it binds to the AHR-mediated aromatic hydrocarbon response element (AHRE, also XRE or DRE) DNA motif [69], which leads to an upregulated transcription of a battery of xenobiotic-metabolizing enzymes (XMEs) [57], which are collectively referred to as "AHR gene battery" [73] (Figure 21). These target genes are encoding phase I and phase II xenobiotic-metabolizing enzymes, which are vital for detoxification of xenobiotics [69, 73]. The main enzymes encoded by AHR affected genes that are involved in phase I of xenobiotic metabolism are CYP1A1, CYP1A2, CYP1B1, NQO1 and ALDH3A1, whereas UGT1A and GSTA1 are connected to phase II [57, 69, 73].

Gene expression analysis revealed an upregulation of CYP1A1, CYP1B1, ALDH3A1, NQO1 and UGT1A5 already 1h after blue light irradiation, which is stable up to 3h (Figure 21). CYP1A1, CYP1B1, ALDH3A1 and NQO1 show an even higher upregulation in gene expression 24h after irradiation, whereas UGT1A remains at the same level. This gene-regulation downstream of AHR activation strengthens the hypothesis that AHR is activated due to photo-oxidation of tryptophan after blue light irradiation. Moreover, activation of metabolism of xenobiotics by CYPs can lead to an activation of steroid hormone biosynthesis with NQO1 and ALDH3A1 likewise involved [58, 79, 80] fitting to the findings of upregulated genes in the pathway of steroid hormone biosynthesis in gene expression analysis for all tested time points after blue light irradiation (Table 7 and Figure 18).

Another overall consequence of AHR activated gene expression is generation of electrophilic reactive intermediates which induce reactive oxygenated metabolite (ROM)-mediated oxidative stress [69]. This triggers, besides the AHR dependent gene activation via AHRE, the additional Nrf2 dependent gene activation via the electrophile response element (EPRE, (also ARE) DNA motif [69] resulting in expression of phase II detoxification enzymes [81, 82], thereby reducing oxidative stress [82].

In its inactive state the transcription factor Nrf2 is bound to the substrate adaptor protein Kelch-like ECH-associated protein 1 (Keap1), which mediates the ubiquitination and subsequent proteasomal degradation of Nrf2 by a Cullin3-dependent E3 ubiquitin ligase complex [83, 84]. After AHR induces ROM-mediated oxidative stress Keap1 is not able to bind to Nrf2 anymore as critical cysteine residues of the protein are oxidized thereby changing its conformation. Subsequently, the unbound Nrf2 is translocated to the nucleus activating gene expression via EPRE

[84]. Target genes are partially consistent with AHR activated AHRE transcribed genes comprising inter alia ALDH3A1, NQO1 and UGT1A [85]. This is in agreement with the gene expression results (Figure 21). Additionally, gene expression of Nrf2 itself is upregulated after blue light irradiation (Figure 21) causing a higher level of Nrf2 transcription factor and more effective activation of the downstream process for reducing oxidative stress, which was shown before by Miao and colleagues in 2005 [86]. Furthermore, Keap1 can degrade the inhibitor of kappa light polypeptide gene enhancer in B-cells kinase beta (IKKβ), which leads to an inhibition of activation of nuclear factor of kappa light polypeptide gene enhancer in B-cells 1 (NF-κB) [84, 87] and thereby to an anti-inflammatory response [88]. Moreover, AHR can directly interact with the transcription factor JunB to modulate skin immune responses, which was shown to play an important role in suppression of psoriatic lesions in keratinocytes [76]. This can be observed in gene expression analysis where, besides the NF-κB signaling pathway, above all inflammatory pathways are downregulated (Table 7 and Figure 18).

Cell cycle arrest pathway can be directly activated through ROS production [58, 89], however, AHR activation can influence the cell cycle, too [71]. After binding retinoblastoma 1 (RB1) [90], the AHR-RBI complex can block E2F-mediated transcription of S-phase genes like e.g. CDKN1B [71, 91, 92], resulting in an inhibition of normal progression of G_1- to S-phase in cell cycle [71]. CDKN1B is downregulated 1h and 3h after blue light irradiation (Figure 21), additionally to ROS induced cell cycle arrest (Table 7 and Figure 18). This explains the decrease of cell metabolism and proliferation with blue light. Moreover, cell cycle arrest was verified with BrdU FACS, where even though cell number was lower after irradiation, irradiated cells shifted to S-phase. This effect was more pronounced after consecutive irradiations (Figure 13) and lead to the conclusion, that the S-phase is slowed down after 30min (41.4J/cm²) blue light irradiation. Interestingly, at the time point 24h after one blue light irradiation, CDKN1B is slightly downregulated (Figure 21). These findings fit to the gene expression results of the pathway of DNA replication, which was downregulated for 1h and 3h after irradiation but slightly upregulated 24h after irradiation (Table 7 and Figure 18) and would explain why the metabolism is again at the normal level 48h after one irradiation (Figure 9).

Next to its function as transcription factor the AHR-ligand complex can associate with cell division cycle 37 control protein (Cdc37) and the non-receptor tyrosine kinase Src

causing the dissociation of the latter. Consequently, Src translocation into the cell membrane is promoted where it phosphorylates the epidermal growth factor receptor (EGFR, also ERBB), which activates ERK1/2 (also MAPK3/1) target gene expression leading to cell survival [73, 93]. The crucial time point for the cell to decide between cell survival and apoptosis after blue light irradiation seems to be during the first hour after irradiation. Here, oxidative stress is induced, which was described with an increase of H_2O_2 production 30min after blue light irradiation followed by a decrease already 1h after irradiation. An early upregulation of ERK1/2 occurs 1h after irradiation (Table 8) on gene expression level triggering cell survival pathways. This cell survival effect is emphasized by the additional downregulation of TFN signaling pathway (Table 7 and Figure 18) containing TRADD, which can signal apoptosis [69, 73]. TRADD is downregulated for all tested time points after blue light irradiation with a maximum after 3h (Figure 21).

Finally, AHR activation triggers the induction of AHRR gene expression 3h after blue light irradiation (Figure 21) which is known to lead to a dimerization of AHRR with ANRT and results in an inhibition of AHR function. Therefore, AHRR activation by AHR represents a regulatory biofeedback loop in the xenobiotic signal transduction pathway [57, 94, 95].

4.2 Proliferative phase

Viability tests demonstrated the activation of cell metabolism and proliferation after one 7.5min (10.35J/cm²) blue light irradiation, with BrdU FACS pointing to a shift of irradiated cells to the S-phase of cell cycle. However, consecutive irradiations lead to a decrease in metabolism and proliferation and a shift of irradiated cells to G_0/G_1-phase. ROS measurement confirmed a high increase of ROS directly after irradiation but could be balanced to normal level quite fast. Additionally, apoptosis test using FACS excluded any apoptotic induction of the used light dosage. Gene expression results were less pronounced than for 30min (41.4J/cm²) blue light irradiation. Nevertheless, they were fitting to preceding experiments and supported the hypothesis of AHR being a possible target for blue light irradiation and pointed out the importance of dosage when using PBM.

AHR activation via photo-oxidation of tryptophan was the main hypothesis for the photobiomodulatory effect of 30min (41.4J/cm²) blue light irradiation connected to cell

protection with decreased proliferation, increased production of steroid hormones and prevention of inflammatory responses. Likewise for 7.5min (10.35J/cm²) of blue light irradiation AHR induced gene transcription was deregulated with CYP1A1, ALDH3A1 and NQO1 upregulated 3h and 24h after irradiation. GSTA1 was considerably upregulated 3h after irradiation and CYP1B1 24h after irradiation. Furthermore, UGT1A was upregulated 1h after irradiation (Figure 32). Corresponding to that the pathway analysis revealed an upregulation of AHR signaling pathway, as well as metabolism of xenobiotics by CYPs and steroid hormone biosynthesis (Figure 31), which involves inter alia NQO1 and ALDH3A1 [58, 79, 80]. However, deregulation for these genes as well as activation of the named pathways was significantly less compared to 30min (41.4J/cm^2) of blue light irradiation fitting to the dose dependency of PBM.

XTT, cell counting and BrdU labeling were performed to investigate the metabolism and cell proliferation of HaCaT cells at different time points after a 7.5min (10.35J/cm²) irradiation with blue light (Figure 23 - Figure 26). The metabolism was increased for all time points after irradiation up to at least 72h (Figure 23). Also proliferation was increased 24h after irradiation (Figure 25). However, consecutive irradiations did not lead to a prolongation of this effect and even lead to a shift of irradiated cells to G_0/G_1-phase in BrdU FACS with 3 consecutive irradiations each 24h (Figure 26). Consequently it is not suggested to irradiate every 24h, if a proliferative effect is desired.

AHR can directly influence the cell cycle by binding to retinoblastoma 1 (RB1) [71, 90]. Consequently, the progression of G_1- to S-phase in cell cycle can be inhibited by blocking the E2F-mediated transcription of S phase genes like e.g. CDKN1B [71, 91, 92]. After an irradiation with 7.5min (10.35J/cm²) blue light, RB1 was downregulated for 1h and 3h and consequently the hypothesis emerged that the translated protein was less available for complexing with AHR. Matching to this hypothesis, CDKN1B was slightly upregulated after 1h and 3h after irradiation (Figure 32). Furthermore, the pathway of DNA replication was upregulated for all three time points (Figure 31) explaining the XTT results described before and the slight shift of irradiated cells to S-phase in BrdU FACS (Figure 26). These findings fit to Yin et. al. 2016 who described that in addition to negatively regulating cell proliferation and survival, AHR may also positively regulate these pathways. Differences in the time frame, dosage of

the ligand, category of ligand, cell type or whether the experiment was performed *in vivo* or *in vitro* may be the reason for these dual functions [96].

As a next step H_2O_2 concentrations were measured to examine oxidative stress, which revealed an even higher rise in H_2O_2 30min after irradiation when compared to 30min ($41.4J/cm^2$) blue light irradiation. This result was unexpected as higher H_2O_2 levels could be connected to higher oxidative stress. Further tests have to be performed to explain these results. It might be connected to the increased metabolism of the cells after 7.5min ($10.35J/cm^2$) blue light irradiation, as higher metabolic activity correlates with ROS production in mitochondria. Furthermore, they might fit to the "triphasic" response of ROS production after PBM described by Huang et al. 2011 [97]. ROS measurements were performed after PBM using an 810nm laser resulting in two distinct peaks for mitochondrial ROS in cultured cortical neurons. Their hypothesis was that two kinds of ROS exist leading to the triphasic course; with firstly beneficial ROS produced by low fluences of LLLT leading to the first peak, followed by decreasing of beneficial ROS with increasing fluences and finally harmful ROS produced with high fluences leading to the second peak. "Good" ROS, which are produced through stimulation of mitochondrial electron transport by lower fluences, are able to act as mediators of cell signaling processes. Thereby, beneficial cell signaling pathways can be activated like for example NF-κB [98, 99], which is a redox sensitive transcription factor and is able to induce expression of a large number of gene products connected to cell survival, proliferation [100, 101] and regulation of inflammation [88, 97]. This would match with gene expression analysis where the NF-κB signaling pathway is upregulated 1h and 24h after blue light irradiation (Figure 31) leading to the hypothesis, that although H_2O_2 concentrations were higher after a 7.5min ($10.35J/cm^2$) blue light irradiation compared to 30min ($41.4J/cm^2$) the actual oxidative stress was lesser.

Alongside with AHR, Nrf2 dependent gene activation via the electrophile response element (EPRE, also ARE) DNA motif [69] can be activated by reactive oxygenated metabolite (ROM)-mediated oxidative stress. ROM-mediated oxidative stress is either induced directly by light or as an AHR downstream process. Resulting in expression of phase I and phase II detoxification enzymes [81, 82], which are partially consistent with AHR activated AHRE transcribed genes comprising inter alia ALDH3A1, NQO1, GSTA1 and UGT1A [85], this pathway reduces oxidative stress [82]. Consequently, activation of this Nrf2 dependent gene transcription can be used to evaluate the

latter. Gene expression results fit with the hypothesis that even though H_2O_2 concentrations were higher after a 7.5min (10.35J/cm²) blue light irradiation compared to 30min (41.4J/cm^2) the induced oxidative stress was lower, with UGT1A and GSTA1 not considerably deregulated, as well as Nrf2 itself not regulated (Figure 32).

Furthermore, cell survival can be induced by AHR-ligand complex association with cell division cycle 37 control protein (Cdc37) and the non-receptor tyrosine kinase Src causing the dissociation of the latter. ERK1/2 (also MAPK3/1) target gene expression can be activated subsequently through phosphorylation of the epidermal growth factor receptor (EGFR, also ERBB) by translocated Src [73, 93]. An early upregulation of ERK1 occurs 1h and 3h after irradiation on gene expression level triggering cell survival pathways (Table 11). Underlining this cell survival effect is the downregulation of TRADD 24h after blue light irradiation (Figure 32), which is connected to apoptosis signaling, as well as the downregulated TNF signaling pathway, which was downregulated for all three timepoints after irradiation (Figure 31) [69, 73].

4.3 Conclusion

The effect of PBM using blue light is dose dependent. The biphasic dose response curve of proliferation in HaCaT cells is reflected in the gene expression results. The two used dosages of 7.5min (10.35J/cm²) and 30min (41.4J/cm²) of blue light show some similarities, like production of steroid hormones and induction of cell survival pathways. However, there are some significant differences as for example the level of oxidative stress. Gene expression results show that the oxidative stress dependent Nrf2 transcribed genes were not deregulated for 7.5min (10.35J/cm²) blue light irradiation. However, when increasing the dose to 30min (41.4J/cm²) blue light, Nrf2 transcribed genes were highly upregulated. After activation of AHR with blue light, the dose seems to determine the extent of the downstream effect and therefore the dose dependency seems to be induced by the secondary steps after blue light irradiation, with oxidative stress being one of the most influencing factors. As a summary it can be said that blue light provides us with a promising treatment method for different paradigms with the dose as an important parameter to be selected according to the needs of the patient.

5 SUMMARY

The skin, which is the largest organ of the human body, serves as a protective barrier between the internal milieu and the environment. It functions as the body's first line of defense against infection and regulates its temperature and fluid balance [11]. Keratinocytes are present in all the layers of the epidermis [21], the outermost layer of the skin, and are essentially connected to the pathophysiology of skin diseases such as psoriasis and atopic dermatitis, and play a crucial role in skin wound healing [14, 20]. Keratinocytes are the first cells to be in contact when exposed with external stimuli and are consequently more amenable to non-invasive treatments such as PBM using blue light [21]. The anti-microbial [36], anti-inflammatory [37] and anti-proliferative effects [38, 39] of blue light are already used for different medical treatments like psoriasis [33], neonatal jaundice [34] and back pain [35]. However, little is known about the mechanisms transducing the light induced signals from target molecules over downstream processes and/or gene expression to the biological effects [56] and therefore the aim of this project was to examine the photobiomodulary effect of blue light on the immortalized human keratinocyte cell line HaCaT in detail.

Photobiomodulation using blue light irradiation induces a biphasic dose response curve of metabolism in HaCaT cells with an increase in metabolism and proliferation for low doses and a decrease in metabolism and proliferation for higher doses *in vitro* (Figure 9) [58]. For further tests, 7.5min (10.35J/cm²) respectively 30min (41.4J/cm²) were chosen for subsequent experiments to test the blue light effect after different harvesting times in the proliferative phase respectively the anti-proliferative phase of PBM.

Gene expression evaluation of HaCaT cells after 30min (41.4J/cm²) of blue light irradiation revealed an upregulation of "AHR battery genes" leading to production of phase I and phase II enzymes of xenobiotic metabolism [69, 73]. One important action of this downstream process is to provide a delicate hormesis between promoting and preventing ROM-mediated oxidative stress, which is in agreement with our ROS measurements. H_2O_2 concentrations are increased 30min after blue light irradiation; however, already 1h after irradiation H_2O_2 is metabolized by the cells leading to an

even lower ROS concentration. Furthermore, steroid hormone biosynthesis is activated as a downstream process of "AHR battery gene" expression [39, 79, 80, 89] already 1h after irradiation triggering anti-inflammatory responses [79, 102, 103]. Additionally, inflammation is also decreased due to oxidative stress inhibited NF-κB signaling pathway [84, 87, 88] and interaction with JunB [76]. DNA replication pathway is downregulated resulting in a decrease in cell proliferation due to primary production of ROS [89], AHR-induced downregulation of CDKN1B [71] and prolongation of S-phase. However, ROS concentrations are not reaching a damaging level as cell survival pathways are enhanced by crosstalk of AHR-ligand complex with EGFR. Moreover, reduction of TNF-signaling pathway and downregulation of TRADD gene expression, which are relevant for apoptotic signaling, are consistent with FACS analysis as 24h after blue light irradiation cells are not showing any sign of apoptosis. Finally, it can be concluded that gene expression after 30min ($41.4J/cm^2$) of blue light irradiation shows a time course after blue light irradiation, with early response genes and pathways leading to the identification of AHR as a possible target for PBM with blue light via photo-oxidation of tryptophan resulting, when using this described dose, in a cell protective effect with decreased proliferation, production of steroid hormones and prevention of inflammatory responses. Moreover, the anti- proliferative effect can be prolonged by consecutive irradiations each 24h.

Photobiomodulation with 7.5min ($10.35J/cm^2$) blue light induced a proliferation increase in HaCaT cells until at least up to 24h after irradiation, which was documented in gene expression analysis with upregulation of DNA replication pathway and genes connected to cell cycle. H_2O_2 concentrations were increased 30min after blue light irradiation to an even higher level than after a 30min ($41.4J/cm^2$) blue light irradiation; however, already 1h after irradiation H_2O_2 was metabolized by the cells. The hypothesis was set that even though H_2O_2 concentrations were higher after a 7.5min ($10.35J/cm^2$) blue light irradiation compared to 30min ($41.4J/cm^2$) the actual oxidative stress was lower. This was explained with the triphasic ROS production-curve induced by PBM described by Huang et al. 2011 [97] and could be linked to gene expression analysis results, where for example oxidative stress dependent Nrf2 transcribed genes were not deregulated. It was not only shown that ROS production was not damaging the cells but even that cell survival pathways were enhanced by crosstalk of EGFR with the AHR-ligand

complex. Furthermore, apoptotic signaling was downregulated as TRADD gene expression and TNF-signaling pathway were reduced. Comparable with 30min (41.4J/cm²) blue light irradiation, gene expression analysis revealed an upregulation of "AHR battery genes" after 7.5min (10.35J/cm²) blue light leading to production of phase I and phase II enzymes of xenobiotic metabolism [69, 73] and steroid hormone biosynthesis as a downstream process of "AHR battery gene" expression [39, 79, 80, 89]. However, deregulation of genes and pathways occurred to a smaller extent. Finally, it can be concluded that PBM with blue light, when using 7.5min (10.35J/cm²), activates AHR and results in a cell protective effect with increased proliferation, production of steroid hormones and induction of cell survival pathways. Furthermore, it is suggested not to use consecutive irradiations each 24h if a proliferative effect is desired.

6 REFERENCES

1. Durmuş, S, Çakır, T, Özgür, A, Guthke, R: A review on computational systems biology of pathogen–host interactions. *Front Microbiol,* 6**:** 235, 2015.
2. PubMed*,* 2016. Retrieved from: https://www.ncbi.nlm.nih.gov/pubmed/.
3. O'Mara-Eves, A, Thomas, J, McNaught, J, Miwa, M, Ananiadou, S: Using text mining for study identification in systematic reviews: a systematic review of current approaches. *Systematic Reviews,* 4**:** 1-22, 2015.
4. Ananiadou, S, Thompson, P, Nawaz, R, McNaught, J, Kell, DB: Event-based text mining for biology and functional genomics. *Brief Funct Genomics,* 14**:** 213-230, 2015.
5. Balan, PF, Gerits, A, Vanduffel, W: A practical application of text mining to literature on cognitive rehabilitation and enhancement through neurostimulation. *Front Syst Neurosci,* 8**:** 1-14, 2014.
6. Hearst, MA: Untangling text data mining. *Proceedings of the 37th annual meeting of the Association for Computational Linguistics on Computational Linguistics.* College Park, Maryland, Association for Computational Linguistics, 1999 pp 3-10.
7. Abbe, A, Grouin, C, Zweigenbaum, P, Falissard, B: Text mining applications in psychiatry: a systematic literature review. *Int J Methods Psychiatr Res,* 25**:** 86-100, 2016.
8. Fleuren, WWM, Alkema, W: Application of text mining in the biomedical domain. *Methods,* 74**:** 97-106, 2015.
9. Huang, C-C, Lu, Z: Community challenges in biomedical text mining over 10 years: success, failure and the future. *Brief Funct Genomics,* 17**:** 132-144, 2016.
10. Averbis. Retrieved from: https://averbis.com/text-mining/.
11. Wang, JX, Fukunaga-Kalabis, M, Herlyn, M: Crosstalk in skin: melanocytes, keratinocytes, stem cells, and melanoma. *J Cell Commun Signal,* 10**:** 191-196, 2016.
12. Di Meglio, P, Duarte, JH, Ahlfors, H, Owens, ND, Li, Y, Villanova, F, Tosi, I, Hirota, K, Nestle, FO, Mrowietz, U, Gilchrist, MJ, Stockinger, B: Activation of the aryl hydrocarbon receptor dampens the severity of inflammatory skin conditions. *Immunity,* 40**:** 989-1001, 2014.
13. Di Meglio, P, Perera, GK, Nestle, FO: The multitasking organ: recent insights into skin immune function. *Immunity,* 35**:** 857-869, 2011.
14. Shirakata, Y: Regulation of epidermal keratinocytes by growth factors. *J Dermatol Sci,* 59**:** 73-80, 2010.
15. Shilov, VN, Sergienko, VI: Oxidative stress in keratinocytes as an etiopathogenetic factor of psoriasis. *Bull Exp Biol Med,* 129**:** 309-313, 2000.
16. Slominski, AT, Zmijewski, MA, Skobowiat, C, Zbytek, B, Slominski, RM, Steketee, JD: Sensing the environment: regulation of local and global homeostasis by the skin's neuroendocrine system. *Adv Anat Embryol Cell Biol,* 212**:** 1-115, 2012.
17. Sobajo, C, Behzad, F, Yuan, XF, Bayat, A: Silk: A Potential Medium for Tissue Engineering. *Eplasty,* 8**:** 438-446, 2008.
18. Botchkarev, VA, Gdula, MR, Mardaryev, AN, Sharov, AA, Fessing, MY: Epigenetic regulation of gene expression in keratinocytes. *J Invest Dermatol,* 132**:** 2505-2521, 2012.

19. Slominski, AT, Zmijewski, MA, Semak, I, Zbytek, B, Pisarchik, A, Li, W, Zjawiony, J, Tuckey, RC: Cytochromes p450 and skin cancer: role of local endocrine pathways. *Anticancer Agents Med Chem,* 14**:** 77-96, 2014.

20. Schroder, JM: The role of keratinocytes in defense against infection. *Curr Opin Infect Dis,* 23**:** 106-110, 2010.

21. Hu, SC-S, Lan, C-CE: High-glucose environment disturbs the physiologic functions of keratinocytes: Focusing on diabetic wound healing. *J Dermatol Sci,* 84**:** 121-127.

22. Sabino, CP, Deana, AM, Yoshimura, TM, da Silva, DF, Franca, CM, Hamblin, MR, Ribeiro, MS: The optical properties of mouse skin in the visible and near infrared spectral regions. *J Photochem Photobiol B,* 160**:** 72-78, 2016.

23. Sowa, P, Rutkowska-Talipska, J, Rutkowski, K, Kosztyla-Hojna, B, Rutkowski, R: Optical radiation in modern medicine. *Postepy dermatologii i alergologii,* 30**:** 246-251, 2013.

24. Anders, JJ, Lanzafame, RJ, Arany, PR: Low-level light/laser therapy versus photobiomodulation therapy. *Photomed Laser Surg,* 33**:** 183-184, 2015.

25. Shirasu, N, Nam, SO, Kuroki, M: Tumor-targeted photodynamic therapy. *Anticancer Res,* 33**:** 2823-2831, 2013.

26. Whelan, HT, Smits, RL, Jr., Buchman, EV, Whelan, NT, Turner, SG, Margolis, DA, Cevenini, V, Stinson, H, Ignatius, R, Martin, T, Cwiklinski, J, Philippi, AF, Graf, WR, Hodgson, B, Gould, L, Kane, M, Chen, G, Caviness, J: Effect of NASA light-emitting diode irradiation on wound healing. *J Clin Laser Med Surg,* 19**:** 305-314, 2001.

27. Huang, YY, Gupta, A, Vecchio, D, de Arce, VJ, Huang, SF, Xuan, W, Hamblin, MR: Transcranial low level laser (light) therapy for traumatic brain injury. *J Biophotonics,* 5**:** 827-837, 2012.

28. Mester, E, Mester, AF, Mester, A: The biomedical effects of laser application. *Lasers Surg Med,* 5**:** 31-39, 1985.

29. Peplow, PV, Chung, TY, Ryan, B, Baxter, GD: Laser photobiomodulation of gene expression and release of growth factors and cytokines from cells in culture: a review of human and animal studies. *Photomed Laser Surg,* 29**:** 285-304, 2011.

30. Karu, TI, Kolyakov, SF: Exact action spectra for cellular responses relevant to phototherapy. *Photomed Laser Surg,* 23**:** 355-361, 2005.

31. Arany, PR, Nayak, RS, Hallikerimath, S, Limaye, AM, Kale, AD, Kondaiah, P: Activation of latent TGF-beta1 by low-power laser in vitro correlates with increased TGF-beta1 levels in laser-enhanced oral wound healing. *Wound Repair Regen,* 15**:** 866-874, 2007.

32. Khan, I, Tang, E, Arany, P: Molecular pathway of near-infrared laser phototoxicity involves ATF-4 orchestrated ER stress. *Sci Rep,* 5**:** 10581, 2015.

33. Pfaff, S, Liebmann, J, Born, M, Merk, HF, von Felbert, V: Prospective Randomized Long-Term Study on the Efficacy and Safety of UV-Free Blue Light for Treating Mild Psoriasis Vulgaris. *Dermatology,* 231**:** 24-34, 2015.

34. Kumar, P, Chawla, D, Deorari, A: Light-emitting diode phototherapy for unconjugated hyperbilirubinaemia in neonates. *Cochrane db syst rev***:** Cd007969, 2011.

35. Ueberall, MA, Müller-Schwefe, G: Wirksamkeit und Verträglichkeit von blauem LED-Licht in der praktischen Behandlung von Kreuz-/Rücken- bzw. Schulter-/Nackenschmerzen unter Alltagsbedingungen. *Der Schmerz.* Hamburg, Springer Medizin, 2014 pp 71-72.

36. Dai, T, Gupta, A, Murray, CK, Vrahas, MS, Tegos, GP, Hamblin, MR: Blue light for infectious diseases: Propionibacterium acnes, Helicobacter pylori, and beyond? *Drug Resist Updat,* 15**:** 223-236, 2012.

37. Prindeze, NJ, Moffatt, LT, Shupp, JW: Mechanisms of action for light therapy: a review of molecular interactions. *Exp Biol Med,* 237**:** 1241-1248, 2012.

38. Liebmann, J, Born, M, Kolb-Bachofen, V: Blue-light irradiation regulates proliferation and differentiation in human skin cells. *J Invest Dermatol,* 130**:** 259-269, 2010.

39. Becker, A, Distler, E, Klapczynski, A, Arpino, F, Kuch, N, Simon-Keller, K, Sticht, C, van Abeelen, FA, Gretz, N, Oversluizen, G: Blue light inhibits proliferation of melanoma cells. In: SPIE (Ed.) *SPIE BiOS.* San Francisco, International Society for Optics and Photonics, 2016 pp 969503-969513.

40. Li, Y, Zhang, J, Xu, Y, Han, Y, Jiang, B, Huang, L, Zhu, H, Xu, Y, Yang, W, Qin, C: The Histopathological Investigation of Red and Blue Light Emitting Diode on Treating Skin Wounds in Japanese Big-Ear White Rabbit. *PLoS One,* 11**:** e0157898, 2016.

41. Sutherland, JC: Biological effects of polychromatic light. *Photochem Photobiol,* 76**:** 164-170, 2002.

42. Huang, YY, Chen, AC, Carroll, JD, Hamblin, MR: Biphasic dose response in low level light therapy. *Dose-Response,* 7**:** 358-383, 2009.

43. Karu, T: Primary and secondary mechanisms of action of visible to near-IR radiation on cells. *J Photochem Photobiol B,* 49**:** 1-17, 1999.

44. AlGhamdi, KM, Kumar, A, Moussa, NA: Low-level laser therapy: a useful technique for enhancing the proliferation of various cultured cells. *Lasers Med Sci,* 27**:** 237-249, 2012.

45. Tang, E, Arany, P: Photobiomodulation and implants: implications for dentistry. *J Periodontal Implant Sci,* 43**:** 262-268, 2013.

46. Calabrese, EJ: The future of hormesis: where do we go from here? *Crit Rev Toxicol,* 31**:** 637-648, 2001.

47. Stebbing, AR: Hormesis--the stimulation of growth by low levels of inhibitors. *Sci Total Environ,* 22**:** 213-234, 1982.

48. Calabrese, EJ: Hormetic dose-response relationships in immunology: occurrence, quantitative features of the dose response, mechanistic foundations, and clinical implications. *Crit Rev Toxicol,* 35**:** 89-295, 2005.

49. Lanzafame, RJ, Stadler, I, Kurtz, AF, Connelly, R, Peter, TA, Sr., Brondon, P, Olson, D: Reciprocity of exposure time and irradiance on energy density during photoradiation on wound healing in a murine pressure ulcer model. *Lasers Surg Med,* 39**:** 534-542, 2007.

50. Oron, U, Yaakobi, T, Oron, A, Hayam, G, Gepstein, L, Rubin, O, Wolf, T, Ben Haim, S: Attenuation of infarct size in rats and dogs after myocardial infarction by low-energy laser irradiation. *Lasers Surg Med,* 28**:** 204-211, 2001.

51. Hawkins, D, Abrahamse, H: Effect of multiple exposures of low-level laser therapy on the cellular responses of wounded human skin fibroblasts. *Photomed Laser Surg,* 24**:** 705-714, 2006.

52. Chow, RT, Heller, GZ, Barnsley, L: The effect of 300 mW, 830 nm laser on chronic neck pain: a double-blind, randomized, placebo-controlled study. *Pain,* 124**:** 201-210, 2006.

53. Lubart, R, Lavi, R, Friedmann, H, Rochkind, S: Photochemistry and photobiology of light absorption by living cells. *Photomed Laser Surg,* 24**:** 179-185, 2006.

54. Sommer, AP, Pinheiro, AL, Mester, AR, Franke, RP, Whelan, HT: Biostimulatory windows in low-intensity laser activation: lasers, scanners, and NASA's light-emitting diode array system. *J Clin Laser Med Surg,* 19**:** 29-33, 2001.

55. Martius, F: Das Arndt-Schulz Grundgesetz. *Muench Med Wschr,* 70**:** 1005-1006, 1923.

56. Chen, AC, Arany, PR, Huang, YY, Tomkinson, EM, Sharma, SK, Kharkwal, GB, Saleem, T, Mooney, D, Yull, FE, Blackwell, TS, Hamblin, MR: Low-level laser therapy activates NF-kB via generation of reactive oxygen species in mouse embryonic fibroblasts. *PLoS One,* 6**:** e22453, 2011.

57. Brauze, D, Fijalkiewicz, K, Szaumkessel, M, Kiwerska, K, Bednarek, K, Rydzanicz, M, Richter, J, Grenman, R, Jarmuz-Szymczak, M: Diversified expression of aryl hydrocarbon receptor dependent genes in human laryngeal squamous cell carcinoma cell lines treated with beta-naphthoflavone. *Toxicol Lett,* 231**:** 99-107, 2014.

58. Becker, A, Sticht, C, Dweep, H, van Abeelen, FA, Gretz, N, Oversluizen, G: Impact of blue LED irradiation on proliferation and gene expression of cultured human keratinocytes. In: SPIE (Ed.) *SPIE BiOS.* San Francisco, International Society for Optics and Photonics, 2015 pp 930909-930921.

59. Becker, A, Klapczynski, A, Kuch, N, Arpino, F, Simon-Keller, K, De La Torre, C, Sticht, C, van Abeelen, FA, Oversluizen, G, Gretz, N: Gene expression profiling reveals aryl hydrocarbon receptor as a possible target for photobiomodulation when using blue light. *Sci Rep,* 6**:** 33847, 2016.

60. Meyer, D, Hornik, K, Feinerer, I: Text mining infrastructure in R. *J Stat Softw,* 25**:** 1-54, 2008.

61. Dai, M, Wang, P, Boyd, AD, Kostov, G, Athey, B, Jones, EG, Bunney, WE, Myers, RM, Speed, TP, Akil, H, Watson, SJ, Meng, F: Evolving gene/transcript definitions significantly alter the interpretation of GeneChip data. *Nucleic Acids Res,* 33**:** e175, 2005.

62. Subramanian, A, Tamayo, P, Mootha, VK, Mukherjee, S, Ebert, BL, Gillette, MA, Paulovich, A, Pomeroy, SL, Golub, TR, Lander, ES, Mesirov, JP: Gene set enrichment analysis: a knowledge-based approach for interpreting genome-wide expression profiles. *Proc Natl Acad Sci U S A,* 102**:** 15545-15550, 2005.

63. Sena, LA, Chandel, NS: Physiological roles of mitochondrial reactive oxygen species. *Mol Cell,* 48**:** 158-167, 2012.

64. Yun, J, Finkel, T: Mitohormesis. *Cell Metab,* 19**:** 757-766, 2014.

65. Ristow, M, Schmeisser, K: Mitohormesis: Promoting Health and Lifespan by Increased Levels of Reactive Oxygen Species (ROS). *Dose-Response,* 12**:** 288-341, 2014.

66. Schieber, M, Chandel, NS: ROS function in redox signaling and oxidative stress. *Curr Biol,* 24**:** R453-462, 2014.

67. Kawagishi, H, Finkel, T: Unraveling the truth about antioxidants: ROS and disease: finding the right balance. *Nat Med,* 20**:** 711-713, 2014.

68. Ristow, M: Unraveling the truth about antioxidants: mitohormesis explains ROS-induced health benefits. *Nat Med,* 20**:** 709-711, 2014.

69. Nebert, DW, Roe, AL, Dieter, MZ, Solis, WA, Yang, Y, Dalton, TP: Role of the aromatic hydrocarbon receptor and [Ah] gene battery in the oxidative stress response, cell cycle control, and apoptosis. *Biochem Pharmacol,* 59**:** 65-85, 2000.

70. Ma, Q, Lu, AY: CYP1A induction and human risk assessment: an evolving tale of in vitro and in vivo studies. *Drug Metab Dispos,* 35**:** 1009-1016, 2007.

71. Nebert, DW, Dalton, TP, Okey, AB, Gonzalez, FJ: Role of aryl hydrocarbon receptor-mediated induction of the CYP1 enzymes in environmental toxicity and cancer. *J Biol Chem,* 279**:** 23847-23850, 2004.

72. Rannug, A, Fritsche, E: The aryl hydrocarbon receptor and light. *Biol Chem,* 387**:** 1149-1157, 2006.

73. Hao, N, Whitelaw, ML: The emerging roles of AhR in physiology and immunity. *Biochem Pharmacol,* 86**:** 561-570, 2013.

74. Waller, CL, McKinney, JD: Three-dimensional quantitative structure-activity relationships of dioxins and dioxin-like compounds: model validation and Ah receptor characterization. *Chem Res Toxicol,* 8**:** 847-858, 1995.

75. Denison, MS, Nagy, SR: Activation of the aryl hydrocarbon receptor by structurally diverse exogenous and endogenous chemicals. *Annu Rev Pharmacol Toxicol,* 43**:** 309-334, 2003.

76. Colonna, M: AHR: making the keratinocytes thick skinned. *Immunity,* 40**:** 863-864, 2014.

77. Taylor, BL, Zhulin, IB: PAS domains: internal sensors of oxygen, redox potential, and light. *Microbiol Mol Biol Rev,* 63**:** 479-506, 1999.

78. Gu, YZ, Hogenesch, JB, Bradfield, CA: The PAS superfamily: sensors of environmental and developmental signals. *Annu Rev Pharmacol Toxicol,* 40**:** 519-561, 2000.

79. Nebert, DW, Wikvall, K, Miller, WL: Human cytochromes P450 in health and disease. *Philos Trans R Soc Lond B Biol Sci,* 368**:** 20120431, 2013.

80. Sugimoto, H, Shiro, Y: Diversity and substrate specificity in the structures of steroidogenic cytochrome P450 enzymes. *Biol Pharm Bull,* 35**:** 818-823, 2012.

81. Hosoya, T, Maruyama, A, Kang, MI, Kawatani, Y, Shibata, T, Uchida, K, Warabi, E, Noguchi, N, Itoh, K, Yamamoto, M: Differential responses of the Nrf2-Keap1 system to laminar and oscillatory shear stresses in endothelial cells. *J Biol Chem,* 280**:** 27244-27250, 2005.

82. Nerland, DE: The antioxidant/electrophile response element motif. *Drug Metab Rev,* 39**:** 235-248, 2007.

83. Zhang, DD, Lo, SC, Cross, JV, Templeton, DJ, Hannink, M: Keap1 is a redox-regulated substrate adaptor protein for a Cul3-dependent ubiquitin ligase complex. *Mol Cell Biol,* 24**:** 10941-10953, 2004.

84. Espinosa-Diez, C, Miguel, V, Mennerich, D, Kietzmann, T, Sanchez-Perez, P, Cadenas, S, Lamas, S: Antioxidant responses and cellular adjustments to oxidative stress. *Redox Biol,* 6**:** 183-197, 2015.

85. Hayes, JD, Dinkova-Kostova, AT: The Nrf2 regulatory network provides an interface between redox and intermediary metabolism. *Trends Biochem Sci,* 39**:** 199-218, 2014.

86. Miao, W, Hu, L, Scrivens, PJ, Batist, G: Transcriptional regulation of NF-E2 p45-related factor (NRF2) expression by the aryl hydrocarbon receptor-xenobiotic response element signaling pathway: direct cross-talk between phase I and II drug-metabolizing enzymes. *J Biol Chem,* 280**:** 20340-20348, 2005.

87. Lee, DF, Kuo, HP, Liu, M, Chou, CK, Xia, W, Du, Y, Shen, J, Chen, CT, Huo, L, Hsu, MC, Li, CW, Ding, Q, Liao, TL, Lai, CC, Lin, AC, Chang, YH, Tsai, SF, Li, LY, Hung, MC: KEAP1 E3 ligase-mediated downregulation of NF-kappaB signaling by targeting IKKbeta. *Mol Cell,* 36**:** 131-140, 2009.

88. Wardyn, JD, Ponsford, AH, Sanderson, CM: Dissecting molecular cross-talk between Nrf2 and NF-kappaB response pathways. *Biochem Soc Trans,* 43**:** 621-626, 2015.

89. Holmstrom, KM, Finkel, T: Cellular mechanisms and physiological consequences of redox-dependent signalling. *Nat Rev Mol Cell Biol,* 15**:** 411-421, 2014.

90. Ge, NL, Elferink, CJ: A direct interaction between the aryl hydrocarbon receptor and retinoblastoma protein. Linking dioxin signaling to the cell cycle. *J Biol Chem,* 273**:** 22708-22713, 1998.

91. Kolluri, SK, Weiss, C, Koff, A, Gottlicher, M: p27(Kip1) induction and inhibition of proliferation by the intracellular Ah receptor in developing thymus and hepatoma cells. *Genes Dev,* 13**:** 1742-1753, 1999.

92. Puga, A, Barnes, SJ, Dalton, TP, Chang, C, Knudsen, ES, Maier, MA: Aromatic hydrocarbon receptor interaction with the retinoblastoma protein potentiates repression of E2F-dependent transcription and cell cycle arrest. *J Biol Chem,* 275**:** 2943-2950, 2000.

93. Fritsche, E, Schafer, C, Calles, C, Bernsmann, T, Bernshausen, T, Wurm, M, Hubenthal, U, Cline, JE, Hajimiragha, H, Schroeder, P, Klotz, LO, Rannug, A, Furst, P, Hanenberg, H, Abel, J, Krutmann, J: Lightening up the UV response by identification of the arylhydrocarbon receptor as a cytoplasmatic target for ultraviolet B radiation. *Proc Natl Acad Sci U S A,* 104**:** 8851-8856, 2007.

94. Haarmann-Stemmann, T, Abel, J: The arylhydrocarbon receptor repressor (AhRR): structure, expression, and function. *Biol Chem,* 387**:** 1195-1199, 2006.

95. Mimura, J, Ema, M, Sogawa, K, Fujii-Kuriyama, Y: Identification of a novel mechanism of regulation of Ah (dioxin) receptor function. *Genes Dev,* 13**:** 20-25, 1999.

96. Yin, J, Sheng, B, Qiu, Y, Yang, K, Xiao, W, Yang, H: Role of AhR in positive regulation of cell proliferation and survival. *Cell Prolif,* 49**:** 554- 560, 2016.

97. Huang, YY, Sharma, SK, Carroll, J, Hamblin, MR: Biphasic dose response in low level light therapy - an update. *Dose-Response,* 9**:** 602-618, 2011.

98. Chandel, NS, Trzyna, WC, McClintock, DS, Schumacker, PT: Role of oxidants in NF-kappa B activation and TNF-alpha gene transcription induced by hypoxia and endotoxin. *J Immunol,* 165**:** 1013-1021, 2000.

99. Groeger, G, Quiney, C, Cotter, TG: Hydrogen peroxide as a cell-survival signaling molecule. *Antioxid Redox Signal,* 11**:** 2655-2671, 2009.

100. Karin, M, Lin, A: NF-kappaB at the crossroads of life and death. *Nat Immunol,* 3**:** 221-227, 2002.

101. Brea-Calvo, G, Siendones, E, Sanchez-Alcazar, JA, de Cabo, R, Navas, P: Cell survival from chemotherapy depends on NF-kappaB transcriptional up-regulation of coenzyme Q biosynthesis. *PLoS One,* 4**:** e5301, 2009.

102. Adcock, IM, Lane, SJ: Corticosteroid-insensitive asthma: molecular mechanisms. *J Endocrinol,* 178**:** 347-355, 2003.

103. Barnes, PJ: How corticosteroids control inflammation: Quintiles Prize Lecture 2005. *Br J Pharmacol,* 148**:** 245-254, 2006.

7   CURRICULUM VITAE AND PUBLICATIONS

PERSONALIEN

Name und Vorname: Anja Becker

Geburtsdatum: 02.09.1989

Geburtsort: Bad Bergzabern, Deutschland

Familienstand: ledig

Vater: Paul Becker

Mutter: Margot Becker

SCHULISCHER WERDEGANG

2002 – 2009   Gymnasium im Alfred- Grosser- Schulzentrum Bad
Bergzabern

UNIVERSITÄRER WERDEGANG

01.10.2009- 10.03.2013   B.Sc. Biologische Chemie, University of Applied Sciences
Mannheim, Deutschland
Note: 1,9

01.11.2012- 28.02.2013   Bachelorarbeit "The Influence of N-acyl-dopamine
Derivatives on TRPV1, NFκB- Pathway and their Capacity
to Induce the Unfolded Protein Response"
Nephrologisches Forschungslabor, V. Medizinische Klinik,
Medizinische Fakultät Mannheim der Universität
Heidelberg, Deutschland
Prof. Dr. rer. nat. Benito Yard

01.03.2013- 05.08.2014   M.Sc. Biomedical Science and Technology, University of
Applied Sciences Mannheim, Deutschland
Note: 1,4

10.02.2014- 05.08.2014   Masterarbeit "Influence of Blue LED Irradiation on Human Skin Cells"

Zentrum für Medizinische Forschung (ZMF), Medizinische Fakultät Mannheim der Universität Heidelberg, Deutschland

Prof. Dr. med. Norbert Gretz

In Zusammenarbeit mit Philips Group Innovation, Research, High Tech Campus Eindhoven, The Netherlands

Dr. Gerrit Oversluizen

PUBLICATIONS

Becker, A, Distler, E, Klapczynski, A, Arpino, F, Kuch, N, Simon-Keller, K, Sticht, C, van Abeelen, FA, Gretz, N, Oversluizen, G: Blue light inhibits proliferation of melanoma cells. In: SPIE (Ed.) *SPIE BiOS.* San Francisco, International Society for Optics and Photonics, 2016 pp 969503-969513.

Becker, A, Sticht, C, Dweep, H, van Abeelen, FA, Gretz, N, Oversluizen, G: Impact of blue LED irradiation on proliferation and gene expression of cultured human keratinocytes. In: SPIE (Ed.) *SPIE BiOS.* San Francisco, International Society for Optics and Photonics, 2015 pp 930909-930921.

Becker, A, Klapczynski, A, Kuch, N, Arpino, F, Simon-Keller, K, De La Torre, C, Sticht, C, van Abeelen, FA, Oversluizen, G, Gretz, N: Gene expression profiling reveals aryl hydrocarbon receptor as a possible target for photobiomodulation when using blue light. *Sci Rep,* 6**:** 33847, 2016.

8 ACKNOWLEDGEMENTS